The Role of CASK in Central Nervous System Function and Disorder

Paras A Patel

Dissertation Submitted to Virginia Polytechnic Institute and State University as Partial Requirement to Fulfill the Degree of

Doctor of Philosophy

in

Translational Biology, Medicine, and Health

Committee Members

Konark Mukherjee, MBBS, PhD

Michael A Fox, PhD

Daniel F English, PhD

Sujith Vijayan, PhD

May 5th, 2022

Roanoke, Virginia, USA

Keywords: CASK, synapse, MICPCH, cerebellum, degeneration

The Role of CASK in Central Nervous System Function and Disorder

Paras A Patel

Abstract

Understanding how different regions of the central nervous system (CNS) are affected by genetic insults is critical to advancing the study of CNS pathologies. The cerebellum is one such region which is disproportionately hypoplastic in the majority of cases of *CASK* gene mutation in humans. CASK is an enigmatic multi-domain scaffolding protein which plays a vital role in organizing protein complexes at the pre-synapse through interactions with both active zone proteins and trans-synaptic adhesion molecules such as liprins-α and neurexins. Mutations in the X-linked *CASK* gene in humans are largely post-natally lethal in the hemizygous condition and result in microcephaly with pontine and cerebellar hypoplasia (PCH) and also optic nerve hypoplasia (ONH) in heterozygous mutations. Herein, I used various molecular and genetic strategies to uncover the role of the CASK protein in brain function and pathogenesis of cerebellar hypoplasia associated with CASK mutations/deletions. First, using the face- and construct-validated heterozygous CASK knockout (*Cask*$^{+/-}$) murine model, I conducted bulk RNA-sequencing and proteomics experiments from whole brain lysates to uncover changes in the *Cask*$^{+/-}$ brain. RNA-sequencing revealed the majority of changes to be broadly categorized into metabolic, nuclear, synaptic, and extracellular-matrix associated transcripts. Proteomics revealed the majority of changes cluster as synaptic proteins, metabolic proteins, and ribosomal subunits. Thus, absence of CASK in

half of brain cells seems to affect synaptic protein content, cell metabolism, and protein homeostasis. Extending these observations, I conducted GFP-trap immunoprecipitation followed by tandem mass spectroscopy to reveal protein complexes in which CASK participates. Commensurate with proteomic changes, CASK was found to complex with synaptic proteins, metabolic proteins, cytoskeletal elements, ribosomal subunits, and protein folding machinery. Next, in order to investigate the pathogenesis of CASK-linked cerebellar hypoplasia, I utilized a human case of early truncation wherein the 27th arginine of CASK is converted to a stop codon. Immunohistochemical analysis of this brain revealed an upregulation of glial fibrillary acidic protein, a common marker for degenerative cell death. To mechanistically test the hypothesis that cerebellar hypoplasia results from cell death rather than developmental failure, I created a murine model wherein CASK is deleted from the majority of cerebellar cells post-development using Cre recombinase driven by the *Calb2* promoter. Deleting CASK from all cerebellar granule neurons post-migration indeed leads to degeneration of the cerebellum via massive depletion of granule cells while sparing Purkinje cells. Overall, the cerebellum shrinks by approximately half in cross-sectional area and degeneration is accompanied by a collapsing of the molecular layer and of Purkinje cell dendrites. In addition, cerebellar degeneration presents with a profound locomotor ataxia. In conclusion, CASK seems to be affecting brain energy homeostasis and synaptic connections via interactions with metabolic proteins, synaptic proteins, and protein homeostatic elements. Further, alterations in brain volume associated with CASK-linked disorders is the result of degenerative cell death rather than developmental failure as previously posited.

The Role of CASK in Central Nervous System Function and Disorder

Paras A Patel

General Audience Abstract

One of the main challenges facing modern neuroscience is the question of how constitutive mutations in genes present in every cell can cause different effects on different parts of the brain. CASK is one such gene which is expressed in every cell of the brain and, when mutated, typically results in an overall smaller brain volume. However, the cerebellum is one region of the brain involved in motor coordination which is disproportionately smaller than the rest of the brain. Through this gene, I investigate here two questions principally: (1) what is the role of the CASK protein in cells? And (2) how is the cerebellum differentially affected?

Firstly, I conduct a molecular investigation into what changes in the brain of a mouse model of CASK deletion which recapitulates the majority of human cases found in girls. This genetic model results in half of cells in the body lacking CASK and leads to smaller brain volume with disproportionate reduction in cerebellum size, as in the human subjects. Using a variety of molecular and biochemical methods, I uncover that several classes of proteins are changed in this brain, primarily those associated metabolism and cell-to-cell communication. Further, my experiments indicate that CASK interacts with many of these proteins.

Next, I use human cases as well as a novel mouse model to uncover the trajectory of CASK-linked reduction in cerebellar size. The human case indicates molecular

signatures of cell death, a surprising finding given that CASK-linked disorders are thought to result from developmental failure. Investigating this mechanistically in a mouse model, I uncover that when CASK is deleted after development, cerebellar cells still die and the cerebellum actually shrinks.

Thus, my work herein elucidates potential roles for the CASK molecule in cells and shows, for the first time, that CASK-linked cerebellar size diminishment is degenerative in nature rather than developmental. This degeneration of the cerebellum occurs very early on in infancy and so was missed until now. The most important implication is that a degenerative process could be halted with therapies other than relying exclusively on genetic therapies

Acknowledgments

This is going to be a long one.

I will start by generally stating my deep regard for everyone who took the time for me when they did not have to. When there was no obligation, and indeed you were exceedingly busy with other concerns, those are the moments I remember most fondly. We often say that our time is valuable. I believe that it is our attention that is yet more valuable – consciously or unconsciously, we direct it towards what we value most in every given moment.

Firstly, I would like to thank each of my committee members for their thoughtful consideration of this document and of the five years of work that it distils:

Dr. Vijayan: you were a lamp in the darkness of signal processing and electrophysiological analysis. When I was in my second year of my PhD, you took the time to meet with me individually and review the figures I had generated while self-teaching signal processing in MATLAB. Taking your course on this topic in the final year of my PhD was the perfect completion of this.

Dr. English: Your welcoming nature and excellent mentorship while personally teaching me *in vivo* recording techniques and analysis will stay with me throughout my life. I never expected our first meeting about joining my committee would turn into such an adventure. Here I would document exactly how much this has and continues to mean to me. The way I see it, I came to you with my hat in my hand and you showed up for me better than I could have ever expected.

Dr. Fox: You and your lab have been a bastion throughout my graduate journey. Through all the late nights and unexpected necessity for antibodies, you all have been there when you did not have to. I have always been able to lean on you when feeling adrift and will never forget how you welcomed me into your lab, invited me to your lab meetings, and generally supported me beyond every expectation. Genuinely, thank you for all that you have done.

Dr. Mukherjee: You have probably tuned out from the sappiness by now. But needless to say, you have been an excellent mentor throughout everything. I remember the very first time we spoke, you said “it’s Konark, like the Sun Temple in India”. I had no idea what to expect and have been surprised, delighted, frustrated, enthused, annoyed, and entranced ever since. I would formally express how lucky I have been to have found such a great match for my PhD advisor.

Although not on my dissertation committee or officially my advisor, I consider Dr. Leslie LaConte to be as close of a mentor. Over these years, she has been a consistent voice of reason. It is astounding how much time and effort she is able to devote to our lab and mentorship of the students therein. In my mind, her greatest attribute is that she does this with no obligation whatsoever – she demonstrates daily a genuine passion for science and mentorship that I hope to emulate moving forward. Every lab meeting has been made more fruitful, both scientifically and personally, by your contribution.

Additionally, I must acknowledge Drs. Alexei Morozov and Michelle Olsen, who mentored me as a rotation student. Dr. Morozov: your instruction in stereotaxic surgery was the most beautiful introduction to graduate school that I could have asked for. On a practical level, it gave me the skills necessary to engage with systems neuroscience later in my graduate career without having to meander through the basic skills. On an abstract level, it demonstrated the realities of what this field demands. Dr. Olsen: I frequently recall fondly the day you sat with me individually to teach me how to patch a cell. The fact that you took time after-hours to teach a rotation student how to break into a cell speaks volumes about your character and approach to mentorship.

I would also like to thank all of my peers and friends. Though all have shaped me into the scientist I am today, I would particularly highlight Drs. Ubadah Sabbagh, Rachana Somaiya, Carmen Muñoz-Ballestar, and Rachel Padget, as well as Earl Gilbert and Kaiser Arndt. Via thousands of hours of conversation about science and life, you have

molded my intellectual and personal life over these last five years documented here in this dissertation.

Speaking of those who have shaped my intellectual life: I must acknowledge the Big Lick of Science podcast team and those who made it possible. In the early days, myself and Dr. Somaiya shared a vision for communicating the science done at Virginia Tech to the public. With the direct mentorship of Drs. Shannon Farris and Ubadah Sabbagh, we were able to build something real out of nothing in order to construct an apparatus to deliver science to the community that made us.

The support staff and animal facility technicians at Virginia Tech and the Fralin Biomedical Research Institute also have been vital in completing the work laid out here.

Finally, I must acknowledge my family. Harsha, Atul, and Nilam Patel have been the most excellent support network and safe havens during this journey. Harsha and Atul immigrated to the United States with no degrees, or money, or prospects. And they built a life for us here in Roanoke, VA. Whatever is laid out here pales in comparison.

Table of Contents

Introduction

Neurological disorders are hard to treat. The nervous system has several properties which make it difficult to access and more difficult to modify. On a physical level it is encased in bone; on a cellular level it is composed of unique cell types which generally live as long as the organism itself; and on a molecular level, there is a dearth of understanding as to how molecular complexes enable the functions of the central nervous system and its maladies.

Defining pathological trajectories is a necessary first step in understanding and eventually treating diseases of the nervous system. As per the paucity of molecular to cellular correlates, pathological trajectories are often confused. Disorders associated with mutations in the CASK gene are an exemplar of this confusion. The primary disorder associated with loss-of-function mutations in humans is known as Microcephaly with Pontine and Cerebellar Hypoplasia (MICPCH) which may present several months post-natally with an abnormally small head circumference at least two standard deviations below the mean for the age and most often progresses into intellectual disability and motor incoordination (OMIM: 300749). The other major pathology associated with *CASK* mutations is optic nerve hypoplasia presenting with a thinned optic nerve studded more sparsely than average with the axons of retinal ganglion cells (Liang et al. 2017; Kerr et al. 2019).

Herein, I elaborate progress on understanding CASK-linked pathologies through three phases: (1) our current understanding of the gene and its protein product; (2) the varied nature of the disorder associated with its loss of function; and (3) novel contributions to adapt our understanding of the pathology riding on a more advanced knowledge of the gene and its protein.

Background

2.1 The *CASK* Gene

On the mammalian X chromosome at the X11.4 locus sits the *CASK* gene. Spanning over 200-400,000 base pairs, depending on the species, 27 exons form the most common mRNA transcript variant of *CASK* (The NCBI Handbook).

Due to the X-linked nature of the *CASK* gene, the expression pattern within a single individual is of note. Males having only one copy of X-linked genes commensurately have only one copy of *CASK*; as such, mutations generally result in more severe pathology and complete loss of function mutations are lethal (Najm et al. 2008; Hackett et al. 2010; Moog et al. 2015; Patel, PA et al. 2022). However, females having two copies undergo the process of random X chromosome inactivation wherein the majority of genes on a randomly chosen X chromosome are permanently inactivated in each cell during early embryogenesis (Lyon, 1961; Reviewed in: Panning et al. 2008). This inactivation results in mosaic expression wherein a given cell expresses genes from one X chromosome or the other. Thus, when mutations present in an X-linked gene, mosaicism is observed in the mutation and cells either have the mutated or normal copy. During normal development, in the absence of skewing, nearly half of cells exclusively express genes from one X chromosome while the other half from the other chromosome (Lyon, 1961). Under some conditions where genetic mutations result in a failure of cell fate or cell cycle, there may be secondary skewing of X-inactivation where more than 50% of cells express

genes from one X chromosome (Plenge et al. 2002); *CASK* mutations generally do not present with skewing of X-inactivation resulting in half of cells expressing the mutation (Hackett et al. 2010).

2. 2 The Protein

Among a flurry of protein discoveries amidst the molecular biology revolution of the 1980s and 90s, the *CASK* gene was cloned and initially described in a 1996 paper (Hata et al. 1996) and commensurately a multi-domain protein product was uncovered. From N- to C-terminus, *CASK* encodes a Cam kinase (CamK) domain, an SH3 domain, two L27 domains, a PDZ domain, and a guanylate kinase (GuK) domain (Hata et al. 1996; LaConte et al. 2016).

As with other interesting features of this gene and its protein, one of the most intriguing is its CaM-kinase domain. Initial analyses revealed that the CaM-kinase domain lacked a magnesium binding pocket nor another pocket for a divalent cationic cofactor (Boudeau et al. 2006; Lu et al. 2003). As such, it was determined to be one of many so-called pseudokinases without the ability to phosphorylate any substrate despite having catalytic sites. Later it was revealed that indeed the CaM-Kinase domain is able to transfer phosphate groups in the absence of magnesium, and, indeed, its kinase activity is inhibited in the presence of magnesium (Mukherjee et al. 2008).

Via its PDZ domain, CASK is able to bind its substrate, the trans-synaptic adhesion molecule neurexin (Mukherjee et al. 2008; LaConte et al. 2016; LaConte et al. 2018).

While the precise function of neurexin phosphorylation by CASK remains unknown, it has recently been brought to light that lack of CASK binding to neurexin most frequently exacerbates CASK linked pathologies when compared to loss of other key interactors (LaConte et al. 2018).

Through the lens of point mutations to the *CASK* gene found in human populations, a trove of functional data emerges describing the function of CASK, the role of each domain, interactions between domains, and potential function of binding to other proteins. Molecular analysis of misfolding mutations affords an early opportunity to understand the phenotypic manifestations and functional loss that occurs in the absence of functional CASK directly in humans. Further, a more specific functional characterization can be obtained by observing truncation mutations which ablate certain domains, but not others. Yet more specific functional analysis of individual domain function obtains when mutations do not cause misfolding but do cause disease in humans. Such cases provide the ability to investigate a specific phenotype which may emerge from the loss of a single interactor or individual domain's functionality.

2. 3 Associated Pathologies

The primary disorder in humans associated with loss of CASK function is MICPCH, which is characterized by a small head circumference usually becoming first apparent several months after birth. MICPCH is also characterized by a disproportionately small cerebellum and pontine structure of the brain stem (Hackett et al. 2010; Moog et al. 2015;

OMIM: 300749). The other disorder noted to occur with *CASK* mutation is optic nerve hypoplasia wherein the optic nerve is disproportionately thinned with loss of retinal ganglion cells (RGCs) (Hackett et al. 2010; Liang et al. 2017; Kerr et al. 2019).

Functional losses associated with MICPCH most often include intellectual disability, autism spectrum disorder diagnosis, failure to develop language from the babbling stage, and motor incoordination including severe hypotonia (Burglen et al. 2012; Moog et al. 2011; Hackett et al. 2010). Visual deficits and nystagmus may also be noted with mutations to the *CASK* gene in humans (Hackett et al. 2010).

However, it should be noted that MICPCH does not always manifest with *CASK* mutations in human (Hackett et al. 2010; others). Additionally, diminished head circumference is not always associated with disproportionate cerebellar volume reduction or optic nerve hypoplasia (Cristofoli et al. 2018).

Epileptic encephalopathies are a more complicated feature of the spectrum of disorders associated with *CASK* mutation. Rare cases in boys where *CASK* mutations encode a non-functional protein present with severe epilepsy and infantile spasms (Moog et al. 2015). However, epileptic discharges are not often seen in girls with heterozygous mutations which form the majority of cases due to post-natal lethality in males (Moog et al. 2015). Girls otherwise exhibit the phenotypic spectrum of MICPCH (Burglen et al. 2012; Moog et al.; Hackett et al. 2010). This pattern raises questions as to the association between CASK and the excitation/inhibition balance which is characteristic of epileptic disorders (Bozzi, 2017). It has been documented that in *Cask*-null neurons *in vitro* exhibit an increase in the frequency of excitatory miniature post-synaptic currents (mEPSC) and

a decrease in the frequency of inhibitory miniature post-synaptic currents (mIPSC) with no change in the amplitude of either of these currents (Atasoy et al. 2007). Further, these changes have been recapitulated in *ex vivo* acute slices from heterozygous *Cask* knockout mice (Mori et al. 2019). Despite these changes seen in neuronal culture and slice, the remaining fact that humans with heterozygous mutations do not always exhibit epilepsy confuses the issue.

2.4 Affected Regions of the CNS

While CASK-linked disorders may present with autonomic dysfunction, this may be attributed to central dysfunction reverberating out into the PNS (Mukherjee et al. 2020; Patel PA et al. 2022). Further, the most apparent disruptions to nervous system function are the hypoplasias of the cerebellum and optic nerve mentioned above as well as the diminished size of virtually the entire central nervous system manifesting as microcephaly. Below, I will describe the gross and cellular anatomy of the affected regions of the CNS as well as their general physiological properties to provide context for the rationale and outcomes of the experiments detailed in the remainder of this document.

2. 4.1 The Optic Nerve and Subcortical Visual System

The primary entry of detectable photons into the nervous system occurs at a CNS structure protruding out of the brain itself called the retina. This specialized light-detecting

region is composed principally of six main cell types: rods and cones which are light-detecting cells; bipolar, horizontal, and amacrine cells which convey light information immediately from rods and cones downstream (bipolar cells) and also modify the information at the level of the retina (horizontal and amacrine cells); and finally retinal ganglion cells (RGCs) which are the only output of the retina to the remainder of the brain (Martersteck et al. 2017; Kang et al. 2004; Liang et al. 2017). The axons of RGCs are what form the optic nerve, which is a heavily myelinated nerve extending from the retina to over 40 regions of the mammalian brain (Kang et al. 2004). Importantly for image forming vision, the optic nerve projects to the dorsal lateral geniculate nucleus (dLGN) of the thalamus which acts predominantly as a relay to primary visual cortex with minimal information transformation occurring at the level of the dLGN itself (Martersteck et al. 2017). Herein, I will focus on the anatomy and physiology of the optic nerve itself due to the associated hypoplasia in CASK-linked disorders.

Composed of RGC axons which span the outer surface of the retina before converging at the optic disc, the optic nerve projects through the retina via the posterior orbit and optic canal. The axons then converge at the optic chiasm where they will either decussate to reach the contralateral thalamus or not decussate to innervate the ipsilateral thalamus (Seabrook et al. 2017). These axons ultimately reach the dLGN where RGC terminals synapse onto thalamic relay neurons in either a one-to-one or many-to-one convergent fashion for information relay and processing (reviewed in: Seabrook et al. 2017; Morgan, 2017).

The nerve itself is composed of no neuronal soma, but is highly vascularized and enriched with glia (Hayreh, 1969; Butt et al. 2004). As such, the optic nerve contains the soma of endothelial cells forming the vasculature, oligodendrocytes participating in the myelination of RGC axons, and fibrous astrocytes playing a regulatory function (Butt et al. 2004).

2.4.2 Alterations of the Optic Nerve with CASK Mutation or Deletion

The most prominent result of CASK-loss on the optic nerve is the diminished cross-sectional area seen in mouse models of *Cask* heterozygous deletion, *Cask* hypomorphism (*Cask*^{floxed}), and *Cask* neuronal knockout (*Cask*^{nKO}) resultant from Cre expression in neurons driven the *Syn1* promoter (Liang et al. 2017; Kerr et al. 2019; unpublished observations). Diminished volume of the optic nerve can also be observed in magnetic resonance images taken from human cases of heterozygous *CASK* mutation or complete loss (Liang et al. 2017).

Diminished cross-sectional area of the optic nerve is likely attributed to the loss of RGC axons which is observed within optic nerves taken from CASK knockout animals. Electron micrographs from *Cask* heterozygous knockout mice demonstrate a reduced number of RGC axons as well as an increased inter-axonal space (Liang et al. 2017) which is accompanied by a reduction in the number of RGC soma observed in the ganglion cell layer at the level of the retina compared to controls (Liang et al. 2017; Kerr et al. 2019). Interestingly, RGC absence was found to be the result of RGC cell death

rather than primary failure in RGC development and this cell death is not due to a cell-intrinsic role of CASK (Kerr et al. 2019).

2.4.3 The Cerebellum

At the other side of the CNS is the cerebellum hypoplastic in CASK-linked disorders. Sitting at the back of the brain, the cerebellum is a region composed of repeats of a highly stereotyped circuit consisting of five main neuron types: glutamatergic granule cells extending parallel fibers up into the molecular layer of the cerebellar cortex; glutamatergic climbing fibers coming up from neurons whose soma reside the inferior olivary nucleus of the brainstem; the GABAergic Purkinje cell onto which both glutamatergic cell types synapse onto and which is the only output of the cerebellar cortex; neurons of the deep cerebellar nuclei which receive inhibitory input from Purkinje cells and subsequently project out to almost the entire rest of the brain; and a variety of interneuron subtypes performing local GABAergic modulation of the cells within the cerebellar cortex (Apps et al. 2005).

Developmentally, cells of the cerebellum primarily arise from the rhombic lip during early embryogenesis and initially migrate in a sequential order. First, Purkinje cells align to form what is known as the Purkinje cell plate which will eventually become the single-file row of Purkinje cell seen in the mature cerebellum. Later, granule cells begin to differentiate on the distal side of the Purkinje cell plate to form what is known as the external granular layer (EGL); these nascent granule cells will then migrate along glial

tracts post-natally through the Purkinje cell layer to form a mature internal granular layer (IGL) (Komuro et al. 2013). The migration of granule cells inward to form the IGL is what gives the cerebellum its three dimensional volume and characteristic foliation. As maturation of the cerebellum progresses postnatally, climbing fiber axons will wrap around immature Purkinje cell soma while Purkinje cells will begin to elaborate their extensive, two dimensional dendritic arbors (Miyata et al. 2010). As the dendrites mature, climbing fiber axons will move up from the soma to form progressively more distal synapses onto the dendrites of the Purkinje cells in order to eventually innervate a single Purkinje cell with up to hundreds of excitatory synapses (reviewed in: van Welie et al. 2011).

In addition to the neuron types residing in the cerebellum, it is a highly vascularized structure with accompanying endothelial cells (Delion et al. 2017) as well as extensive glial presence. Oligodendrocytes within the cerebellum primarily myelinate the efferent Purkinje cell axons and afferent climbing fiber axons. Interestingly, astrocytes within the cerebellum take on an unusual morphology relative to other regions of the brain; the cerebellum contains two primary types of astrocytes: the astrocytes of the granule cell layer and white matter which resemble typical protoplasmic astrocytes such as those seen in the neocortex and also the Bergmann glia which reside perisomatic to Purkinje cells and extend their processes up through the molecular layer perfectly perpendicular to the single-file arrangement of the Purkinje cell layer. These Bergmann glia resemble radial glia of the neocortex in morphology and indeed have been implicated in providing

a physical substrate for migration of granule cells from the EGL to the IGL (Buffo et al. 2013).

At a gross morphology level, the cerebellum is a foliated structure, even in mouse, which is largely isolated from the rest of the brain except via axon tracts running through the pontine structure of the brainstem known as the cerebellar peduncles (Jimsheleishvili et al. 2021).

As the Purkinje cell is the only output of the cerebellar cortex, it plays a central role in the motor processing which occurs there. This large GABAergic cell has correspondingly strange physiological properties. They have an intrinsic firing rate of 40-100Hz which presumably occurs without any glutamatergic stimulus (Reviewed in: Apps et al. 2005; Streng et al. 2018). Further, they display two unique kinds of action potential: a “simple” spike which occurs at the intrinsic 40-100Hz rate and resembles a typical action potential waveform which is modulated by glutamatergic input from granule cells as well as a “complex” spike which occurs at approximately 1Hz and is led by the simultaneous discharge of up to hundreds of climbing fiber synapses onto a single Purkinje cell. The unique complex spike is composed of a sharp high-amplitude depolarization thought to be mediated by the initial sodium current followed by two to five spikelets with no afterhyperpolarization observed in between each spikelet mediated by secondary calcium entry into the proximal dendrites of the Purkinje cell (Streng et al. 2018).

The function of either simple or complex spikes is still a matter of active investigation (Streng et al. 2018). However, it has been observed that complex spike generation is followed by a brief pause in simple spike firing on the order of 10-30

milliseconds (Streng et al. 2018). While the function of Purkinje cell output remains to be specifically determined, experiments ablating granule cell firing via calcium channel inactivation have demonstrated that this excitatory input is not necessary for Purkinje cell simple or complex spike generation and that granule cell input does not play a role in normal motor function but does serve a function during motor learning (Galliano et al. 2013; Giovannucci et al. 2017). This observation is interesting given the data presented herein where granule cell death is associated with severe ataxia even after motor learning and cerebellar function have obtained.

2.4.4 Outputs of the Cerebellum

While the cerebellar cortex is composed entirely of repeats of the circuit described above, the Purkinje cell subsequently outputs to a nucleus within the cerebellar white matter known as the deep cerebellar nuclei (DCN) (Apps et al. 2005). The DCN project out from the cerebellum to innervate vast swaths of the brain, first sending axons through the cerebellar peduncles in the pontine brainstem then out to regions as diverse as the thalamus, cortex, striatum, and hippocampus (Baumel et al. 2009, Xiao et al. 2018, Bohne et al. 2019).

References

1. Apps, R., Garwicz, M. (2005). Anatomical and physiological foundations of cerebellar information processing. Nat Rev Neurosci. 6: 297-311.

2. Atasoy, D. et al. (2007). "Deletion of CASK in mice is lethal and impairs synaptic function." Proceedings of the National Academy of Sciences of the United States of America **104**(7): 2525-2530.

3. Baumel, Y., Jacobson, G. A., Cohen, D. (2009). “Implications of functional anatomy on information processing in the deep cerebellar nuclei”. Front Cell Neurosci. **3**(14).

4. Bohne, P. et al. (2019). “A New Projection From the Deep Cerebellar Nuclei to the Hippocampus *via* the Ventrolateral and Laterodorsal Thalamus in Mice”. Front Neural Circuits. **13**(51).

5. Boudeau, J. et al. (2006). “Emerging roles of pseudokinases”. Trends in Cell Biology. **16**(9): 443-52.

6. Bozzi, Y. et al. (2018). “Neurobiological bases of autism-epilepsy comorbidity: a focus on excitation/inhibition imbalance”. Eur J Neurosci. **47**(6): 534-48.

7. Buffo, A., Rossi, F. (2013). “Origin, lineage and function of cerebellar glia”. Progress in Neurobiology. **109**: 42-63.

8. Burglen, L. et al. (2012). "Spectrum of pontocerebellar hypoplasia in 13 girls and boys with CASK mutations: confirmation of a recognizable phenotype and first description of a male mosaic patient." Orphanet J Rare Dis **7**: 18.

9. Butt, A. M. et al. (2004). “Functions of optic nerve glia: axoglial signalling in physiology and pathology”. Eye (Lond). **18**(11): 1110-21.

10. Cristofoli F. et al. (2018). “Novel *CASK* mutations in cases with syndromic microcephaly”. Hum Mutat. **39**(7): 993-1001.

11. Delion M., Dinomais, M., Mercier, P. (2017). “Arteries and Veins of the Cerebellum”. Cerebellum. **16**: 880-912.
12. Galliano, E. et al. (2013). “Silencing the majority of cerebellar granule cells uncovers their essential role in motor learning and consolidation”. Cell Rep. **3**(4): 1239-51.

13. Giovannucci A. et al. (2017). “Cerebellar granule cells acquire a widespread predictive feedback signal during motor learning”. Nat Neurosci. **20**(5): 727-34.

14. Hackett, A. et al. (2010). "CASK mutations are frequent in males and cause X-linked nystagmus and variable XLMR phenotypes." Eur J Hum Genet **18**(5): 544-552.

15. Hata, Y. et al. (1996). "CASK: a novel dlg/PSD95 homolog with an N-terminal calmodulin-dependent protein kinase domain identified by interaction with neurexins." J Neurosci **16**(8): 2488-2494.

16. Hayreh, S. S. (1969). “Blood supply of the optic nerve head and its role in optic atrophy, glaucoma, and oedema of the optic disc”. Br J Ophthalmol. **53**(11): 721-48.

17. Hsueh, Y. et al. (2000). “Nuclear translocation and transcription by the membrane-associated guanylate kinase CASK/LIN-2”. Nature. **404**: 298-302.

18. Jimsheleishvili, S., Dididze, M. (2021). “Neuroanatomy, Cerebellum”. In: StatPearls [Internet]. Treasure Island (FL): StatPearls Publishing; 2022 Jan-

19. Kang, K., Shapley, R.M., Sompolinsky, H. (2004). “Information Tuning of Populations of Neurons in Primary Visual Cortex”. Journal of Neuroscience. 24(15): 3726-3735.

20. Kerr, A. et al. (2019). "Non-Cell Autonomous Roles for CASK in Optic Nerve Hypoplasia." Invest Ophthalmol Vis Sci **60**(10): 3584-3594.

21. Kumoro, H., Rakic, P. (1998). “Distinct Modes of Neuronal Migration in Different Domains of Developing Cerebellar Cortex”. Journal of Neuroscience. **18**(4): 1478-90.

22. LaConte, L. E. et al. (2016). "CASK stabilizes neurexin and links it to liprin-alpha in a neuronal activity-dependent manner." Cell Mol Life Sci **73**(18): 3599-3621.

23. LaConte, L. E. W. et al. (2018). "Two microcephaly-associated novel missense mutations in CASK specifically disrupt the CASK-neurexin interaction." Hum Genet **137**(3): 231-246.

24. Liang, C. et al. (2017). "Optic Nerve Hypoplasia Is a Pervasive Subcortical Pathology of Visual System in Neonates." Investigative Ophthalmology & Visual Science **58**(12): 5485-5496.

25. Lu, C. S. et al. (2003). “Regulation of the Ca2+/CaM-Responsive Pool of CaMKII by Scaffold-Dependent Autophosphorylation”. Neuron. **40**: 1185-97.

26. Lyon, M. (1961). “Gene action in the X-chromosome of the mouse (*Mus musculus* L.)”. Nature **190**:372-373.

27. Martersteck, E. et al. (2017). “Diverse Central Projection Patterns of Retinal Ganglion Cells”. Cell Rep. 18(8): 2058-2072.

28. Miyata, T. et al. (2010). “Migration, early axonogenesis, and Reelin-dependent layer-forming behavior of early/posterior-born Purkinje cells in the developing mouse lateral cerebellum”. Neural Development. **5**(23).

29. Morgan, J. L. (2017). “A connectomic approach to the lateral geniculate nucleus”. Vis Neurosci. **34**: E014.

30. Moog, U. et al. (2011). "Phenotypic spectrum associated with CASK loss-of-function mutations." J Med Genet **48**(11): 741-751.

31. Moog, U. et al. (2015). "Phenotypic and molecular insights into CASK-related disorders in males." Orphanet J Rare Dis **10**: 44.

32. Mori, T. et al. (2019). "Deficiency of calcium/calmodulin-dependent serine protein kinase disrupts the excitatory-inhibitory balance of synapses by down-regulating GluN2B." Mol Psychiatry **24**(7): 1079-1092.

33. Mukherjee, K. et al. (2008). "CASK functions as a Mg2+-independent neurexin kinase." Cell **133**(2): 328-339.

34. Najm, J. et al. (2008). "Mutations of CASK cause an X-linked brain malformation phenotype with microcephaly and hypoplasia of the brainstem and cerebellum." Nat Genet **40**(9): 1065-1067.

35. Patel, P. A. et al. (2020). "Haploinsufficiency of X-linked intellectual disability gene CASK induces post-transcriptional changes in synaptic and cellular metabolic pathways." Exp Neurol **329**: 113319.

36. Patel, P. A. et al. (2022). “Complete loss of the X-linked gene CASK causes severe cerebellar degeneration”. Journal of Medical Genetics. Published Online First: 11 February 2022.

37. Panning, B. (2008). “X-chromosome inactivation: the molecular basis of silencing”. Journal of Biology. **7**(30).

38. Plenge, R.M. et al. (2002). “Skewed X-chromosome inactivation is a common feature of X-linked mental retardation disorders”. Am J Hum Genet. **71**(1): 168-73.

39. Patil, N. et al. (1995). “A potassium channel mutation in weaver mice implicates membrane excitability in granule cell differentiation”. Nat Genet. **11**(2): 126-9.

40. Salazar, J. J. et al. (2018). “Anatomy of the Human Optic Nerve: Structure and Function”. In: Ferrari, F. M. editor, Optic Nerve [Internet].

41. Schweighofer, N., Doya, K., Lay, F. (2001). “Unsupervised learning of granule cell sparse codes enhances cerebellar adaptive control”. Neuroscience. **103**(1): 35-50.

42. Seabrook, T. A. et al. (2017). “Architecture, Function, and Assembly of the Mouse Visual System”. Annu Rev Neurosci. **40**: 499-538.

43. Srivastava, S. et al. (2016). "X-linked intellectual disability gene CASK regulates postnatal brain growth in a non-cell autonomous manner." Acta Neuropathol Commun **4**: 30.

44. Streng, M.L., Popa, L.S., Ebner, T.J. (2018). “Complex Spike Wars: a New Hope”. Cerebellum. 17(6): 735-746.

45. The NCBI handbook [Internet]. Bethesda (MD): National Library of Medicine (US), National Center for Biotechnology Information; 2002 Oct. Available from http://www.ncbi.nlm.nih.gov/books/NBK21101

46. van Welie I. et al. (2011). “The metamorphosis of the developing cerebellar microcircuit”. Curr Opin Neurobiol. **21**(2-14): 245-53.

47. Xiao L. et al. (2018). “Regulation of striatal cells and goal-directed behavior by cerebellar outputs”. Nat Commun. **9**(3133).

48. Zhang, Y. et al. (2014). “An RNA-sequencing transcriptome and splicing database of glia, neurons, and vascular cells of the cerebral cortex”. J Neurosci. **34**(36): 11929-47.

Outline

The following four sections will outline the results of my thesis work as well as the methods used, split into four papers published in *Investigative Ophthalmology and Visual Science*, *Experimental Neurology*, *Molecular Genetics and Genomic Medicine*, and the *Journal of Medical Genetics*. Briefly, the main goal of my thesis work was to define pathological trajectories and phenotypes associated with CASK-linked disorders in order to better understand how diminishments in volume of certain regions of the CNS can occur. In Chapter 3.1, I investigate the optic nerve and the mechanisms underlying diminishment of its size. In Chapter 3.2, I investigate molecular complexes and changes in the face-

validated heterozygous *Cask* deletion model. Chapter 3.3 is a description of a case of a human with an early truncation in *CASK* precluding functional protein formation. Finally, in Chapter 3.4, I investigate another case of early truncation and generate a novel mouse model to test the pathological trajectory of diminished size of the cerebellum in CASK-linked disorders across genetic backgrounds.

Preface: Chapter 3.1 details work elucidating the effects of CASK mutation and cell-type specific deletion on the structure and function of the optic nerve. The work was primarily carried out by Dr. Alicia Kerr in the laboratory of Dr. Michael fox. It was published in *Investigative Ophthalmology and Visual Science* in 2019.

3.1 Non-cell autonomous roles for CASK in ONH

Authors: Alicia Kerr[1,2], Paras Patel[1,2], Leslie E. W. LaConte[1,3], Chen Liang[1], Ching-Kang Chen[4], Veeral Shah[4,5], Michael Fox[1,6,7*], Konark Mukherjee[1,8*]

Affiliations:

[1]Center for Neurobiology Research, Fralin Biomedical Research Institute at Virginia Tech Carilion, Roanoke, Virginia, United States.

[2]Graduate Program in Translational Biology, Medicine, and Health, Virginia Tech, Blacksburg, Virginia, United States.

[3]Department of Basic Science Education, Virginia Tech Carilion School of Medicine, Roanoke, Virginia, United States.

[4]Department of Ophthalmology, Baylor College of Medicine, Houston, Texas, United States.

[5]Texas Children's Hospital, Houston, Texas, United States.

[6]Department of Biological Sciences, Virginia Tech, Blacksburg, Virginia, United States.

[7]Department of Pediatrics, Virginia Tech Carilion School of Medicine, Roanoke, Virginia, United States.

[8]Department of Psychiatry and Behavioral Medicine, Virginia Tech Carilion School of Medicine, Roanoke, Virginia, United States.

*Correspondence to: konark@vtc.vt.edu and mafox1@vtc.vt.edu

Konark Mukherjee and Michael Fox

2 Riverside Circle

Roanoke, VA USA 24016

Abstract

PURPOSE:

Heterozygous mutations in the essential X-linked gene CASK associate with Optic Nerve Hypoplasia (ONH) and other retinal disorders in girls. CASK$^{+/-}$ heterozygous knockout mice with mosaic CASK expression exhibit ONH with a loss of retinal ganglion cells (RGCs) but no changes in retinal morphology. It remains unclear if CASK deficiency selectively affects RGCs or also affects other retinal cells. Furthermore, it is not known if CASK expression in RGCs is critical for optic nerve (ON) development and maintenance.

METHODS:

The visual behavior of CASK$^{+/-}$ mice was assessed and electroretinography (ERG) was performed. Using a mouse line with a floxed CASK gene that expresses ~40% CASK globally in all cells (hypomorph) under hemizygous and homozygous conditions, we investigated effects of CASK reduction on the retina and ON. CASK was then completely deleted from RGCs to examine its cell-autonomous role. Finally, for the first time we describe a hemizygous CASK missense mutation in a boy with ONH.

RESULTS:

CASK$^{+/-}$ heterozygous mutant mice display reduced visual contrast sensitivity, but ERG is indistinguishable from wildtype. CASK hypomorph mice exhibit ONH, but deletion of CASK from RGCs in this background does not exacerbate the condition. The boy with ONH harbors a missense mutation (p.Pro673Leu) that destabilizes CASK and weakens the crucial CASK-neurexin interaction.

CONCLUSIONS:

Our results demonstrate that mosaic or global reduction in CASK expression and/or function disproportionately affects RGCs. CASK expression in RGCs does not appear critical for cell survival, indicating a non-cell autonomous role for CASK in the development of ON.

Word count=248

Introduction

Optic Nerve Hypoplasia (ONH) is the most common cause of childhood blindness in developed nations, and its incidence is on the rise(Kong, Fry et al. 2012, Khaper, Bunge et al. 2017). ONH involves thinning of the optic nerve (ON) and is typically associated with loss of retinal ganglion cells (RGCs) and their axons(Katagiri, Nishina et al. 2017). Most cases of ONH are non-genetic in nature, and the etiogenesis of ONH has therefore remained obscure. Genetically identified forms of ONH are typically associated with transcription factors that are directly involved in the development of RGCs(Chen, Yin et al. 2017). In many instances of ONH, however, RGCs initially begin to develop and connect with the brain, but development stalls or RGCs undergo atrophy before complete ON development(Frisén and Holmegaard 1978, Hoyt and Good 1992). Therefore, to better understand the etiopathogenesis of ONH, face-validated animal models of this disease need to be investigated.

We have demonstrated that haploinsufficiency of the X-linked gene *CASK* (Calcium/calmodulin Activated Serine Kinase) produces ONH in both humans and mice(Liang, Kerr et al. 2017). Like many forms of human ONH, CASK-linked ONH does not affect formation of RGCs(Liang, Kerr et al. 2017). The protein product of this gene (also CASK) is a peripheral scaffolding protein(Butz, Okamoto et al. 1998), and its role in RGC development or survival remains unknown. In addition to ONH, mutations in *CASK* are also associated with other retinopathies, including retinal dystrophy, indicating that retinal cells distal to RGCs may also be affected(Moog, Uyanik et al. 1993, Burglen, Chantot-Bastaraud et al. 2012, LaConte, Chavan et al. 2019). In previous work(Liang,

Kerr et al. 2017) on mice exhibiting CASK-linked ONH, we did not observe any change in lamination or loss of non-RGC retinal cells. Here, we investigate the effect of *CASK* haploinsufficiency on the function of retinal cells and determine if CASK deficiency produces an RGC-specific pathology in a cell-autonomous fashion.

Our results demonstrate that *CASK* haploinsufficiency produces isolated RGC pathology. We also demonstrate that global reduction of CASK by ~60% as observed in *CASK*$^{fl/fl}$ mice is sufficient to induce RGC loss. Surprisingly, we find that despite this disproportionate sensitivity of RGCs to CASK deficiency, CASK expression in an RGC is not important for its survival or maintenance. Finally, using a human case report, we demonstrate that a hemizygous partial- loss of function mutation in CASK is sufficient to produce ONH. Taken together, these results suggest that 1) global reduction in CASK expression or function adversely affect RGC survivaland 2) CASK deficiency produces a developmental RGC pathology via a non-cell autonomous mechanism.

Methods

Statement of ethics

All experiments were performed in accordance with Virginia Tech IACUC and IRB guidelines and approved protocols.

Visual behavior tasks

The two-alternative forced-swim task was performed as previously described(Monavarfeshani, Stanton et al. 2018). The method is based on finding a hidden platform in response to visual cues. See supplement for full methods.

Electroretinography

Stimulus-dependent transcorneal potential changes from both eyes were simultaneously recorded using the UTAS BigShot system (LKC Technologies, Gaithersburg, MD). Photopic recordings ensued immediately after scotopic recordings by exposing the animals to a white background light of 30 Cd/m^2 intensity for 10 min followed by flashes of 25 Cd/s/m^2 in intensity and presented at 1 Hz frequency for 90 sec. See supplement for full methods.

Analysis of human CASK sequence variant

The human CASK sequence variant, p.Pro673Leu, was examined biochemically and *in silico* as previously described by us(LaConte, Chavan et al. 2014, LaConte, Chavan et al. 2018, LaConte, Chavan et al. 2019). Details of the methodology are in the supplementary files.

Immunoblots and immunohistochemistry

Detailed methodology described in supplementary section. IHC was performed as previously described (Liang, Kerr et al. 2017).

In situ hybridization (ISH)

ISH was performed on 16 µm sections as previously described(Su, Gorse et al. 2010, Su, Chen et al. 2016). Sense and antisense riboprobes were generated against full-length *CASK* IMAGE Clone (catalog number MMM1013-202761641, Dharmacon, Lafayette, CO). Riboprobes were synthesized using digoxigenin (DIG) (Roche, Mannheim, Germany) and the MAXI-Script In Vitro Transcription Kit (Ambion, Austin, TX). Probes were hydrolyzed to ~500 base pairs. Images were obtained on a Zeiss LSM700 confocal microscope.

Animals

Cask$^{+/-}$ female mice generated in-house(Srivastava, McMillan et al. 2016) were crossed with C57BL6 male mice to generate *CASK*$^{(+/-)}$ female pups and their *Cask*$^{+/+}$ female littermates. *Calb2-Cre* (stock #010774), *Rosa-stop-tdT* (Ai9) (stock #007909), *Cask*$^{fl/fl}$ (stock #006382) were all obtained from Jackson Laboratories. Genotyping was done using a PCR-based method with primer pairs given in Supplementary Table 1. All mice used in these experiments were between 3 and 6 months old.

Optic Nerve toluidine blue staining and electron microscopy

ON analysis was performed as previously described(Liang, Kerr et al. 2017). Details of the methodology are in the supplementary files.

Results

Heterozygous loss of CASK produces behavioral but not electroretinographical deficits in vision

We previously described that heterozygous loss of *Cask* (*Cask*$^{+/-}$) in mice results in ONH(Liang, Kerr et al. 2017). To assess visual function in *Cask*$^{+/-}$ mice, we used a two-alternative forced-swim task. In this task, mice learn to associate a visual cue of a sine-grating with a hidden platform used to escape the water (Figure 1A)(Prusky, West et al. 2000, Huberman and Niell 2011). Mice genetically devoid of RGCs are unable to perform this task(Monavarfeshani, Stanton et al. 2018). We first assessed the ability of *Cask*$^{+/-}$ mice (and female wild-type littermates) to learn this task. *Cask*$^{+/-}$ mice and controls were trained for 8 days on a vertical grating (0.17 cycles per degree [cpd]) on the S+ monitor

above a hidden platform (compared to a gray screen on the S- monitor). When their ability to locate the hidden platform in ten trials (per day) exceeded 70%, they were considered to have successfully discriminated between the visual cues(Li, Chen et al. 2005). *Cask*$^{+/-}$ mice and female littermate controls performed at similar rates through the 8 days of training, and by the end of this training both genotypes were performing at near 100% accuracy (Figure 1B).

By changing the spatial frequency of the S+ sine-grating, we were able to test visual acuity of mutant and control mice. Although *Cask*$^{+/-}$ mice performed slightly worse than littermate controls, there was no significant difference in performance regardless of the spatial frequency of the gratings (Figure 1C). We then altered the contrast of the gratings. *Cask*$^{+/-}$ mice performed statistically worse than littermate controls in these tasks, and their performance consistently worsened (compared with littermates) as the contrast of the grating decreased (Figure 1D). Thus in addition to ONH and reduced RGCs, *Cask*$^{+/-}$ mice exhibit readily noticeable decreased visual performance.

To assess whether this behavioral deficit was due to ONH (and RGC loss) or from defects within the retina, electoretinograms (ERGs) were recorded on *Cask*$^{+/-}$ mice and controls. ERG waveforms are well-documented to reflect neural activity from the outer retina, with the a-wave reflecting photoreceptor activity(Brown 1968) and the b-wave reflecting activity of the depolarizing bipolar cells(Stockton and Slaughter 1989, Gurevich and Slaughter 1993). Under photopic conditions, ERG b-wave responses appeared similar between *Cask*$^{+/-}$ and wild-type littermates (Figure 1E). Moreover, the average photopic b-wave amplitudes elicited by light flashes of 25 Cd/sec/m^2 in intensity showed no difference

between genotypes (Figure 1F). Likewise, scotopic a-wave amplitudes were also comparable between *Cask*$^{+/-}$ and wild-type littermates (Figure 1G, H). By fitting the ensemble scotopic b-wave amplitudes vs. retinal illuminance to a modified Naka-Rushton function for maximum rod- and cone-driven responses and their half-saturating light intensities(Tracy, Kolesnikov et al. 2015), we further found their ERG responses to be very similar (Figure 1I). Taken together, these results indicate that outer retinal function is normal in *Cask*$^{+/-}$ mice and thus suggest that the observed deficit in visual behavior is likely due to the loss of RGCs and their axonal thinning.

Global reduction in CASK expression produces ONH

Due to random X-inactivation, *CASK* heterozygous mutations result in a mosaic condition, with ~50% of brain cells generating 100% of CASK and ~50% of cells being CASK-null. In our experiments designed to understand the cellular role of CASK in RGCs and ON development, such mosaicism is a confounding variable. A global CASK loss-of-expression mutation, in either a hemizygous male or homozygous female mouse, is a useful model to help disentangle this confound. *Cask*$^{-/-}$ mice do not survive, but a conditional allele of *Cask* (*Cask*$^{fl/fl}$) generated previously was shown to cause a global reduction in CASK expression (~40% of wild-type expression) due to selection cassette interference(Atasoy, Schoch et al. 2007). This *Cask*$^{fl/fl}$ mouse has also been reported to have microcephaly and cerebellar hypoplasia(Najm, Horn et al. 2008, Srivastava, McMillan et al. 2016).

Here, we confirm that CASK expression in the ON of *Cask*$^{fl/fl}$ mice (Figure 2A) is similarly reduced; we therefore used these mice to determine if uniform reduction in CASK

expression impacts the developing visual system. Toluidine blue sections show that *Cask*$^{fl/fl}$ ONs are thin and hypoplastic compared to littermate *Cask*$^{+/+}$ controls (Figure 2B), demonstrating that global reduction of CASK in all cells results in ONH.

Next, we evaluated RGC numbers in *Cask*$^{fl/fl}$, *Cask*$^{fl/+}$, and controls using a marker for RGCs (RBPMS)(Rodriguez, Muller et al. 2014) and a Nissl Stain. We saw a dose-dependent decrease in RGCs in the presence of the floxed allele of CASK (Figure 2D): one floxed allele (*Cask*$^{fl/+}$) significantly reduced RGC numbers compared to controls (CASK$^{+/+}$), and homozygous floxed alleles (*Cask*$^{fl/fl}$) significantly reduced RGC numbers compared to both heterozygotes (*Cask*$^{fl/+}$) and controls (*Cask*$^{+/+}$) (Figure 2E). This decrease is comparable to what we previously found in *Cask*$^{+/-}$ retinas (*Cask*$^{+/-}$ 27.2 ± 3.1 RBPMS^{+} cells; *Cask*$^{fl/fl}$ 30.6 ± 2.9 RBPMS^{+} cells)(Liang, Kerr et al. 2017). We also evaluated total numbers of cells in the RGC layer using a NeuroTrace stain to verify that RBPMS is not sensitive to CASK deficiency. *Cask*$^{fl/fl}$ mice have a reduction in total numbers of NeuroTrace-positive cells in the RGC layer compared to *Cask*$^{+/+}$ mice (Figure 2F). We saw no difference in the average area of each RGC, based on measurement of RBPMS signal (WT 57.8 ± 8.6 μm^2; CASK 61.4 ± 8.7 μm^2). Finally, we explored potential axonopathy in *Cask*$^{fl/fl}$ mice. RGC axon number and diameter were evaluated using TEM of ON cross sections from *Cask*$^{fl/fl}$ and control mice (Figure 2G). No reduction in the density of axons in *Cask*$^{fl/fl}$ samples was observed compared to CASK$^{+/+}$ ONs (Figure 2H), but we did observe a significant decrease in the average cross-sectional area of axons in *Cask*$^{fl/fl}$ ON (WT 1.54 ± 0.70 μm^2, CASK 1.20 ± 0.52 μm^2, $p < 0.05$). RGC axons in the ON can be classified as fine or coarse, based on diameter[36,37]. Previous analysis

in *Cask*$^{+/-}$ mice revealed a loss of both fine and coarse RGC axons[7]. When plotting RGC axon diameter, we could identify an inflection point between axon types in *Cask*$^{fl/fl}$ and controls (Fig 2I; 2.208 μm^2 in controls). By separating the fine and coarse axons and averaging axon size for each type, we observed that both fine (Figure 2J) and coarse axons (Figure 2K) were significantly reduced in *Cask*$^{fl/fl}$ ON. Myelination patterns were evaluated in TEM images, and *Cask*$^{fl/fl}$ ON myelination appeared normal in adulthood. However, analysis of the ON at P12 showed a difference in total myelinated axon numbers compared to *Cask*$^{+/+}$ (Supplemental Fig. 1). This difference was no longer apparent by P18, suggesting that global reduction in CASK delays the onset of myelination. Overall, our data suggest RGCs are extremely sensitive to level of CASK expression.

CASK is expressed in Retinal Ganglion Cells

To analyze the role of CASK in RGC development, we first asked if RGCs express detectable levels of CASK using *in situ* hybridization (Figure 3A). Riboprobes against *Cask* mRNA were developed and revealed widespread expression in all three nuclear layers (Figure 3B); no appreciable reactivity in these regions (versus synaptic regions) was observed with a sense riboprobe (Figure 3C). Importantly, we observed significant reactivity of the CASK antisense riboprobe in the ganglion cell layer (GCL), suggesting CASK is generated by RGCs. Results were validated by showing CASK immunoreactivity in the GCL using IHC (Figure 3D).

RGC-derived CASK is not required for RGC survival

Due to the above-described sensitivity of RGCs to CASK levels, we next wanted to evaluate whether RGCs were dependent upon CASK expression for survival. To remove CASK from RGCs, we sought a driver line that generated Cre recombinase in RGCs to excise the floxed *CASK* allele. One option was *Calretinin-Cre* (*Calb2-Cre*). Calretinin is generated by RGCs, as well as some types of horizontal and amacrine cells in the developing and adult retina (Nag 1999, Georgi and Reh, 2010, Bastianelli et al 1995). Importantly Calretinin is not generated by thalamic relay cells. Furthermore, Calretinin (and Cre in *Calb2-Cre* mice) is generated in RGCs at neonatal ages in RGCs (Monavarfeshani and Georgi and Reh, 2010). The percentage of RGCs in which *Calb2-Cre* exhibited recombination activity was quantified by crossing with a reporter line (*Rosa-stop-tDT* Ai9). As expected, widespread expression of tdT was observed in the retinas of *Calb2-Cre::Rosa-stop-tdT* mice (Figure 4A, A'). Cross-section analysis showed that tdT expression is present in cells of the inner nuclear layer and GCL (Figure 4B) (77 $\pm$ 2.5% of DAPI-labeled cells in the GCL were tdT$^+$; n=4 mice). Since misplaced amacrine cells also reside in the GCL and may also express Cre in this driver line (Figure 4C), we used immunostaining for RBPMS to assess the percent of RGCs expressing Cre in this line (Figure 4C'). We found 91.1 $\pm$ 2.4% (n=4 mice) of RBPMS cells were tdT$^+$ in *Calb2-Cre::Rosa-stop-tdT.* Furthermore, 87.6 $\pm$ 5.1% of the tdT$^+$ cells were immunoreactive for RBPMS. It remains possible that ~9% of RGCs that do not generate Cre in Calb2-Cre mice belong to a small number of distinct subtypes of RGCs, such as intrinsically photosensitive RGCs (ipRGCs). This was not expected, based on scRNAseq analysis of murine RGCs, which has shown Calb2 (also known as calretinin) in all subtypes of RGCs

(Rheaume et al., 2018), but to address this possibility, we used IHC to show that ipRGCs and other subtypes of RGCs are labeled in Calb2-Cre mice (Supplemental Figure 2).

To assess the requirement for CASK in RGCs, *Cask*$^{fl/fl}$::*Calb2-Cre*$^{+/+}$ mice were generated. These mutants have a global reduction in CASK expression (as described above), as well as a complete loss of CASK in ~91% of RGCs. We compared the ON of *Cask*$^{fl/fl}$::*Calb2-Cre*$^{+/+}$ mice with *Cask*$^{fl/fl}$ mice using toluidine blue staining as described earlier (Figure 5A). Surprisingly, there was no further reduction in the size of ON when CASK was abolished from most RGCs (Figure 5B). Furthermore, when RGC's were labeled with RBPMS and NeuroTrace (Figure 5C), no significant loss of RGCs or overall cells in the GCL layer in the *Cask*$^{fl/fl}$::*Calb2-Cre*$^{+/+}$ mice was observed as compared to *Cask*$^{fl/fl}$, suggesting that lack of CASK expression in remaining RGCs does not affect their survival (Figure 5D,E). Finally, axonal morphology in the ON of these mutants (Figure 5F) was assessed; there were no differences in axonal density of *Cask*$^{fl/fl}$::*Calb2-Cre*$^{+/+}$ or *Cask*$^{fl/fl}$ mice (Figure 5G). Overall our data indicate that CASK expression in RGCs is not a requisite for RGC development or survival.

<u>Partial loss of function mutation of CASK in a 3-year-old boy with ONH</u>

CASK loss in males is neurodevastating and can be associated with ONH(Moog, Bierhals et al. 2015) and epileptic encephalopathies(Burglen, Chantot-Bastaraud et al. 2012, Saitsu, Kato et al. 2012). Missense mutations that decrease CASK function, however, are frequently present in males with X-linked intellectual disability who survive well into adulthood. These cases typically have been reported to display nystagmus, strabismus and even reduced visual acuity. An analysis of the optic nerve in these cases, however,

has not been described. Here we report a 3-year-old boy with a milder condition exhibiting microcephaly and severe pontocerebellar hypoplasia (MICPCH) similar to haploinsufficient females (Figure 6A) and ON thinning (Figure 6B). This subject presented with decreased visual acuity (20/130; Teller acuity test) and horizontal nystagmus (with a pendular jerk of small amplitude and frequency) that did not dampen with convergence, indicating that it may be central in origin. These phenotypes (thin ON, non-retinal defects) led to the diagnosis of ONH. Exome sequencing uncovered a *CASK* variant c.2018C>T (p.Pro673Leu) that was absent from the parents and had not been identified or reported in any other database.

We expressed recombinant CASK containing the P673L variation ($CASK^{P673L}$) fused with GFP protein for biochemical analysis. Wild-type CASK ($CASK^{WT}$) expressed in HEK293 cells diffusely fills the cytosol (Figure 6C), whereas expression of $CASK^{P673L}$ results in an aggregation of protein (Figure 6D), indicating that this protein may be partially misfolded or prone to aggregation compared to wild-type. $CASK^{P673L}$ also exhibits higher insolubility, supporting the notion that this protein variant may have a propensity to misfold (Figure 6E).

We employed molecular dynamics (MD) simulations to simulate the impact of the P673L mutation on the structure of CASK. Three 100 ns MD simulation trajectories were run using a model of the CASK wild-type and $CASK^{P673L}$ PDZ-SH3-GK (PSG) supradomain(LaConte, Chavan et al. 2018). The radius of gyration of a protein structure model can be used to evaluate how compactly a protein structure is folded. In our simulations, $CASK^{P673L}$'s average radius of gyration (2.51 nm) over the course of the three

trajectories is slightly, significantly larger than CASK^{WT} (2.48 nm) and the mutated structure explores a larger range of radii throughout the simulations (Supplemental Figure 1), suggesting that the P673L mutation prevents the domain from folding as compactly and stably as it does in the wild-type structure. The P673L mutation also changes the overall fold of the PDZ domain more significantly (Figure 6F) than other previously examined mutations in this domain (RMSD difference between CASK^{P673L} and wildtype is 3.1nm; CASK^{M519T} RMSD difference is 2.49 nm; CASK^{G659D} RMSD difference is 2.11 nm), an important observation given CASK's known interactions with proteins containing PDZ-binding domains(Hata, Butz et al. 1996, Fairless, Masius et al. 2008, Mukherjee, Sharma et al. 2008). A comparison of secondary structure propensity and mobility at each residue (b-factors) throughout the MD simulations helps further specify the impact of a given mutation; in the case of CASK^{P673L}, of particular interest is the notable absence in helical propensity and mobility of the α-C helix of the CASK^{P673L} PDZ domain(Zeng, Ye et al. 2018); this particular alpha helix is purported to be involved in coupling the PDZ and SH3 domains to allow for ligand binding. The P673L variation in CASK's SH3 domain disrupts packing between all three of the domains, causing a reorientation of the domains with respect to each other (Fig. 6F). This disruption in packing may indicate that CASK^{P673L} is more likely to adopt a conformation that oligomerizes. In sum, these structural differences point to a CASK^{P673L} structure which is slightly less compact than its wild-type counterpart and has alterations in the region predicted to interact with known binding partners such as neurexin(Cohen, Woods et al. 1998, Biederer and Sudhof 2001,

Biederer, Sara et al. 2002, Mukherjee, Sharma et al. 2008, Pak, Danko et al. 2015, LaConte, Chavan et al. 2016).

Based on the structural changes predicted by MD in CASK^{P673L}, we next tested these in silico predictions by determining whether the mutation indeed impairs CASK-neurexin binding in vitro by using a previously described recruitment assay where distribution of GFP-CASK can be altered from cytoplasmic to membrane-bound upon co-expression of neurexin-1β (Figure 6C, 6G). For this recruitment assay, analysis was done only on cells where GFP-CASK^{P673L} was not aggregating. Upon co-expressing neurexin-1β, CASK^{P673L} and neurexin-1β did not co-localize on the membrane (Figure 6H), revealing that neurexin is unable to efficiently recruit the remaining soluble fraction of CASK^{P673L} from the cytosol. In order to quantitatively measure the change in CASK^{P673L} affinity towards neurexin, we performed GST pulldown assays using the cytosolic tail of neurexin-1 fused to the GST protein, which revealed that the affinity of CASK^{P673L} for neurexins is reduced by ~80% compared to CASK^{WT} (Figure 6I, J).

Overall, these results suggest that the P673L sequence variation affects the structure of CASK sufficiently to increase misfolding and impair but not abolish its interaction with neurexins. Such a reduction in functional CASK is sufficient to produce ONH manifestation, indicating RGCs may be highly sensitive to CASK functional deficiency. Furthermore, our data point to the strong possibility that other boys with CASK missense mutations may also have ONH.

Discussion

Although the prevalence of ONH is on the rise, the mechanism that underlies its onset and progression remains unknown. ONH is likely a heterogeneous disorder with differing etiologies that share similar downstream pathogenesis. Many cases of ONH arise much later in perinatal and postnatal development and are associated with environmental factors(Hoyt and Billson 1986, Lambert, Hoyt et al. 1987). The mechanism of this later-onset ONH is not clear. Mouse models which target genes involved in RGC development often lead to complete non-development of eyes (anophthalmy) (Taranova, Magness et al. 2006) or of the ON itself(Brown, Patel et al. 2001) and thus do not recapitulate ONH. Heterozygous deletion of CASK produces ONH and microcephaly in girls and female mice(Moog, Kutsche et al. 2011, Burglen, Chantot-Bastaraud et al. 2012, Srivastava, McMillan et al. 2016, Liang, Kerr et al. 2017). We have shown that microcephaly linked to CASK mutation may stem from loss of PDZ domain-mediated interactions with proteins like neurexin(LaConte, Chavan et al. 2018). Analysis of a CASK variant ($CASK^{P673L}$) in a male subject with microcephaly and ONH suggests that both microcephaly and ONH are likely to result from disruption of PDZ domain-mediated interactions of CASK. $CASK^{P673L}$'s interaction with neurexin, however, is not entirely abolished but merely reduced, indicating that this mutation causes partial loss of function in CASK. Such global CASK partial loss-of-function is compatible with survival but sufficient to produce ONH. Intriguingly, CASK mutations have also been associated with retinopathies(Burglen, Chantot-Bastaraud et al. 2012, LaConte, Chavan et al. 2019). These observations pose an interesting question: do CASK mutations produce isolated ONH or are the ON

pathologies reflective of a broader retinal disorder? Answering this question is not only critical for more accurately classifying the ocular phenotypes seen with CASK mutations but is also crucial for validating CASK mutant mice as tools to investigate mechanisms underlying ONH.

Cask$^{+/-}$ mice display a postnatal decrease in the number of RGCs, thinning of the ON, and atrophy of RGC axons(Liang, Kerr et al. 2017). Despite deficits in RGCs, no defects are observed in other cells or in lamination of the *Cask*$^{+/-}$ retina(Liang, Kerr et al. 2017). *Cask*$^{+/-}$ mice also exhibit significantly decreased contrast sensitivity. Based on retinal morphology and ERG data, we suggest that this visual deficit is due to RGC pathology and not due to defects in retinal circuitry. CASK haploinsufficiency thus specifically affects RGCs to produce ONH. Furthermore, we demonstrate that global reduction of CASK expression by ~60% is also sufficient to induce ONH, indicating that RGCs are extremely sensitive to CASK loss. Why are RGCs disproportionately affected by CASK loss? The anatomy and physiology of RGCs are unique; they are the predominant action potential-generating neurons within the retina and have extremely long, myelinated axons, unlike other retinal cells. In other brain regions, *Cask* loss or mutation appears to disproportionately affect projection neurons, such as those in pontocerebellar circuits(Burglen, Chantot-Bastaraud et al. 2012).

Since the CASK hypomorph line is based on a floxed CASK allele, we also used this line to delete all CASK expression from RGCs. Surprisingly, total loss of CASK from RGCs did not exacerbate the ONH phenotype, indicating RGC-derived CASK is not critical for RGC survival. How then does CASK reduction produce ONH? There are at least three

possible explanations. First, although the discernible pathology of ONH appears late in the course of development, it is possible that the biological insult required for ONH occurs earlier in development before the Cre-mediated deletion of CASK gene. This, however, does not explain why RGCs are more susceptible. Secondly, similar to the experimental models of glaucoma, it is possible that certain RGC subtypes(Puyang, Chen et al. 2015, Daniel, Meyer et al. 2019) are highly susceptible to CASK deficiency and are already lost in the CASK hypomorph line, hence no further decrease would be observed upon targeted deletion of CASK in the remaining RGCs. This would, however, suggest that the mosaic *Cask*$^{+/-}$ mutant should have a milder phenotype than the global *Cask*$^{fl/fl}$ mutant, which is not the case. A third, more plausible explanation may be that the effect seen on RGCs is non-cell-autonomous in origin. A strong argument for this possibility is that in *Cask*$^{+/-}$ mice, we do not observe secondary selection (apoptosis) of neurons resulting from random X-linked inactivation, suggesting that neurons lacking CASK do not exhibit reduced survival(Srivastava, McMillan et al. 2016, Liang, Kerr et al. 2017). Further experiments are required in the future to fully investigate these three alternative mechanisms.

Importantly, CASK is present not only in neurons but also in glial and endothelial cells(Weigand, Boeckel et al. 2012, Horng, Therattil et al. 2017). Aberrant functioning of these cell populations is likely to affect survival and health of RGCs by producing changes in retinal metabolism and vascularization. ONH has been associated with mitochondrial cytopathies(Taban, Cohen et al. 2006, Edvardson, Porcelli et al. 2013), peroxisomal disorders(Pfeifer and Martinot 2017), and nutritional deprivation(Garcia-Filion and

Borchert 2013, Khaper, Bunge et al. 2017), all of which point toward a possible metabolic derangement. Similarly, altered vasculature, such as vascular tortuosity, has been suggested to be one of the hallmarks of ONH(Lambert, Hoyt et al. 1987, Kaur, Jain et al. 2013, Cheng, Yen et al. 2015). Overall our data suggest that an in-depth study of CASK mutant mice may uncover a common underlying pathobiogenesis of ONH.

Acknowledgments

The authors thank the participation and cooperation of families and children with *CASK* mutation in our studies. We thank Vrushali Chavan for technical help. Ching-Kang Chen is the Alice McPherson Retina Research Foundation Endowed Chair at Baylor College of Medicine and is supported by grants from the National Institute of Health (EY026930 and EY002520). Work in the Fox and Mukherjee laboratories is supported by the National Institutes of Health (EY024712 [KM], AI124677 [MAF] and EY021222 [MAF]).

References

1. Khaper T, Bunge M, Clark I et al. (2017). Increasing incidence of optic nerve hypoplasia/septo-optic dysplasia spectrum: Geographic clustering in Northern Canada. *Paediatr Child Health*;22:445-453.

2. Kong L, Fry M, Al-Samarraie M, Gilbert C, Steinkuller PG. (2012). An update on progress and the changing epidemiology of causes of childhood blindness worldwide. *J AAPOS*;16:501-507.

3. Katagiri S, Nishina S, Yokoi T et al. (2017). Retinal Structure and Function in Eyes with Optic Nerve Hypoplasia. *Sci Rep*;7:42480.

4. Chen CA, Yin J, Lewis RA, Schaaf CP. (2017) Genetic causes of optic nerve hypoplasia. *J Med Genet*;54:441-449.

5. Frisén L, Holmegaard L. (1978) Spectrum of optic nerve hypoplasia. *Brit J Ophthalmol*;62:7-15.

6. Hoyt CS, Good WV. (1992). Do we really understand the difference between optic nerve hypoplasia and atrophy? *Eye (Lond)*;6 (Pt 2):201-204.

7. Liang C, Kerr A, Qiu Y et al. (2017). Optic Nerve Hypoplasia Is a Pervasive Subcortical Pathology of Visual System in Neonates. *Invest Ophthalmol Vis Sci*;58:5485-5496.

8. Butz S, Okamoto M, Sudhof TC. (1998). A tripartite protein complex with the potential to couple synaptic vesicle exocytosis to cell adhesion in brain. *Cell*;94:773-782.

9. Burglen L, Chantot-Bastaraud S, Garel C et al. (2012). Spectrum of pontocerebellar hypoplasia in 13 girls and boys with CASK mutations: confirmation of a

recognizable phenotype and first description of a male mosaic patient. *Orphanet J Rare Dis*;7:18.

10. LaConte LEW, Chavan V, DeLuca S et al. (2019). An N-terminal heterozygous missense CASK mutation is associated with microcephaly and bilateral retinal dystrophy plus optic nerve atrophy. *American Journal of Medical Genetics Part A*;179:94-103.

11. Moog U, Uyanik G, Kutsche K. (1993). CASK-Related Disorders. In: Adam MP, Ardinger HH, Pagon RA et al. (eds), *GeneReviews((R))*. Seattle (WA).

12. Monavarfeshani A, Stanton G, Van Name J et al. (2018). LRRTM1 underlies synaptic convergence in visual thalamus. *Elife*;7.

13. LaConte LE, Chavan V, Mukherjee K. (2014). Identification and glycerol-induced correction of misfolding mutations in the X-linked mental retardation gene CASK. *PLoS One*;9:e88276.

14. LaConte LEW, Chavan V, Elias AF et al. (2018). Two microcephaly-associated novel missense mutations in CASK specifically disrupt the CASK-neurexin interaction. *Hum Genet*;137:231-246.

15. Su JM, Chen J, Lippold K et al. (2016). Collagen-derived matricryptins promote inhibitory nerve terminal formation in the developing neocortex. *Journal of Cell Biology*;212:721-736.

16. Su JM, Gorse K, Ramirez F, Fox MA. (2010). Collagen XIX Is Expressed by Interneurons and Contributes to the Formation of Hippocampal Synapses. *Journal of Comparative Neurology*;518:229-253.

17. Srivastava S, McMillan R, Willis J et al. (2016). X-linked intellectual disability gene CASK regulates postnatal brain growth in a non-cell autonomous manner. *Acta Neuropathol Com*;4.

18. Huberman AD, Niell CM. What can mice tell us about how vision works? (2011). *Trends in Neurosciences*;34:464-473.

19. Prusky GT, West PWR, Douglas RM. (2000). Behavioral assessment of visual acuity in mice and rats. *Vision Res*;40:2201-2209.

20. Li S, Chen D, Sauve Y, McCandless J, Chen YJ, Chen CK. (2005). Rhodopsin-iCre transgenic mouse line for Cre-mediated rod-specific gene targeting. *Genesis*;41:73-80.

21. Brown KT. (1968). Electroretinogram - Its Components and Their Origins. *Vision Res*;8:633-+.

22. Gurevich L, Slaughter MM. (1993). Comparison of the waveforms of the ON bipolar neuron and the b-wave of the electroretinogram. *Vision Res*;33:2431-2435.

23. Stockton RA, Slaughter MM. (1989). B-Wave of the Electroretinogram - a Reflection of on Bipolar Cell-Activity. *J Gen Physiol*;93:101-122.

24. Tracy CM, Kolesnikov AV, Blake DR et al. (2015). Retinal Cone Photoreceptors Require Phosducin-Like Protein 1 for G Protein Complex Assembly and Signaling. *Plos One*;10.

25. Atasoy D, Schoch S, Ho A et al. (2007). Deletion of CASK in mice is lethal and impairs synaptic function. *Proc Natl Acad Sci U S A*;104:2525-2530.

26. Najm J, Horn D, Wimplinger I et al. (2008). Mutations of CASK cause an X-linked brain malformation phenotype with microcephaly and hypoplasia of the brainstem and cerebellum. *Nat Genet*;40:1065-1067.

27. Rodriguez AR, Muller LPD, Brecha NC. (2014). The RNA binding protein RBPMS is a selective marker of ganglion cells in the mammalian retina. *Journal of Comparative Neurology*;522:1411-1443.

28. Moog U, Bierhals T, Brand K et al. (2015). Phenotypic and molecular insights into CASK-related disorders in males. *Orphanet Journal of Rare Diseases*;10.

29. Saitsu H, Kato M, Osaka H et al. (2012). CASK aberrations in male patients with Ohtahara syndrome and cerebellar hypoplasia. *Epilepsia*;53:1441-1449.

30. Fairless R, Masius H, Rohlmann A et al. (2008). Polarized Targeting of Neurexins to Synapses Is Regulated by their C-Terminal Sequences. *Journal of Neuroscience*;28:12969-12981.

31. Hata Y, Butz S, Sudhof TC. (1996). CASK: a novel dlg/PSD95 homolog with an N-terminal calmodulin-dependent protein kinase domain identified by interaction with neurexins. *J Neurosci*;16:2488-2494.

32. Mukherjee K, Sharma M, Urlaub H et al. (2008). CASK Functions as a Mg2+-independent neurexin kinase. *Cell*;133:328-339.

33. Zeng ML, Ye F, Xu J, Zhang MJ. (2018). PDZ Ligand Binding-Induced Conformational Coupling of the PDZ-SH3-GK Tandems in PSD-95 Family MAGUKs. *J Mol Biol*;430:69-86.

34. Biederer T, Sudhof TC. (2001). CASK and protein 4.1 support F-actin nucleation on neurexins. *J Biol Chem*;276:47869-47876.

35. LaConte LEW, Chavan V, Liang C et al. (2016). CASK stabilizes neurexin and links it to liprin-alpha in a neuronal activity-dependent manner. *Cell Mol Life Sci*;73:3599-3621.

36. Pak C, Danko T, Zhang YS et al. (2015). Human Neuropsychiatric Disease Modeling using Conditional Deletion Reveals Synaptic Transmission Defects Caused by Heterozygous Mutations in NRXN1. *Cell Stem Cell*;17:316-328.

37. Biederer T, Sara Y, Mozhayeva M et al. (2002). SynCAM, a synaptic adhesion molecule that drives synapse assembly. *Science*;297:1525-1531.

38. Cohen AR, Woods DF, Marfatia SM, Walther Z, Chishti AH, Anderson JM. (1998). Human CASK/LIN-2 binds syndecan-2 and protein 4.1 and localizes to the basolateral membrane of epithelial cells. *J Cell Biol*;142:129-138.

39. Hoyt CS, Billson FA. (1986). Optic-Nerve Hypoplasia - Changing Perspectives. *Aust Nz J Ophthalmol*;14:325-331.

40. Lambert SR, Hoyt CS, Narahara MH. (1987). Optic-Nerve Hypoplasia. *Surv Ophthalmol*;32:1-9.

41. Taranova OV, Magness ST, Fagan BM et al. (2006). SOX2 is a dose-dependent regulator of retinal neural progenitor competence. *Genes Dev*;20:1187-1202.

42. Brown NL, Patel S, Brzezinski J, Glaser T. (2001). Math5 is required for retinal ganglion cell and optic nerve formation. *Development*;128:2497-2508.

43. Moog U, Kutsche K, Kortum F et al. (2011). Phenotypic spectrum associated with CASK loss-of-function mutations. *J Med Genet*;48:741-751.

44. Daniel S, Meyer KJ, Clark AF, Anderson MG, McDowell CM. (2019). Effect of ocular hypertension on the pattern of retinal ganglion cell subtype loss in a mouse model of early-onset glaucoma. *Exp Eye Res*;107703.

45. Puyang Z, Chen H, Liu X. (2015). Subtype-dependent Morphological and Functional Degeneration of Retinal Ganglion Cells in Mouse Models of Experimental Glaucoma. *J Nat Sci*;1:e103.

46. Horng S, Therattil A, Moyon S et al. (2017). Astrocytic tight junctions control inflammatory CNS lesion pathogenesis. *J Clin Invest*;127:3136-3151.

47. Weigand JE, Boeckel JN, Gellert P, Dimmeler S. (2012). Hypoxia-Induced Alternative Splicing in Endothelial Cells. *Plos One*;7.

48. Edvardson S, Porcelli V, Jalas C et al. (2013). Agenesis of corpus callosum and optic nerve hypoplasia due to mutations in SLC25A1 encoding the mitochondrial citrate transporter. *Journal of Medical Genetics*;50:240-245.

49. Taban M, Cohen BH, David Rothner A, Traboulsi EI. (2006). Association of optic nerve hypoplasia with mitochondrial cytopathies. *J Child Neurol*;21:956-960.

50. Pfeifer CM, Martinot CA. (2017). Zellweger syndrome: Depiction of MRI findings in early infancy at 3.0 Tesla. *Neuroradiol J*;30:442-444.

51. Garcia-Filion P, Borchert M. (2013). Prenatal determinants of optic nerve hypoplasia: review of suggested correlates and future focus. *Surv Ophthalmol*;58:610-619.

52. Cheng HC, Yen MY, Wang AG. (2015). Neuroimaging and clinical features of patients with optic nerve hypoplasia in Taiwan. *Taiwan J Ophthalmol*;5:15-18.

53. Kaur S, Jain S, Sodhi HB, Rastogi A, Kamlesh. (2013). Optic nerve hypoplasia. *Oman J Ophthalmol*;6:77-82.

Figure 1.

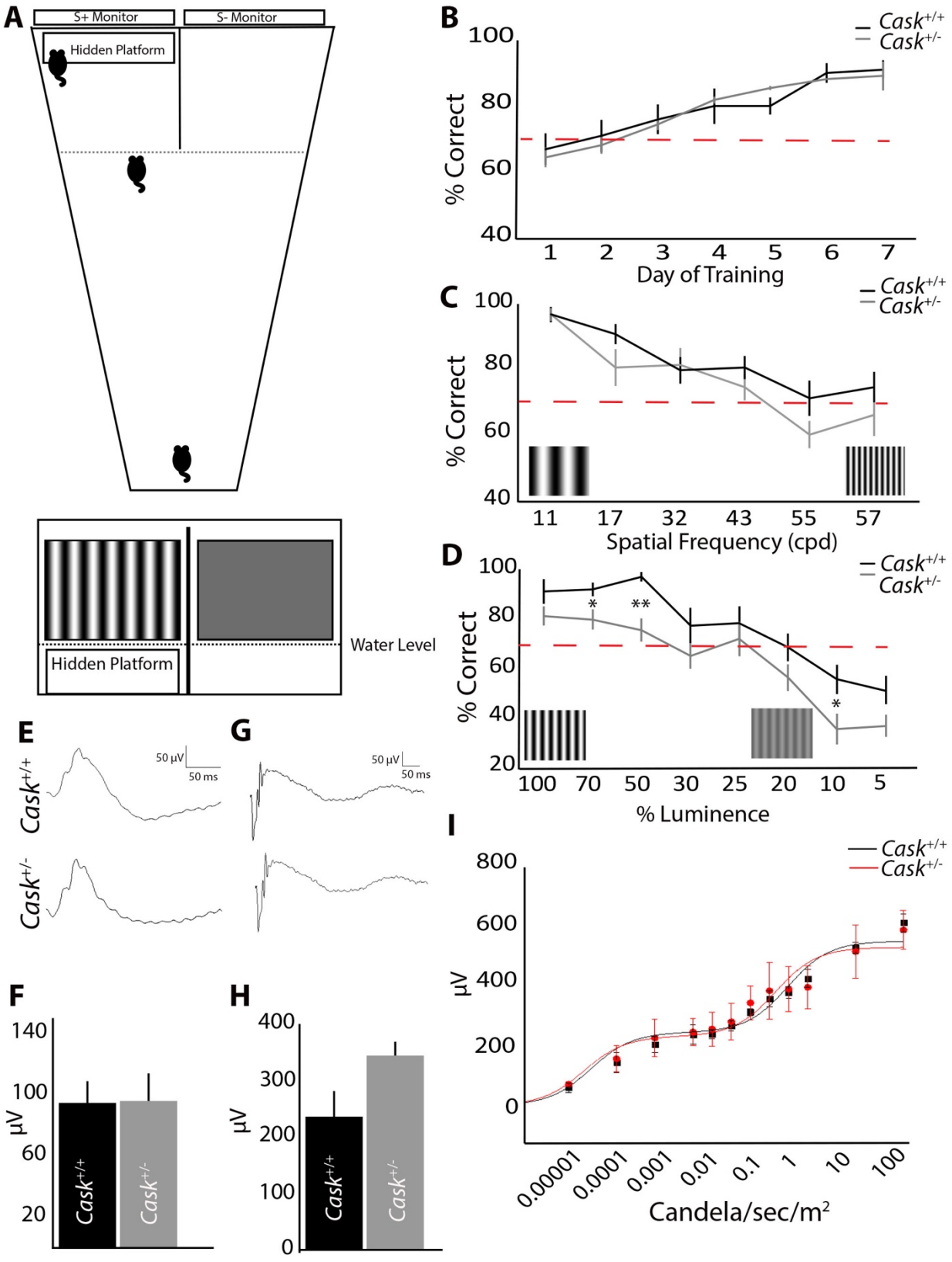
A
S+ Monitor
S- Monitor
Hidden Platform
Water Level
Hidden Platform
B
Cask+/+
Cask+/-
% Correct
Day of Training
C
Spatial Frequency (cpd)
D
% Luminence
E
G
50 µV
50 ms
F
H
µV
I
Candela/sec/m2

Figure 1. Heterozygous loss of CASK produces behavioral but not electrophysiological deficits in vision. (A) Schematic of two-alternative forced-swim test with a choice between a sine-positive grating (S+) and a sine-negative grating (S-). (B) *Cask*$^{+/-}$ and wild-type littermates learn the task at a similar rate. (C) Increasing the spatial frequency of sine-grating leads to similar decrease in *Cask*$^{+/-}$ and control mice performance. (D) *Cask*$^{+/-}$ mice perform significantly worse than controls when contrast (%luminence) is decreased. (E-H) Electroretinography in both photopic (E) and scotopic conditions (G). n=3 mice per genotype. There were no statistical differences in photopic b-wave amplitudes (F) or scotopic a-wave amplitudes (H). A Naka-Rushton fit of scotopic b-wave amplitudes vs. retinal illuminance for maximum rod- and cone-driven responses reveal comparable fits between *Cask*$^{+/+}$ and *Cask*$^{+/-}$ mice (I). For all panels, data is plotted as mean±SEM. * indicates $p<0.05$, ** indicates $P<0.01$ by two-way ANOVA.

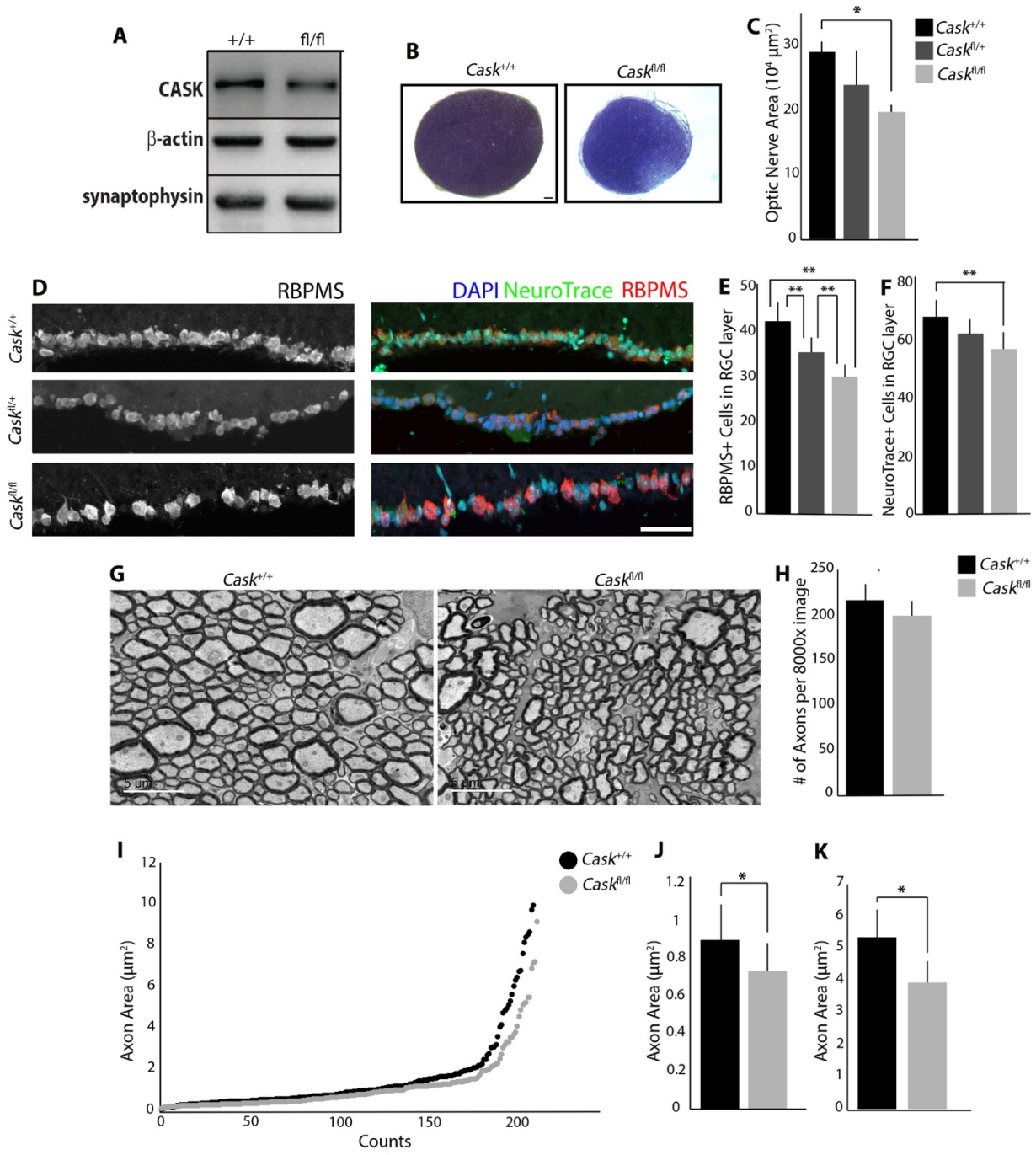

Figure 2: Global reduction in CASK expression produces ONH. (A) Immunoblot shows reduced levels of CASK in *Cask*$^{fl/fl}$ ON compared to wild-type controls. (n=3 mice per genotype). (B) Toluidine blue staining shows reduced ON size in *Cask*$^{fl/fl}$ mice compared to wild-type controls. Scale bar = 50μm. (C) Quantification of reduced cross-sectional

area in *Cask*$^{fl/fl}$ compared with *Cask*$^{fl/+}$ and *Cask*$^{+/+}$ (n=4 mice per genotype). (D) Reduction in number of cells in GCL layer using RBPMS (RNA-Binding Protein with Multiple Splicing) and NeuroTrace. Scale bar = 50 μm. (E) Quantification of reduced number of RBPMS+ cells in GCL of *Cask*$^{fl/fl}$ compared with *Cask*$^{fl/+}$ and *Cask*$^{+/+}$, and *Cask*$^{fl/+}$ compared to *Cask*$^{+/+}$ (n=10 mice per genotype). (F) Quantification of reduced number of NeuroTrace+ cells in GCL of *Cask*$^{fl/fl}$ compared with *Cask*$^{+/+}$ (n=6 mice per genotype). (G) TEM of RGC axons in the ON of *Cask*$^{fl/+}$ and wild-type controls. Scale bar = 5 μm. (H) Quantification of density of axons per image in *Cask*$^{fl/fl}$ mice (n=4 mice per genotype). (I-K) Analysis of axon area in *Cask*$^{fl/fl}$ ON and wild-type controls. Quantification of the average size of fine axons (J) and course axons (K). For all panels, data is plotted as mean±SEM; *indicates $p<0.05$, **indicates $p<0.01$ by two-way ANOVA.

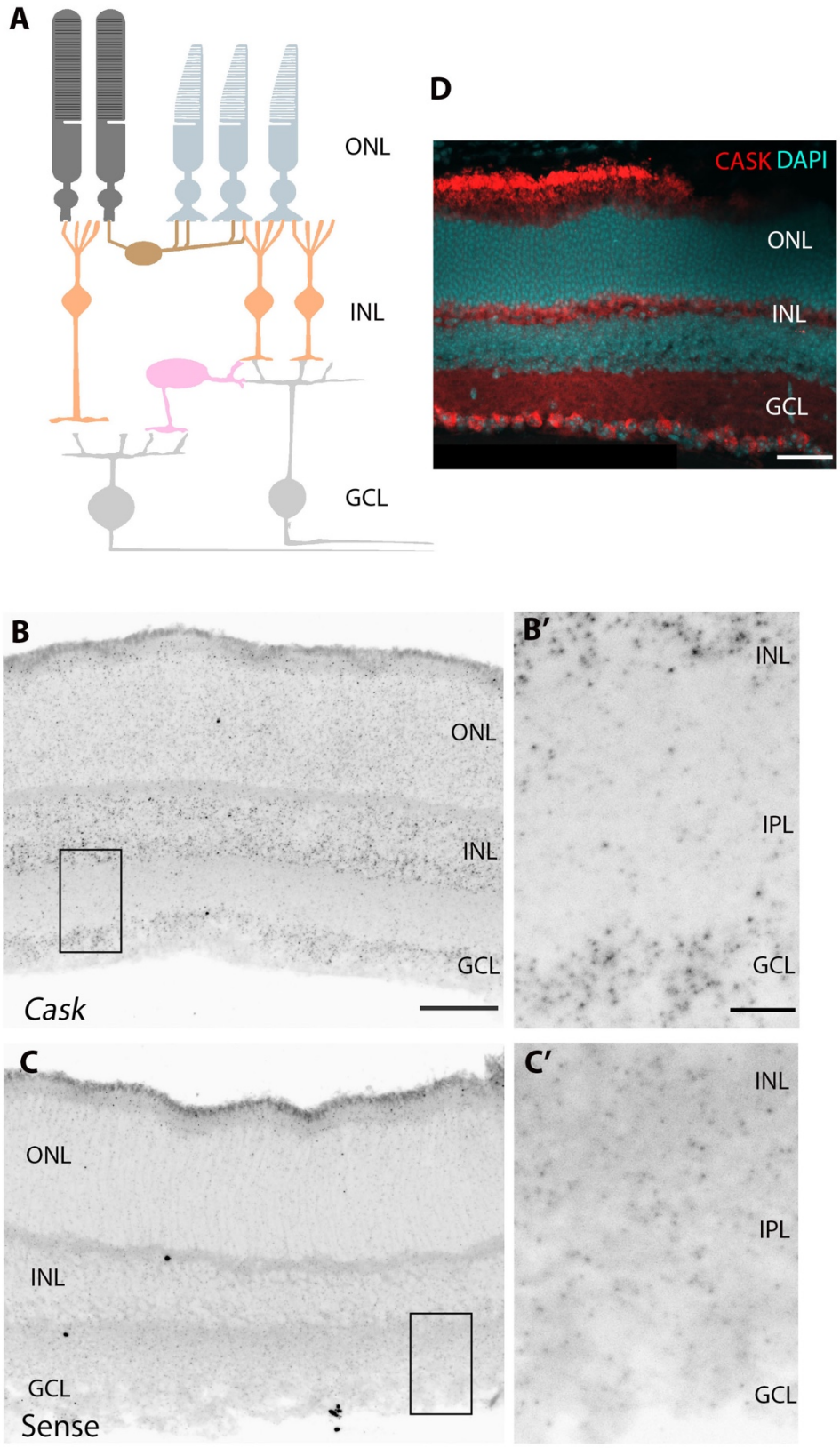
A
ONL
INL
GCL
D
CASK DAPI
ONL
INL
GCL
B
ONL
INL
GCL
Cask
B′
INL
IPL
GCL
C
ONL
INL
GCL
Sense
C′
INL
IPL
GCL

Figure 3. CASK is expressed in Retinal Ganglion Cells. (A) Schematic of mouse retina. ONL – outer nuclear layer, INL- inner nuclear layer, GCL- ganglion cell layer. (B) *In situ* hybridization shows *Cask* mRNA is expressed in the INL and GCL of the P14 retina. Scale bar = 50μm. B' shows higher magnification of expression in GCL. Scale bar = 10μm. (C) No appreciable signal was detected in the GCL with the sense riboprobe. C' shows higher magnification of GCL in C. (D) CASK immunoreactivity in the GCL of P21 retina. Scale bar = 50μm.

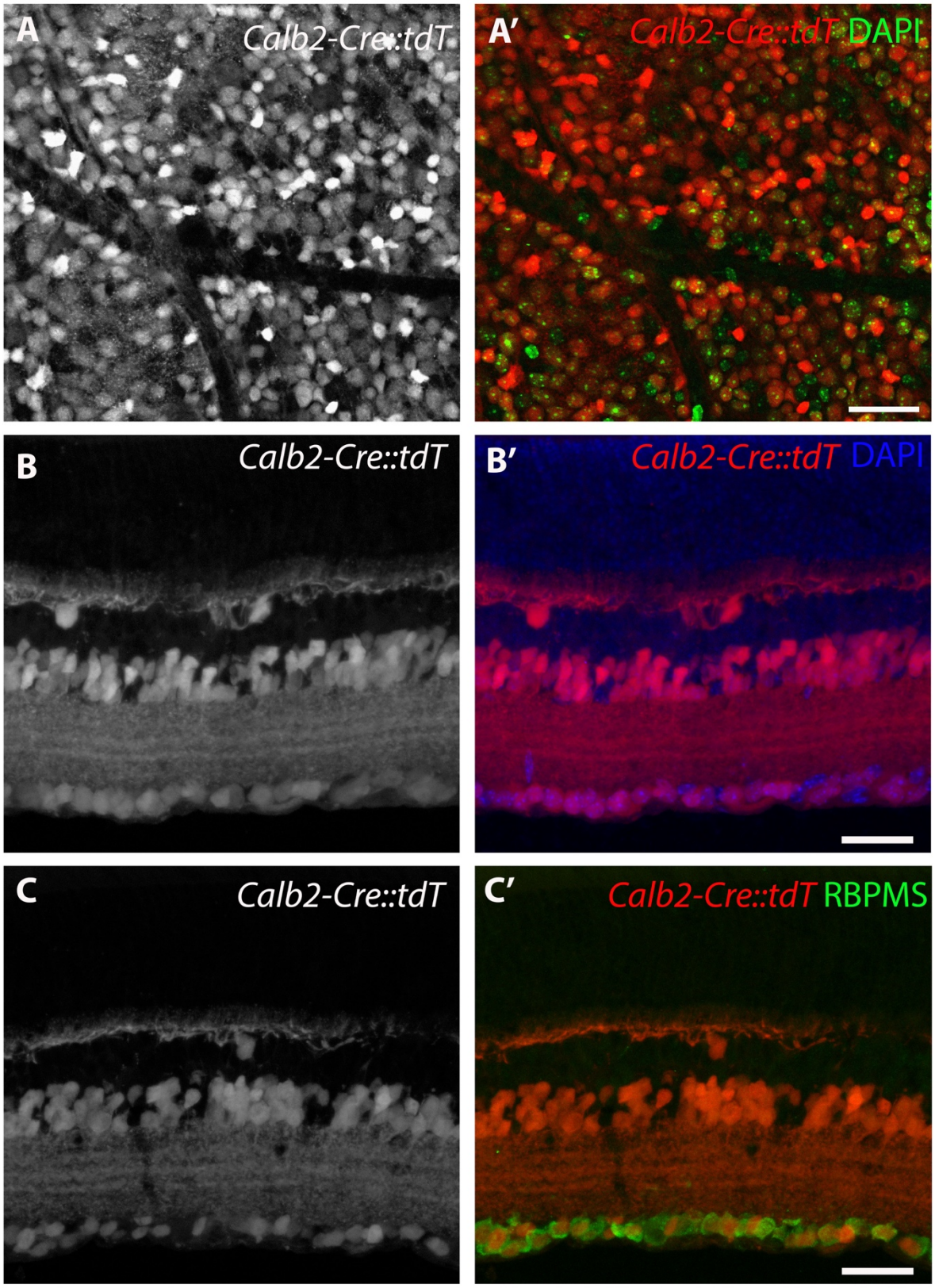
A
Calb2-Cre::tdT
A'
Calb2-Cre::tdT DAPI
B
Calb2-Cre::tdT
B'
Calb2-Cre::tdT DAPI
C
Calb2-Cre::tdT
C'
Calb2-Cre::tdT RBPMS

Figure 4: Calb2-Cre labels Retinal Ganglion Cells. (A) Retinal whole mount of the GCL of *Calb2-Cre::Rosa-stop-tdT* (*Calb2-Cre::tdT*). Note the large number of cells labeled with tdT. (B) Retinal cross section of *Calb2-Cre::tdT* shows tdT^+ cells in the INL and GCL. (C) tdT^+ cells in the GCL of *Calb2-Cre::tdT* co-label with RBPMS. For all panels, scale bar = 50μm.

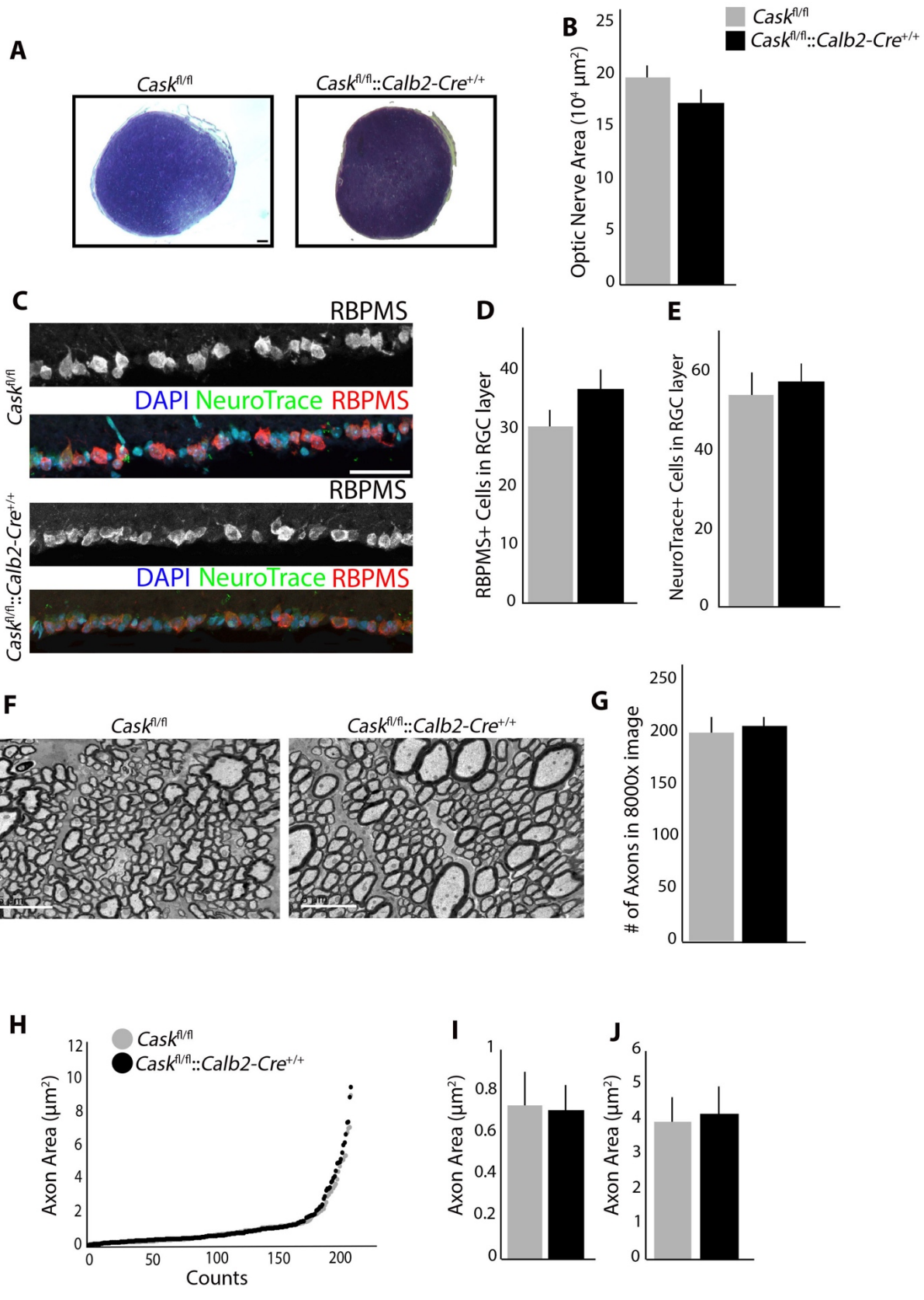
A
Cask^fl/fl
Cask^fl/fl::Calb2-Cre^+/+
B
Cask^fl/fl
Cask^fl/fl::Calb2-Cre^+/+
Optic Nerve Area (10^4 µm^2)
25
20
15
10
5
0
C
RBPMS
Cask^fl/fl
DAPI NeuroTrace RBPMS
RBPMS
Cask^fl/fl::Calb2-Cre^+/+
DAPI NeuroTrace RBPMS
D
RBPMS+ Cells in RGC layer
40
30
20
10
0
E
NeuroTrace+ Cells in RGC layer
60
40
20
0
F
Cask^fl/fl
Cask^fl/fl::Calb2-Cre^+/+
G
# of Axons in 8000x image
250
200
150
100
50
0
H
Cask^fl/fl
Cask^fl/fl::Calb2-Cre^+/+
Axon Area (µm^2)
12
10
8
6
4
2
0
0
50
100
150
200
Counts
I
Axon Area (µm^2)
1
0.8
0.6
0.4
0.2
0
J
Axon Area (µm^2)
6
5
4
3
2
1
0

Figure 5: RGC-derived CASK is not required for RGC survival. (A) Toluidine blue staining shows no reduction in ON size in *Cask*$^{fl/fl}$::*Calb2-Cre*$^{+/+}$ compared to *Cask*$^{fl/fl}$. Scale bar = 50μm. (B) Quantification of cross-sectional area in *Cask*$^{fl/fl}$::*Calb2-Cre*$^{+/+}$ compared to *Cask*$^{fl/fl}$. (n=4 mice per genotype). (C) No reduction in number of cells in GCL layer using RBPMS (RNA-Binding Protein with Multiple Splicing) or NeuroTrace. Scale bar = 50 μm. (D) Quantification of number of cells in GCL using RBPMS in *Cask*$^{fl/fl}$::*Calb2-Cre*$^{+/+}$ compared to *Cask*$^{fl/fl}$. (n=10 mice per genotype). (E) Quantification of number of cells in GCL using NeuroTrace in *Cask*$^{fl/fl}$::*Calb2-Cre*$^{+/+}$ compared to *Cask*$^{fl/fl}$. (n=6 mice per genotype). (F) TEM of RGC axons in the ON in *Cask*$^{fl/fl}$::*Calb2-Cre*$^{+/+}$ compared to *Cask*$^{fl/fl}$. Scale bar = 5 μm. (G) Quantification of density of axons per image in *Cask*$^{fl/fl}$::*Calb2-Cre*$^{+/+}$ compared to *Cask*$^{fl/fl}$. (n=4 mice per genotype). (H-J). Analysis of axon area in *Cask*$^{fl/fl}$::*Calb2-Cre*$^{+/+}$ ON compared to *Cask*$^{fl/fl}$. Quantification of the average size of fine axons (I) and course axons (J). For all panels data is plotted as mean±SEM.

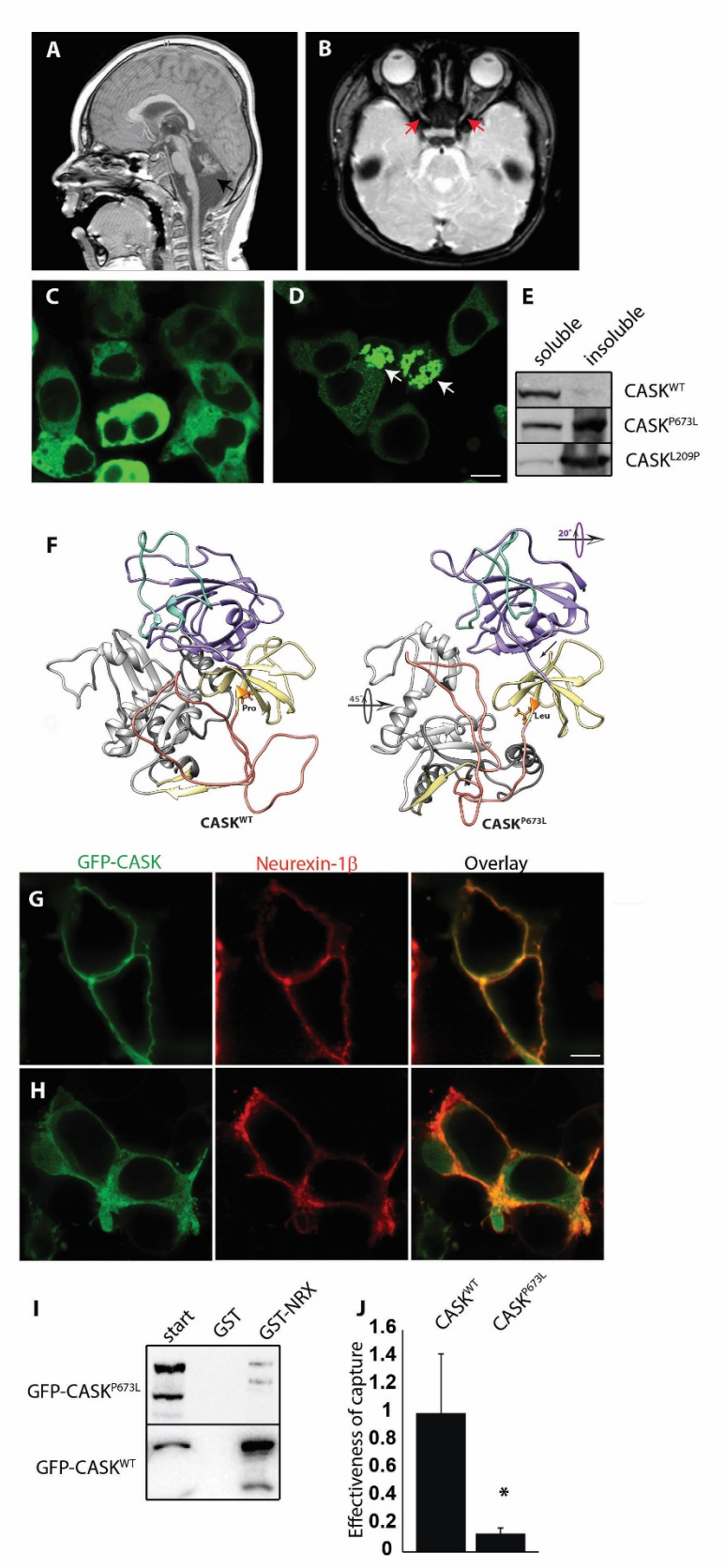
A
B
C
D
E
soluble
insoluble
CASK^WT
CASK^P673L
CASK^L209P
F
Pro
Leu
CASK^WT
CASK^P673L
GFP-CASK
Neurexin-1β
Overlay
G
H
I
start
GST
GST-NRX
GFP-CASK^P673L
GFP-CASK^WT
J
CASK^WT
CASK^P673L
Effectiveness of capture
1.6
1.4
1.2
1
0.8
0.6
0.4
0.2
0
*

Figure 6: Partial loss-of function of CASK in 3-year-old boy produces ONH. (A-B) *CASK* variant in a 3-year-old boy with microcephaly and severe pontocerebellar hypoplasia with *CASK* variant c.2018C>T (p.Pro673Leu) mutation. T2-weighted magnetic brain resonance images show small cerebellum (black arrow) and thinning of optic nerve (red arrow). (C) Expression of WT-CASK-GFP fusion protein in HEK293 cells shows localization of CASK in cytosol. (D) $CASK^{P673L}$-GFP fusion protein shows cotton-wool aggregates (white arrows). (E) Blot for CASK in soluble and soluble fractions of cell lysate show that $CASK^{P673L}$ is predominantly present in the insoluble fraction, similar to $CASK^{L209P}$, previously described to have aggregation tendencies. (F) Structural models of the PDZ-SH3-GK supradomain of $CASK^{WT}$ (left) and $CASK^{P673L}$ (right). Site of P673L variation shown in orange, PDZ domain in purple, □-C helix in green, SH3 domain in yellow, hook/hinge region in salmon, and GK domain in gray. Arrows indicate structural differences between wild-type and variant structures. (G) Recruitment assay using a known CASK substrate, neurexin-1β, shows that $CASK^{WT}$ colocalizes with neurexin. (H) $CASK^{P673L}$ is mislocalized, with some colocalization with neurexin but substantial amounts visible in the cytosol. (I) GST-NRX is able to capture $CASK^{WT}$ but not $CASK^{P673L}$. (J) Effectiveness of capture for $CASK^{WT}$ and $CASK^{P673L}$ is plotted after normalization to wild-type. Data is plotted as mean±SEM; * indicates $P<0.05$ by two-way ANOVA. n=3. Scale bar for all = 5μm.

Preface: Chapter 3.2 details investigations into the molecular function of the CASK protein involving a face- and construct-validated murine model of CASK mutations as well as *in vitro* analysis of CASK binding partners. The work was primarily carried out by myself working in the laboratory of Dr. Konark Mukherjee. It was published in *Experimental Neurology* in 2020.

3.2 Haploinsufficiency of X-Linked intellectual disability gene CASK induces post-transcriptional changes in synaptic and cellular metabolic pathways

Authors: Patel PA[1,2], Liang C[1], Arora A[1], Vijayan S[3], Ahuja S[4], Wagley PK[5], Settlage R[6], LaConte LEW[7], Goodkin HP[5], Lazar I[4], Srivastava S[7], and Mukherjee K[1,7,8].

Running Title: Synaptic and Metabolic CASK Function

Affiliations:

[1]Center for Neurobiology Research, Fralin Biomedical Research Institute at Virginia Tech Carilion, Roanoke, Virginia, United States.

[2]Graduate Program in Translational Biology, Medicine, and Health, Virginia Tech, Blacksburg, Virginia, United States.

[3]School of Neuroscience, Virginia Tech, Blacksburg, Virginia, United States.

[4]Biological Sciences, Virginia Tech, Blacksburg, Virginia, United States.

[5]Neurology, University of Virginia, Charlottesville, Virginia, USA

[6]Advanced Research Computing, Virginia Tech, Blacksburg, Virginia, United States

[7] Fralin Biomedical Research Institute at Virginia Tech Carilion, Roanoke, Virginia, United States.

[8]Department of Psychiatry and Behavioral Medicine, Virginia Tech Carilion School of Medicine, Roanoke, Virginia, United States.

Affiliation of Liang C has changed to Pediatrics-Nutrition, Baylor College of Medicine, Houston, TX since the time this work was completed.

*Correspondence to: konark@vtc.vt.edu

Konark Mukherjee

2 Riverside Circle

Roanoke, VA USA 24016

Abstract

Heterozygous mutations in the X-linked gene *CASK* are associated with intellectual disability, microcephaly, pontocerebellar hypoplasia, optic nerve hypoplasia and partially penetrant seizures in girls. The *Cask*$^{+/-}$ heterozygous knockout female mouse phenocopies the human disorder and exhibits postnatal microencephaly, cerebellar hypoplasia and optic nerve hypoplasia. It is not known if *Cask*$^{+/-}$ mice also display seizures, nor is known the molecular mechanism by which *CASK* haploinsufficiency produces the numerous documented phenotypes. 24-hour video electroencephalography demonstrates that despite sporadic seizure activity, the overall electrographic patterns remain unaltered in *Cask*$^{+/-}$ mice. Additionally, seizure threshold to the commonly used kindling agent, pentylenetetrazol, remains unaltered in *Cask*$^{+/-}$ mice, indicating that even in mice the seizure phenotype is only partially penetrant and may have an indirect mechanism. RNA sequencing experiments on *Cask*$^{+/-}$ mouse brain uncovers a very limited number of changes, with most differences arising in the transcripts of extracellular matrix proteins and the transcripts of a group of nuclear proteins. In contrast to limited changes at the transcript level, quantitative whole-brain proteomics using iTRAQ quantitative mass-spectrometry reveals major changes in synaptic, metabolic/mitochondrial, cytoskeletal, and protein metabolic pathways. Unbiased protein-protein interaction mapping using affinity chromatography demonstrates that CASK may form complexes with proteins belonging to the same functional groups in which altered protein levels are observed. We discuss the mechanism of the observed changes in the context of known molecular function/s of CASK. Overall, our data indicate that the

phenotypic spectrum of female *Cask*$^{+/-}$ mice includes sporadic seizures and thus closely parallels that of *CASK* haploinsufficient girls; the *Cask*$^{+/-}$ mouse is thus a face-validated model for *CASK*-related pathologies. We therefore surmise that *CASK* haploinsufficiency is likely to affect brain structure and function due to dysregulation of several cellular pathways including synaptic signaling and cellular metabolism.

Word count= 288

Key word: CASK, EEG, Proteomics, iTraq, microcephaly, synapse, mitochondria, ribosome.

Introduction

Heterozygous mutations in the X-linked gene *CASK* are associated with mental retardation and microcephaly with pontine and cerebellar hypoplasia in girls (MICPCH; OMIM #300749) ((Najm, Horn et al. 2008, Moog, Kutsche et al. 2011, Burglen, Chantot-Bastaraud et al. 2012, LaConte, Chavan et al. 2018, LaConte, Chavan et al. 2019)). *CASK* mutations in boys can produce neurodevastating conditions with epileptic encephalopathies (Saitsu, Kato et al. 2012, Moog, Bierhals et al. 2015), but some *CASK* missense mutations in boys are milder and are commonly found in cases of X-linked intellectual disability in normocephalic boys (Hackett, Tarpey et al. 2010). The molecular function of CASK and the mechanism of CASK-linked disorders remain unknown.

CASK (calcium/calmodulin activated serine kinase) is a multi-domain protein belonging to the MAGUK (membrane associated guanylate kinase) class of scaffolding proteins. From N- to C-terminus, CASK is comprised of a CaMK (calcium/calmodulin dependent kinase) domain, two L27 (lin-2/lin-7) domains, a PDZ (PSD95, dlg-1 and ZO1) domain, SH3 (Src homology 3) domain and a GuK (guanylate kinase) domain (Hata, Butz et al. 1996, Butz, Okamoto et al. 1998, Mukherjee, Sharma et al. 2008). Proposed functions for CASK have included, among others, a role as a presynaptic scaffolding molecule (Butz, Okamoto et al. 1998), involvement in Tbr1-mediated transcription (Hsueh, Wang et al. 2000), establishing cell polarity (Caruana 2002), and trafficking of ion channels (Olsen, Liu et al. 2002, Leonoudakis, Conti et al. 2004). Deletion of CASK does not alter active or passive membrane properties of neurons or cell polarity (Atasoy, Schoch et al. 2007, Lozovatsky, Abayasekara et al. 2009, Mori, Kasem et al. 2019), indicating that there may

be molecular redundancy in these CASK functions. Additionally, *Cask* mutations do not alter neuronal migration in mice, suggesting that the Tbr-1/reelin pathway is not the cause of the observed phenotypes (Atasoy, Schoch et al. 2007, Huang 2016, Srivastava, McMillan et al. 2016, Mori, Kasem et al. 2019). Although synapse formation itself remains unaltered in *Cask* mutant mice (Atasoy, Schoch et al. 2007), we have observed a reduction in the number of active zones within the large retinogeniculate synapses of *Cask*$^{+/-}$ mice (Liang, Kerr et al. 2017). Biochemically, CASK interacts with and phosphorylates the cytosolic tail of α-neurexins via its PDZ domain. CASK also links neurexins to presynaptic scaffolding molecules such as Mint1, Caskin and the active zone organizer liprins-α (LaConte, Chavan et al. 2016). In addition to neurexins, the PDZ domain of CASK may also interact with other proteins such as syndecan2, syncam/IGSF4 and parkin, as well as phospholipids (Cohen, Woods et al. 1998, Biederer, Sara et al. 2002, Fallon, Moreau et al. 2002, Ivarsson, Wawrzyniak et al. 2013).

CASK is an evolutionarily conserved protein (Mukherjee, Sharma et al. 2010, LaConte and Mukherjee 2013), and an unbiased analysis of CASK-interacting proteins in Drosophila melanogaster revealed that CASK is also likely to interact with a set of mitochondrial proteins (Mukherjee, Slawson et al. 2014). Using a murine model, we have previously demonstrated that the heterozygous deletion of CASK in female mice is sufficient to produce microcephaly, cerebellar hypoplasia and optic nerve hypoplasia (Srivastava, McMillan et al. 2016, Liang, Kerr et al. 2017), thereby phenocopying the human disorder. Here we use this face-validated model to examine underlying mechanisms of the observed phenotypes. Constitutive CASK deletion in mice does not

affect overall core neuronal functions but performs a selectively essential role (Atasoy, Schoch et al. 2007). Specifically, in human populationCASK haploinsufficiecy produces lack of brain growth after birth which appears to be progressive till brain reaches its adult size (postnatal micerocephaly), lifelong intellectual disability, psychomotor disability along with incompletely penetrant epilepsy. To uncover the role of CASK, in this study we therefore performed unbiased analysis of electrical changes and molecular changes that are present in the whole brain of CASK haploinsufficient adult mice. We also performed an unbiased protein interaction mapping of CASK to understand mechanism of molecular changes. Our data indicate that CASK may participate in multiple cellular pathway including mitochondrial, synaptic and protein metabolism. Dysfunction of these cellular function is likely to underlie the complex neurological condition..

Materials and Methods

Study Approval - Procedures involving animals

All procedures involving the use of animals were approved by the Institutional Animal Care and Use Committee of the University of Virginia and the Institutional Animal Care and Use Committee of the Virginia Polytechnic Institute and State University.

All animals used in proteomics studies were at postnatal day 40 (P40) at the time of sacrifice. Animals used for RNA sequencing and EEG experiments were either P7-P14 for pups or between 2 and 4 months old for adults. P7-P14 was chosen as this is the earliest age that electrographic signals can be measured from mouse pups; between 2 and 4 months was chosen for adult mice so as to observe changes between genotypes

when the phenotype has plateaued. *Cask*$^{+/-}$ mutants and *Cask*$^{+/+}$ wild-type littermates are both from a C57BL/6J background and were backcrossed for at least 25 generations. Mice were genotyped using polymerase chain reaction followed by gel electrophoresis using primers targeted toward the exon 1-intron 1 boundary of CASK.

Electrode Implantation Surgery and EEG Data Acquisition

EEG Recordings on Pups

Pups (P7-P14) were anesthetized using 5% isoflurane for induction and 2-2.5% isoflurane for maintenance adapted from a previously published protocol (Zanelli, Goodkin et al. 2014). Unipolar insulated stainless steel depth electrodes were stereotaxically implanted in the right hippocampus and right parietal cortex, with two reference electrodes on the left parietal cortex and the cerebellum. After the surgery, pups were allowed to recover for 24 hours with the mother. The next day, the pups were connected to a video-EEG monitoring system via a flexible cable connected to the amplifier. The output signal was amplified using a Grass amplifier (Model1, Natus Neurology Incorporated-Grass Products, Warwick, RI), digitized and recorded for later review using Labchart software (ADInstruments, Dunedin, New Zealand).

EEG Recordings on Adults

Female C57BL/6J mice of each genotype (four WT and three *Cask*$^{+/-}$) between 68 and 93 days old were initially anesthetized using 5% isoflurane and head-fixed in a stereotaxic apparatus with continual 3% isoflurane administration throughout the surgery. Burr holes were drilled free-handed through the skull at 3mm anteroposterior and 3mm mediolateral from bregma to expose the dura. Two stainless steel electrodes were lowered into the

hippocampus and overlying cortex; electrode positions were verified in post-hoc analysis by the presence of a characteristic theta peak recorded from hippocampal electrodes. Mice were allowed to recover for at least 6 days post-surgery before recordings began.

PTZ Experiments

Adult mice received an intraperitoneal (IP) injection of 40mg/kg of PTZ. If the animal did not seize for approximately 10 minutes after the first injection, then 20mg/kg of PTZ was injected every approximately 10 minutes until the animal seized. The highest dose received in the study was 80mg/kg of PTZ. Latency to seizure was calculated from the time of the first injection to electrographic seizure onset and duration by the time length of electrographic seizure.

EEG Data Analysis

Raw data were visually inspected within the GRASS Technologies software for epileptiform activity by two trained observers. Upon identification of a seizure, the video recording was inspected to rule out artifacts due to movement or physical alterations in the recording setup. Power spectra were calculated using the EEGlab toolbox in MATLAB2017a. Data were sampled at 400Hz. 20 hour long epochs spanning the full day and majority of the night were used for spectral analysis including periods of sleep and wake as well as all typical locomotor behaviors. No raw data during this 20 hour period was excluded from downstream analysis. The raw data were filtered from 0-50Hz using a finite impulse response (FIR) filter, DC offset was removed, and mean power spectral densities were calculated for each channel independently over 20 hours of recording. The mean power spectral density for hippocampal and cortical electrode

placements were then averaged within each genotype. These genotype averages were then compared between wild type and *Cask*$^{+/-}$ conditions. Subsequently, the 0-50Hz filtered data was manually binned into frequency ranges of 0-4Hz, 4-8Hz, 8-12Hz, 12-15Hz, 15-20Hz, 20-30Hz, and 30-50Hz. Mean power spectral densities for each genotype in each frequency bin were calculated and compared as described above. Data were analyzed for statistical significance ($p<0.05$) using an f-test to determine homogeneity of variation, and then a two-tailed student's t-test with equal variance for all comparisons; n=3 *Cask*$^{+/-}$ mice and 4 WT mice.

RNA Sequencing Analysis

Whole brain RNA was extracted from four *Cask*$^{+/-}$ and four WT adult mice (age 2-4 months) using Aurum™ Total RNA Fatty and Fibrous Tissue kit from Biorad following manufacturer's instructions. RNA sequencing experiments were performed at the Biocomplexity Institute of Virginia Tech on an Illumina Nextseq 500 platform. Strand-specific libraries were constructed using the Illumina's TruSeq Stranded mRNA HT Sample Prep Kit (Illumina, RS-122-2103). PolyA mRNA was extracted and fragmented into 180-200 nucleotide fragments. 16 libraries were created from each mouse and pooled. Briefly, the generated libraries are clustered and sequenced using NextSeq 500/550 High Output kit V2 (75 cycles) (P/N FC-404-2005) to 1 x 75 (400 million clusters). The Illumina NextSeq Control Software v2.1.0.32 with Real Time Analysis RTA v2.4.11.0 was used to provide the management and execution of the NextSeq 500 and to generate BCL files. The BCL files were converted to FASTQ files, adapters trimmed and demultiplexed using bcl2fastq Conversion Software v2.20. The FASTQ files are used

for further analysis. Following sequencing, data was trimmed for both adaptor and quality using a combination of ea-utils and Btrim (Aronesty 2011, Kong 2011). Sequencing reads were then aligned to the genome (Ensembl Mus_musculus.GRCm38.78) using Tophat2/HiSat2 (Kim, Landmead et al. 2015) and counted via HTSeq (Simon Anders 2014). Quality control summary statistics were examined to identify any problematic samples (e.g. total read counts, quality and base composition profiles (+/- trimming)). Following successful alignment and counting, mRNA differential expression was determined using contrasts of and tested for significance using the false discovery rate (FDR) (Benjamini-Hochberg) corrected Likelihood Ratio Test (LRT) in the R-package DESeq2 (Love, Huber et al. 2014). The gene ontology classification of significant changes ($p_{adjusted}$ <0.05) was performed on the NIH DAVID web interface (https://david.ncifcrf.gov/).

iTRAQ Proteomics

Three C57BL/6J mice from each genotype (WT and *Cask*$^{+/-}$) were sacrificed by cervical dislocation, and the brains were hemisected. One hemisphere of each brain was used for isobaric Tagging for Relative and Absolute Quantitation (iTRAQ) Liquid Chromatography Tandem Mass Spectroscopy (LC-MS/MS) (Tannu and Hemby 2006). iTRAQ experiments were performed commercially by MtoZ-Biolabs (Boston, MA, USA). Total brain protein was extracted by physical homogenization in lysis buffer and subjected to trypsin digestion at a concentration of 0.025μg/μL overnight at 37°C. The TMT10plex Isobaric Label Reagent Set from Thermofisher Scientific (USA) dissolved in 41μL anhydrous acetonitrile was used to label peptides. The three WT samples were labelled

with TMT10-126, TMT10-129N, and TMT-129C respectively; the three *Cask*$^{+/-}$ samples were labelled with TMT10-130N, TMT10-130C, and TMT10-131N, respectively. Peptides were subjected to tandem LC-MS/MS using an Easy-nLC1000 chromatograph (Thermofisher Scientific, USA) and an Orbitrap™ Fusion™ Lumos™ Tribrid™ Mass Spectrometer (Thermofisher Scientific, USA).The raw MS/MS data were searched against the UniProt *Mus musculus* protein database using Proteome Discover 2.1 (Thermofisher Scientific, USA) using the following parameters: protein modifications were set to carbamidomethylation (C) (fixed), oxidation (M) (variable); enzyme set to trypsin; maximum missed cleavages set to 2; precursor ion mass tolerance set to 10ppm; MS/MS tolerance set to 20ppm. The resulting proteomic changes between WT and CASK$^{+/-}$ were selected based on significance ($p<0.05$) using a one-tailed Student's t-test assuming equal variance comparing abundance levels for each peptide between the three *Cask*$^{+/-}$ and three WT samples. Only changes with $p<0.05$ between groups were analyzed. Significant changes were categorized into subcellular compartments by using the GO_CC_DIRECT algorithm (NIH DAVID). The changes were also categorized into functional pathways using the KEGG_PATHWAY algorithm to sort them into functional categories (NIH DAVID). We also performed R spider analysis and Profcom GO analysis using the bioprofiling.de web interface (Antonov, Schmidt et al. 2008, Antonov, Schmidt et al. 2010).

Co-Immunoprecipitation Mass Spectroscopy

These experiments were done using methodology described previously (Mukherjee, Slawson et al. 2014). Briefly, lysates of HEK 293 cells expressing either GFP

or GFP-CASK were incubated overnight at 4^{o}C with whole rat brain lysate, to allow in vitro complex formation. Both cellular and brain lysates were made using a solubilizing buffer consisting of 20mM HEPES-KOH (pH7.2), 150mM NaCl, 2mM EDTA, 1% Triton-X 100, 1% sodium deoxycholate and protease inhibitor cocktail. The lysate mixture was filtered through 0.2 micron filter and pre-cleared with glutathione agarose for 2 hours. GFP-Trap beads were subsequently incubated with the lysate mixtures for an hour to precipitate GFP-tagged proteins. Beads were washed thrice with ice cold solubilizing buffer without protease inhibitors. The GFP-Trap beads were then treated with trypsin, and peptide mixtures were then separated by nano-liquid chromatography (1260 Infinity from Agilent Technologies, Santa Clara, CA) and analyzed by tandem mass spectrometry with an LTQ XL^{TM} linear ion trap mass spectrometer (ThermoFisher, Waltham, MA). Separation columns were prepared in-house using 100 µm i.d. fused silica capillaries (Polymicro Technologies Phoenix, AZ) and 5 µm Zorbax SB-C18 particles (Agilent technologies, Santa Clara, CA). The length of the column ranged from 10 cm to 12 cm. Mobile phases A and B consisted of 0.01% TFA in 4 % and 90 % acetonitrile, respectively. The peptides were eluted at a flow rate of ~160-180 nL/min by using a 200 min long gradient with increasing concentrations of solvent B (Lazar, Hoeschele et al. 2017). MS data were acquired via a data-dependent acquisition strategy by performing Zoom/MS2 scans on the 5 most intense peaks in each MS scan. Data were acquired over a mass range of 500 – 1600 m/z. Collision induced dissociation (CID) was performed at a normalized collision energy of 35 %, activation Q 0.250, and activation time of 30 msec. The threshold for triggering MS2 scans was set as 100 counts. The data dependent parameters were set

for exclusion mass width ±1.5 m/z, zoom scan width ± 5 m/z, dynamic exclusion repeat count 1, repeat duration 30 sec, and exclusion duration 60 sec, and exclusion list size of 200. The Thermo Proteome Discoverer 1.4 software package was employed to search the MS/MS spectra against the *Rattus norvegicus* (Rat) protein database (SwissProt/TrEMBL, combined 36081 entries) extracted from UniProt on November 7, 2017 (https://www.uniprot.org) as rat brain homogenate was used for protein interactions. The database search used the Sequest HT algorithm and included fully tryptic peptides with a maximum of 2 missed cleavages, minimum/maximum peptide length of 6/144, precursor ion mass ranging from 500-5000 Da with a precursor ion tolerance of 2 Da and fragment tolerance of 1 Da, no posttranslational modifications, and a stringent FDR of <1 % and relaxed of <3 %. In the case of 0 peptides coming down with GFP, a threshold of at least 2 peptide spectrum matches from a protein coming down with CASK-GFP was qualified as a putative interaction. In cases with background binding with GFP-beads, 3 times more peptides coming down with CASK over GFP alone was used as a threshold to identify putative interactors.

Results

Cask$^{+/-}$ mice display minimal electrographic changes

Mutations in *CASK* may co-occur with partially penetrant epilepsy with the majority not showing any seizures (Moog, Kutsche et al. 2011). Mutations specifically in boys are associated with epileptic encephalopathies during infancy such as Ohtahara syndrome and West syndrome (Saitsu, Kato et al. 2012, Moog, Bierhals et al. 2015). The

mechanism of the seizures remains unknown. Although an imbalance in excitatory and inhibitory synaptic transmission has been noted, these changes are limited to spontaneous action potential-independent release events (Atasoy, Schoch et al. 2007, Mori, Kasem et al. 2019). Evoked excitatory or inhibitory synaptic responses and neuronal excitability remain unchanged in CASK-null neurons (Atasoy, Schoch et al. 2007). The effect of spontaneous release of single vesicles on larger field potentials is uncertain. The electroencephalographic (EEG) signal emerges as a measure for largescale extracellular voltage changes which may result from post-synaptic potentials as well as pre-synaptic currents and action potentials (Buzsaki, Anastassiou et al. 2012).

To better characterize CASK-associated epileptic encephalopathies, we therefore performed video EEG (vEEG) recordings in infant mice at postnatal day 7, 8, 13, and 14. The vEEG recordings in infant CASK$^{+/-}$ mice did not reveal any interictal discharges or seizures (data not shown). We next performed two weeks of 24-hour vEEG recording of adult *Cask*$^{+/-}$ mice, which only revealed a single hippocampal seizure in a single mouse identified visually by two trained observers (Figure 1A). Because we did not observe frequent seizures or interictal discharges, we next performed a power spectral analysis of the EEG signal to determine whether electrographic activity was altered in a non-ictal manner. No significant differences in mean power were found in the entire 0-50Hz range or when binned into biologically relevant frequency bands of delta, theta, alpha, beta, and gamma (Figure 1B,C). Overall, the *Cask*$^{+/-}$ mice displayed a qualitatively and quantitatively normal EEG signature (Figure 1D,E). Although we failed to see more than one readily observable epileptic episodes or resting power spectral differences at the

height of the phenotype in the young and adult mice that we recorded, it may still be that the epileptic threshold in these animals is lowered. We therefore performed a kindling experiment with pentylenetetrazol (PTZ) (Rajasekaran, Zanelli et al. 2010). Our data suggest that CASK$^{+/-}$ mice do not differ from wildtype mice with respect to epileptic threshold (Figure 1F). Overall our data suggest that although seizures may occur in *Cask*$^{+/-}$ mice, overall electrographic signals remain unaltered at the ages of the *Cask*$^{+/-}$ mice that we recorded. Any cellular or molecular changes are thus unlikely to be the result of large-scale changes in activity of neuronal ensembles. Furthermore, our data indicate that an imbalance in spontaneous action potential independent release does not translate into changes in field potentials, and the observed seizures in some cases of MICPCH cannot be accounted for simply by a change in baseline synaptic activity in isolation.

Transcriptional changes in CASK$^{+/-}$ mice

RNA-Sequencing analysis was performed on three *Cask*$^{+/-}$ mice and four wildtype littermates to determine transcriptional changes. In all three *Cask*$^{+/-}$ mice, CASK mRNA was reduced to a similar degree, confirming that the X-chromosome inactivation was not skewed. Significant changes were seen in only a very few transcripts, with 105 transcripts in addition to the CASK transcript reaching statistical significance (p-adjusted value of lower than 0.05). Out of the altered transcripts, 43 transcripts were reduced in amount and 62 transcripts showed an increase (Supplementary figure 1). CASK has been proposed to affect transcription via the Tbr1 pathway (Hsueh, Wang et al. 2000), but we did not see changes in transcription of RNAs downstream of Tbr1, such as reelin or NR2b (Hsueh, Wang et al. 2000, Huang, Chang et al. 2010, Mori, Kasem et al. 2019). This is

consistent with our previous biochemical analysis of MICPCH-associated missense mutations, in which we found that the CASK-Tbr1 interaction does not underlie CASK-associated brain pathology (LaConte, Chavan et al. 2018). Approximately 50% of the reduced transcripts encode soluble (i.e. not nuclear or transmembrane) proteins of the cytosol (as classified by inclusion in GO:0005737), and of these, only 11 transcripts are ascribed functions related to core neuronal function such as synaptic transmission or membrane excitability which are encompassed in the “synapse” category (Figure 2). Note that GO:0005737 includes all proteins which are not nuclear, transmembrane, or extracellular; therefore, figure 2 was manually curated to parse out other subcellular compartments and the “cytoplasm” category refers to transcripts which could not be otherwise grouped. The largest subcellular class of decreased transcripts are identified as nuclear, encoding transcription factors or proteins responsible for mRNA processing or export (Figure 2). Most of the transcription factors that are reduced are known to regulate cell cycle rather than neuronal or synaptic function. The remaining intracellular transcript changes include proteins in metabolic pathways, with five of them belonging to the oxidative phosphorylation pathway in mitochondria and five belonging to the solute carrier family. Intriguingly, the majority of the transcripts in the mitochondrial pathway that are upregulated are not nuclear but rather mitochondrially encoded. Strikingly, the largest class of increased transcripts (24 out of 62) belong to proteins of the extracellular matrix (Figure 2). The relatively small number of changes precluded further meaningful bioinformatics analysis, such as functional pathway analysis. Overall, the most notable changes which rise to a level of significance are found in gene ontology groups associated

with generic descriptions of extracellular region, membrane fraction and cytoplasmic fraction. Our transcriptomic data thus do not support an overall nuclear reprogramming in the brains of CASK heterozygous knockout mice, and we do not observe any specific cellular pathway alteration induced by haploinsufficiency of CASK. The changes noted in transcripts for extracellular proteins are more likely to reflect increased ECM turnover, a phenomenon observed in many developmental disorders (Lu, Takai et al. 2011).

Proteomic changes in CASK$^{+/-}$ mice

Changes at the transcript level may not always be representative of changes at the protein level (Ghazalpour, Bennett et al. 2011, Haider and Pal 2013). An additional factor which complicates interpretation of changes at the transcript level specifically in the setting of CASK reduction is that CASK has been implicated as a scaffolding protein that facilitates the localization and binding of protein complexes *in situ*; if CASK's scaffolding function is reduced or eliminated in a cell, it is possible that this will impact turnover of its binding partners. We therefore decided to examine changes in the levels of brain proteins in *Cask*$^{+/-}$ mice, using sensitive and unbiased iTRAQ mass spectrometry. Comparisons were made between three wild-type (WT) and three *Cask*$^{+/-}$ mice at postnatal day 40. In contrast to the limited number of changes observed at the transcript level, we observed significant changes in 525 different proteins, excluding CASK (Auxiliary Supplementary Excel file 2). CASK was again found to be reduced in all three mutant mice, confirming previous literature (Atasoy, Schoch et al. 2007, Srivastava, McMillan et al. 2016, Mori, Kasem et al. 2019). Of all the changes observed, only a single one correlated with a change noted at the level of transcription: the CART (Cocaine- and Amphetamine-

Regulated Transcript) peptide. CART peptide acts as a neurotransmitter and a hormone. It plays a role in body energy metabolism and body weight (Farzi, Lau et al. 2018), and its promoter is known to be regulated by cyclic adenosine monophosphate response element (Zhang, Wang et al. 2012). All other alterations at the protein level appear to be post-transcriptional in nature. Of the 525 proteins, 246 proteins are decreased and 279 proteins are increased (Figure 3). The largest single organelle group (99 out of 525) identified as having altered protein levels is the mitochondrion; this is an ~2-fold higher number of proteins changed than the number of synaptic protein changes (49 (excluding CASK) out of 525) (Supplementary Figure 1). KEGG pathway analysis included less than half of the proteins observed to be altered but did identify oxidative phosphorylation and cardiac contractility as the top cellular pathways that are disturbed (Supplementary Figure 2), and the proteins involved with these pathways were overlapping. Of the proteins that were increased in the setting of lower CASK levels, many were membrane and cytoplasmic proteins (Figure 3A). In addition to the expected adhesion molecules such as CASK's known interactors, neurexin and syndecan2, other proteins found at increased levels include synaptic proteins, many members of ribosomal, cytoskeletal, proteasome protein families and metabolic proteins (Figure 3A,B and Supplementary Figure 2). Intriguing changes were also found in ion channels and proteins known to be involved in long-term potentiation, axonal guidance, and proteins found at the dopaminergic and glutamatergic synapse (Supplementary Figure 2). Of the proteins found to be increased, only 86 were able to be mapped in the R spider analysis (Antonov, Schmidt et al. 2010), and the only significant pathway alteration identified by this analysis as significant was in

the protein degradation pathway (Figure 3B). Less significant, but notable nonetheless, were changes seen in synaptic pathways. GO analysis of proteins found to be decreased in the brains of *Cask*$^{+/-}$ mice again identified the mitochondrion as the most significant group, with 65 proteins (Figure 3C and Supplementary Figure 4) from the mitochondrial matrix, inner membrane and respiratory chain complex III. KEGG pathway analysis was possible on nearly 50% of the proteins with altered levels and revealed enrichment in mostly metabolic pathways including oxidative phosphorylation, glycolysis/gluconeogenesis, biosynthesis of antibiotics, and amino acids (Supplementary Figure2). R spider analysis included only 67 proteins from the decreased expression group, and several pathways were identified that may be significantly impeded in the *Cask*$^{+/-}$ mouse brain, including the electron transport chain, NADH metabolic processes and oxaloacetate metabolism (Figure 3D). The population of proteins found to be decreased in the *Cask*$^{+/-}$ mouse brain was enriched with proteins that play a role in intracellular protein transport and mRNA processing (Figure 3D). The proteomic data thus explains at a protein expression level the mitochondrial dysfunction we previously observed in the *Cask*$^{+/-}$ mouse brain (Srivastava, McMillan et al. 2016).

CASK can phosphorylate the presynaptic adhesion molecule neurexin1 and link it to the active zone organizers liprins-α. CASK has also been speculated to play a role in the trafficking of post-synaptic molecules and to participate in Tbr1-mediated gene regulation, particularly that of reelin and NR2b (Wang, Hong et al. 2004). Recently it has been reported that CASK null cells in *Cask*$^{+/-}$ mice may express lower amounts of NR2b (Atasoy, Schoch et al. 2007, Mori, Kasem et al. 2019). A mitochondrial and trafficking

function of CASK has also been suggested (Leonoudakis, Conti et al. 2004, Mukherjee, Slawson et al. 2014, Srivastava, McMillan et al. 2016). To gain a more comprehensive understanding of the changes induced in the *Cask*$^{+/-}$ mouse brain, we therefore did a heat map analysis on the three functional groups with the largest change (synaptic, protein biosynthesis, and mitochondrial; Figure 3) to examine which of the above pathways are most affected in *Cask*$^{+/-}$ mice.

First we examined bona fide presynaptic and postsynaptic proteins. We observed changes in many categories of presynaptic proteins. Five major active zone proteins (liprin-α4, Rims1, piccolo, bassoon and munc13) are all decreased in the *Cask*$^{+/-}$ mice. We also found changes in proteins involved in synaptic vesicle cycling, including decreases in Munc18c, synaptotagmin-12, rabphilin and SNAP25 and an increase in tomosyn (Figure 4). Overall the changes in these proteins suggest that loss of CASK should affect synaptic vesicle recycling negatively. On the postsynaptic side, postsynaptic density proteins are almost entirely increased. In a striking contrast to expected and previously published data (Mori, Kasem et al. 2019), levels of NR2b protein are increased in the setting of lower CASK expression (Figure 4). Within the protein biosynthetic pathway, most of the RNA processing proteins are decreased, whereas ribosomal subunits are increased in abundance. Mitochondrial proteins operating in the oxidative phosphorylation pathway are mostly decreased, with the exception of an increase in a subset of mitochondrial proteins (Figure 4). We also observed changes in several cytoskeletal molecules, including tubulins. Overall these data confirm a synaptic function

for CASK and also indicate that CASK additionally participates in mitochondrial and protein biosynthetic pathways.

Putative protein complexes in which CASK participates

Previous experiments examining protein interactions in *Drosophila melanogaster* were done using transgenic flies expressing a transgene of CASK fused with YFP (yellow fluorescence protein); a GFP-Trap matrix was employed to capture interacting partners. YFP-CASK can rescue CASK loss-of-function in Drosophila ((Slawson, Kuklin et al. 2011) and unpublished observations), and GFP-CASK maintains all of its known interactions (LaConte, Chavan et al. 2014, Mukherjee, Slawson et al. 2014, LaConte, Chavan et al. 2016, LaConte, Chavan et al. 2018, LaConte, Chavan et al. 2019). In these Drosophila experiments, both synaptic and mitochondrial proteins were pulled down by CASK (Mukherjee, Slawson et al. 2014). Because both of these categories of protein (synaptic and mitochondrial) were identified in the proteomic study described here (Figure 4), and since the protein changes cannot be explained by changes in either electrical activity (Figure 1) or nuclear reprogramming (Figure 2), we investigated CASK interacting partners in a mammalian system with a focus on non-plasma membrane proteins. Because we have previously shown that using antibodies to internal epitopes of CASK for immunoprecipitation sometimes inhibits binding of crucial interactors due to steric hindrance (LaConte, Chavan et al. 2016), we once again used a recombinant GFP-CASK pulldown approach with GFP-Trap beads. GFP-CASK expressed in HEK293 cells was used to precipitate all CASK-interacting proteins from rat brain, and mass spectrometry was used for identification. GFP alone was employed as a negative control; 640 GFP

peptides were identified in the GFP-beads sample, while 224 GFP peptides were identified in GFP-CASK beads. Additionally, 2018 CASK peptides were identified in GFP-CASK beads while no CASK peptides were identified on GFP-beads. Based on our candidate inclusion criteria (minimum of two peptides identified and at least 3 times more peptides with GFP-CASK over GFP alone), we identified 170 candidate proteins that interact with CASK either directly or indirectly. A complete list of interactors which met our inclusion criteria can be found in supplemental table 7. Many of the peptides belonged to previously known interactors such as veli, Mint1 and liprins-α. The dataset of putative interacting proteins were mapped using known interactions in the STRING database (Figure 5, supplementary figure 7; (Szklarczyk, Franceschini et al. 2015)). Five major clusters emerged: presynaptic proteins, mitochondrial proteins, ribosomal proteins, chaperone proteins, and cytoskeletal proteins (Figure 5, supplemental figure 7). Based on the STRING (database) mapping derived from previously known interactions on which we have overlaid the list of proteins from our pulldown experiment and the design of the experiment itself, it is likely that proteins pulled down in these experiments may represent both direct and indirect binding partners. In the future it will be critical to validate specific interactions that are described here. However, the similarity of these clusters with the proteomic changes in the brain suggests that CASK most likely forms complexes within these pathways. Furthermore, multiple new interacting partners identified here exhibit changes in their abundance in the iTraq proteomic study such as Nedd4, CamKIIa, Ppp2r1a, Slc25a5, Wars, Uqcrc2 and Tufm (Figure 6A), increasing our confidence in these interactions. Since CASK is a scaffolding protein, lack of CASK may destabilize

interacting molecules and reduce their amount. Strikingly, analysis of 27 direct interacting partners revealed that interacting proteins can either increase or decrease in amount in the *Cask*$^{+/-}$ brain (Figure 6A), suggesting that CASK likely regulates these protein complexes dynamically.

Discussion

Mutations in the gene encoding CASK associate with MICPCH, ONH, growth retardation and often seizures. Seizures are, in fact, a common accompaniment of a multitude of neurodevelopmental disorders (Crino, Miyata et al. 2002). As CASK is a putative synaptic molecule (Butz, Okamoto et al. 1998), one could argue that a shift in steady state (excitatory/inhibitory) E/I balance induced by loss of CASK might lead to epileptiform activity. We were able to record at least one apparent spontaneous seizure, but an extensive analysis of EEG data from adult and young mice failed to reveal significant electrographic changes in *Cask*$^{+/-}$ mice. Overall these data indicate that epilepsy in rodents is likely to have low penetrance with CASK haploinsufficiency; these findings are consistent with clinical data, since many CASK mutation subjects do not exhibit seizures (DeLuca, Wallace et al. 2017, LaConte, Chavan et al. 2018, Kerr, Patel et al. 2019, LaConte, Chavan et al. 2019). Typical epileptic disorders are characterized by epileptiform activity in less than 1% of total brain activity (Staley 2015), indicating that ictogenic triggers may play a role in such cases. *Cask*$^{+/-}$ mice do not display a decreased threshold for seizures after exposure to the kindling agent PTZ, a GABA antagonist. These data suggest that in *Cask*$^{+/-}$ mice, E/I imbalance is unlikely to be the major ictogenic trigger. Our data thus indicate that previously described changes in spontaneous

vesicular release are insufficient to precipitate hypersynchronous neuronal activity required for ictogenesis.

In mammals, CASK was discovered due to its ability to interact with the cytosolic tail of the presynaptic adhesion molecule neurexin (Hata, Butz et al. 1996) and was proposed to be a scaffolding molecule involved in presynaptic assembly (Butz, Okamoto et al. 1998). This idea was challenged since CASK deletion did not affect synapse formation and assembly (Atasoy, Schoch et al. 2007) and also because the CASK-neurexin interaction is not needed for neurexin's synaptogenic activity (Gokce and Sudhof 2013). CASK, however, interacts with other probable presynaptic scaffolds such as Mint1 (Butz, Okamoto et al. 1998), Caskin1 (Tabuchi, Biederer et al. 2002), liprin-α (Olsen, Moore et al. 2005), and rabphilin (Zhang, Luan et al. 2001), and participates in presynaptic specialization (Spangler, Schmitz et al. 2013). We have previously demonstrated that CASK is critical for linking presynaptic adhesion molecules to the active zone via interaction with the liprins-α (LaConte, Chavan et al. 2016). Furthermore, we have demonstrated that CASK haploinsufficiency reduces the number of release sites (active zones) in the large retinogeniculate synapses (Liang, Kerr et al. 2017). Despite our and others' numerous studies, CASK's role in the assembly of the presynaptic active zone remains a subject of debate. The increase in the level of neurexin1 and concomitant decrease in five major presynaptic active zone proteins in the *Cask*$^{+/-}$ mouse brain provide strong evidence for the role of CASK in active zone assembly, formation, and maintenance. Specifically, lack of CASK decreases the levels of: 1) piccolo and 2) bassoon, two large proteins involved in synaptic vesicle clustering (Mukherjee, Yang et

al. 2010); 3) RIM1, a molecule involved in docking, presynaptic short term plasticity and positioning of calcium channels (Castillo, Schoch et al. 2002, Kaeser, Deng et al. 2011); 4) Munc13, a protein involved in the priming of synaptic vesicles (Ashery, Varoqueaux et al. 2000, Rhee, Betz et al. 2002); and 5) liprin-α4, which is involved in active zone organization (Kaufmann, DeProto et al. 2002, Dai, Taru et al. 2006). In summary, lack of CASK affects the biochemical composition of the active zone. In addition to the changes seen in active zone protein levels, we also observe a decrease in a number of proteins that are involved in synaptic vesicle cycling, including the SNARE protein SNAP25 and a number of SNARE fusion-regulating proteins such as Munc18c (Hata, Slaughter et al. 1993), complexin-2 (Tang, Maximov et al. 2006), rabphilin (Deak, Shin et al. 2006) and synaptotagmin-12 (Maximov, Shin et al. 2007). The only presynaptic molecule which is increased is tomosyn, a protein shown to inhibit vesicle fusion by inducing formation of non-fusogenic SNARE complexes (Hatsuzawa, Lang et al. 2003). Based on decreases in the many vital active zone and fusion-related proteins we observe, neurotransmitter release should be negatively impacted in the *Cask*$^{+/-}$ brain.

Cask$^{+/-}$ mouse brain also displays an increase in a number of postsynaptic proteins (Figure 4) like the NR2B subunit of the NMDA receptor and the scaffolding molecules PSD95, SHANK3, SYNGAP1, CaMKII and Homer. Since a parallel increase in mRNA production is not observed (Fig. 2), we suspect that these protein-level increases are not a nuclear response at the level of transcription but rather a change in turnover rate. Proteins associated with the postsynaptic density might, for example, be stabilized by changes in presynaptic function, thus decreasing the turnover rate. In fact, RIM1 knockout

mice also display a modest increase in postsynaptic density proteins (Schoch, Castillo et al. 2002). Reduction or deprivation of presynaptic release also often results in an observed increase in levels of postsynaptic density proteins (Guldner and Ingham 1980, Clarkson, Antunes et al. 2016). Multiple studies have shown that neurons adjust synaptic strength in response to chronically increased or decreased activity in a process called homeostatic synaptic scaling, utilizing mechanisms independent of those traditionally associated with long-term potentiation/depression (Turrigiano 2012, Chowdhury and Hell 2018). As such, decreases observed here in active zone proteins resulting from loss of CASK may induce compensatory changes in protein turnover at the post-synapse. Further, it has recently been shown that changes to presynaptic neurexin composition can differentially affect postsynaptic glutamatergic responses (Aoto, Martinelli et al. 2013, Dai, Aoto et al. 2019), and an increase in presynaptic neurexin may also increase Homer1 in positive excitatory post-synapses (Trotter, Hao et al. 2019). A caveat to this argument is that the reported changes are global and may arise from different synapses and indeed different kinds of neurons. The experimental approach described here does not have the resolution to provide a more detailed description of neuron-specific changes. Furthermore, at a cellular level, both the MICPCH disorder and its animal model presented here are mosaic in regard to the expression of the X-linked gene *CASK* in the female population. Approximately 50% of neurons express normal levels of CASK while approximately 50% express no CASK. Some of the observed changes may also represent compensatory changes in CASK-expressing cells.

Indeed, CASK has also been proposed to be present in the postsynaptic compartment, with evidence suggesting that it interacts with parkin (Fallon, Moreau et al. 2002), syndecan2 (Cohen, Woods et al. 1998), SAP-97 (Sanford, Mays et al. 2004, Lozovatsky, Abayasekara et al. 2009) and CaMKII (Lu, Hodge et al. 2003, Hodge, Mullasseril et al. 2006, Mukherjee, Slawson et al. 2014), as well as potentially playing a role in the trafficking of NMDA receptors (Jeyifous, Waites et al. 2009). Therefore, an alternative and equally intriguing possibility is that CASK plays a cell-autonomous, but negative, role in formation of the postsynaptic density via interaction with postsynaptic molecules, specifically CaMKII. Herein, we, for the first time, demonstrate that this critical interaction with CaMKII first described in the Drosophila literature is evolutionarily conserved (Lu, Hodge et al. 2003, Hodge, Mullasseril et al. 2006, Mukherjee, Slawson et al. 2014). CaMKII plays a crucial role in the postsynaptic compartment in the process of long-term potentiation (LTP). LTP may involve interaction with and phosphorylation of the NR2b subunit of the NMDA receptor by CaMKII (Omkumar, Kiely et al. 1996, Bayer, De Koninck et al. 2001). The increase noted in NR2b and other postsynaptic density proteins may thus be explained by the CASK-CaMKII interaction. Our results suggest that mammalian CASK via interaction with CaMKII may participate in postsynaptic plasticity.

We also demonstrate that CASK interacts with mitochondrial proteins and that a lack of CASK alters levels of mitochondrial proteins. We have previously demonstrated that the CASK$^{+/-}$ mouse brain exhibits reduced mitochondrial respiration (Srivastava, McMillan et al. 2016), but the mechanism for this observation remained unclear. Our proteomic data thus provides a biochemical explanation for our prior observation. Overall,

we find that the mitochondrial proteome is disproportionately affected in the brain of CASK$^{+/-}$ mice (99 of the 525 total proteins found to be altered are mitochondrial; Figure 4). The majority of these changes were decreases and would negatively impact mitochondrial function. Our data suggest a critical role of CASK in regulating mitochondrial function. Strikingly, in our RNA sequencing analysis, we observed increases in mitochondrial DNA encoded genes, indicative of a compensatory response. Future studies are required to determine where and how CASK interacts with the mitochondrial proteins and regulates their function. Interestingly, it also remains unclear how a reduction in mitochondrial function in CASK mutant mice affects overall neurophysiology. Finally, we found protein-level changes suggestive of a role for CASK in protein biosynthetic and degradation pathways, including proteins involved in mRNA processing, ribosomal subunits and proteins belonging to proteasomal pathways. This function of CASK was hitherto unknown and also needs further investigation. Furthermore, a function within protein biosynthesis or degradation pathways by itself may contribute directly to post-transcriptional alterations described here (Figure 6B).

CASK is not a neuron-specific or indeed even a brain-specific molecule (Hata, Butz et al. 1996), and in *Caenorhabdites elegans* (*C. elegans*), deletion of CASK does not produce a neuronal phenotype (Hoskins, Hajnal et al. 1996). Could CASK have a more central cellular function that may explain many of the observed changes reported here? CASK forms a well-characterized and evolutionarily highly conserved tripartite complex with Mint1/X11-α/lin-10 and veli/Mals/lin-7 (Butz, Okamoto et al. 1998, Kaech, Whitfield et al. 1998, Mukherjee, Slawson et al. 2014). Orthologs of all these genes were

discovered in a vulval precursor cell-fate patterning screen in *C.elegans* as early as 1980, which suggests a functional relevance of this complex (Horvitz and Sulston 1980, Ferguson and Horvitz 1985). The vulval differentiation function of these three genes in *C.elegans* is dependent on proper membrane targeting of the tyrosine kinase LET-23. One possibility is that CASK/Mint-1/veli complex may also be involved in polarized and regulated trafficking of proteins from the endoplasmic reticulum/golgi complex in other animal clades. In fact Mint1 and CASK have both been shown to participate in such trafficking (Alewine, Kim et al. 2007, Gross, Lone et al. 2013), which could explain changes in both pre-and post-synaptic molecules. Furthermore recent evidence suggests mitochondrial protein import also involves the endoplasmic reticulum (Hansen, Aviram et al. 2018), and veli has been shown to localize to mitochondria (Ferrari, Crespi et al. 2016). Indeed CASK has been isolated from endoplasmic reticulum-mitochondria contact sites (Poston, Krishnan et al. 2013, Hung, Lam et al. 2017). Future experiments need to address these ideas.

There are number of limitations in this study which include lack of spatial and temporal resolution in the molecular changes and number and age of animals used. Some findings here may also be limited by species differences from human. Furthermore, the study has been done in a highly homogeneous genotypic background, although this allows us to draw statistical significance from a smaller group of animals, it may fail to represent the spectrum of CASK-linked disorders in the highly heterogeneous human subject population. This issue is particularly pertinent in incompletely penetrant phenotypes such as seizures which may derive from a complex interaction of CASK dysfunction and

genotypic background. While it may be possible for us to document more seizures in the C57Bl6 background by increasing number and time periods of recordings, it is more likely that we may observe higher seizure numbers in a different strain of mice. These deficiencies will be addressed in future studies. Overall, the data presented here elucidate several biochemical functions of the CASK protein in multiple aspects of cellular physiology (Figure 6B). Pathology of the CASK-linked brain phenotype is highly complex and involves the entire brain, therefore here we have taken an approach which is highly sensitive, but does not address specific molecular or cell-type roles of CASK. This is to delineate identifiable cellular pathways that are affected by loss of CASK. In the future, we will investigate specific molecular interactions and region and cell-type specific changes to obtain mechanistic insights into this multifaceted neurodevelopmental disorder. Our data here confirm the canonical synaptic role of CASK while furthering the discussion of effects of heterozygous deletion at the whole brain level. Furthermore, non-canonical phenotypic observations such as effects on mitochondrial respiration have been explained at the level of mRNA, protein, and protein-protein interactions. In doing so, these data enhance our understanding of the diverse functions of CASK and the microcephaly produced by clinically relevant heterozygous CASK mutations at a whole brain level.

Declarations

Consent for Publication

Not applicable.

Data Availability

The full datasets generated and analyzed by the experiments described here will be submitted to respective repositories and are available upon reasonable request from the corresponding author.

Competing Interests

The authors declare that they have no competing interests.

Funding

This work was supported by the NIH National Eye Institute (R01EY024712 to KM) and a UVA-VTC seed fund to KM and HG.

Author Contributions

PAP performed experiments, analyzed data, helped in writing the original draft and editing. CL performed experiments and analyzed data. AA performed experiments. SV analyzed data and helped in writing the manuscript. SA performed experiments. PKW performed experiments. RS analyzed data and helped in writing the manuscript. LEWL analyzed data and helped in writing the manuscript. HPG analyzed data and helped in writing the manuscript. IL performed experiments. SS analyzed data and helped in writing the manuscript. KM designed experiments, performed experiments, analyzed data, helped in writing the original draft, and editing.

Acknowledgements

We thank Vrushali Chavan for technical assistance.

References

1. Burglen L, Chantot-Bastaraud S et al. (2012) Spectrum of pontocerebellar hypoplasia in 13 girls and boys with CASK mutations: confirmation of a recognizable phenotype and first description of a male mosaic patient. Orphanet J Rare Dis 7:18. doi:1750-1172-7-18 [pii]

10.1186/1750-1172-7-18

2. Moog U et al. (2011) Phenotypic spectrum associated with CASK loss-of-function mutations. J Med Genet 48 (11):741-751. doi:jmedgenet-2011-100218 [pii]

10.1136/jmedgenet-2011-100218

3. Najm J et al. (2008) Mutations of CASK cause an X-linked brain malformation phenotype with microcephaly and hypoplasia of the brainstem and cerebellum. Nat Genet 40 (9):1065-1067. doi:10.1038/ng.194

4. LaConte LEW et al. (2019) An N-terminal heterozygous missense CASK mutation is associated with microcephaly and bilateral retinal dystrophy plus optic nerve atrophy. Am J Med Genet A 179 (1):94-103. doi:10.1002/ajmg.a.60687

5. LaConte LEW et al. (2018) Two microcephaly-associated novel missense mutations in CASK specifically disrupt the CASK-neurexin interaction. Hum Genet 137 (3):231-246. doi:10.1007/s00439-018-1874-3

6. Moog U et al. (2015) Phenotypic and molecular insights into CASK-related disorders in males. Orphanet J Rare Dis 10:44. doi:10.1186/s13023-015-0256-3

7. Saitsu H et al. (2012) CASK aberrations in male patients with Ohtahara syndrome and cerebellar hypoplasia. Epilepsia 53 (8):1441-1449. doi:10.1111/j.1528-1167.2012.03548.x

8. Hackett A et al. (2010) CASK mutations are frequent in males and cause X-linked nystagmus and variable XLMR phenotypes. Eur J Hum Genet 18 (5):544-552. doi:ejhg2009220 [pii]

10.1038/ejhg.2009.220

9. Butz S, Okamoto M, Sudhof TC (1998) A tripartite protein complex with the potential to couple synaptic vesicle exocytosis to cell adhesion in brain. Cell 94 (6):773-782

10. Hata Y, Butz S, Sudhof TC (1996) CASK: a novel dlg/PSD95 homolog with an N-terminal calmodulin-dependent protein kinase domain identified by interaction with neurexins. J Neurosci 16 (8):2488-2494

11. Mukherjee K et al. (2008) CASK Functions as a Mg2+-independent neurexin kinase. Cell 133 (2):328-339. doi:10.1016/j.cell.2008.02.036

S0092-8674(08)00287-0 [pii]

12. Hsueh YP, Wang TF, Yang FC, Sheng M (2000) Nuclear translocation and transcription regulation by the membrane-associated guanylate kinase CASK/LIN-2. Nature 404 (6775):298-302. doi:10.1038/35005118

13. Caruana G (2002) Genetic studies define MAGUK proteins as regulators of epithelial cell polarity. Int J Dev Biol 46 (4):511-518

14. Leonoudakis D, Conti LR, Radeke CM, McGuire LM, Vandenberg CA (2004) A multiprotein trafficking complex composed of SAP97, CASK, Veli, and Mint1 is associated

with inward rectifier Kir2 potassium channels. J Biol Chem 279 (18):19051-19063. doi:10.1074/jbc.M400284200

M400284200 [pii]

15. Olsen O, Liu H, Wade JB, Merot J, Welling PA (2002) Basolateral membrane expression of the Kir 2.3 channel is coordinated by PDZ interaction with Lin-7/CASK complex. Am J Physiol Cell Physiol 282 (1):C183-195. doi:10.1152/ajpcell.00249.2001

16. Lozovatsky L, Abayasekara N, Piawah S, Walther Z (2009) CASK deletion in intestinal epithelia causes mislocalization of LIN7C and the DLG1/Scrib polarity complex without affecting cell polarity. Mol Biol Cell 20 (21):4489-4499. doi:10.1091/mbc.E09-04-0280

E09-04-0280 [pii]

17. Atasoy D et al. (2007) Deletion of CASK in mice is lethal and impairs synaptic function. Proc Natl Acad Sci U S A 104 (7):2525-2530. doi:0611003104 [pii]

10.1073/pnas.0611003104

18. Mori T et al. (2019) Deficiency of calcium/calmodulin-dependent serine protein kinase disrupts the excitatory-inhibitory balance of synapses by downregulating GluN2B (vol 24, pg 1079, 2019). Mol Psychiatr 24 (7):1093-1093. doi:10.1038/s41380-019-0362-z

19. Huang TNaH, Y.P. (2016) Calcium/calmodulin-dependent serine protein kinase (CASK), a protein implicated in mental retardation and autism-spectrum disorders, interacts with T-Brain-1 (TBR1) to control extinction of associative memory in male mice. Journal of Psychiatry and Neuroscience. doi: 10.1503/jpn.150359

20. Srivastava S et al. (2016) X-linked intellectual disability gene CASK regulates postnatal brain growth in a non-cell autonomous manner. Acta Neuropathol Commun 4:30. doi:10.1186/s40478-016-0295-6

21. Liang C et al. (2017) Optic Nerve Hypoplasia Is a Pervasive Subcortical Pathology of Visual System in Neonates. Invest Ophthalmol Vis Sci 58 (12):5485-5496. doi:10.1167/iovs.17-22399

22. LaConte LEW et al. (2016) CASK stabilizes neurexin and links it to liprin-alpha in a neuronal activity-dependent manner. Cell Mol Life Sci 73 (18):3599-3621. doi:10.1007/s00018-016-2183-4

23. Biederer T et al. (2002) SynCAM, a synaptic adhesion molecule that drives synapse assembly. Science 297 (5586):1525-1531. doi:10.1126/science.1072356

297/5586/1525 [pii]

24. Cohen AR et al. (1998) Human CASK/LIN-2 binds syndecan-2 and protein 4.1 and localizes to the basolateral membrane of epithelial cells. J Cell Biol 142 (1):129-138

25. Fallon L et al. (2002) Parkin and CASK/LIN-2 associate via a PDZ-mediated interaction and are co-localized in lipid rafts and postsynaptic densities in brain. J Biol Chem 277 (1):486-491. doi:10.1074/jbc.M109806200

26. Ivarsson Y et al. (2013) Prevalence, Specificity and Determinants of Lipid-Interacting PDZ Domains from an In-Cell Screen and In Vitro Binding Experiments. Plos One 8 (2). doi:ARTN e54581

10.1371/journal.pone.0054581

27. LaConte L, Mukherjee K (2013) Structural constraints and functional divergences in CASK evolution. Biochem Soc Trans 41 (4):1017-1022. doi:10.1042/BST20130061

28. Mukherjee K et al. (2010) Evolution of CASK into a Mg2+-sensitive kinase. Sci Signal 3 (119):ra33. doi:10.1126/scisignal.2000800

3/119/ra33 [pii]

29. Mukherjee K, Slawson JB, Christmann BL, Griffith LC (2014) Neuron-specific protein interactions of Drosophila CASK-beta are revealed by mass spectrometry. Front Mol Neurosci 7:58. doi:10.3389/fnmol.2014.00058

30. Lu PF, Takai K, Weaver VM, Werb Z (2011) Extracellular Matrix Degradation and Remodeling in Development and Disease. Csh Perspect Biol 3 (12). doi:ARTN a005058 10.1101/cshperspect.a005058

31. Zanelli S, Goodkin HP, Kowalski S, Kapur J (2014) Impact of transient acute hypoxia on the developing mouse EEG. Neurobiol Dis 68:37-46. doi:10.1016/j.nbd.2014.03.005

32. Aronesty E (2011) ea-utils : "Command-line tools for processing biological sequencing data".

33. Kong Y (2011) Btrim: A fast, lightweight adapter and quality trimming program for next-generation sequencing technologies. Genomics 98 (2):152-153. doi:10.1016/j.ygeno.2011.05.009

34. Kim D, Landmead B, Salzberg SL (2015) HISAT: a fast spliced aligner with low memory requirements. Nat Methods 12 (4):357-U121. doi:10.1038/Nmeth.3317

35. Simon Anders PTP, Wolfgang Huber (2014) HTSeq — A Python framework to work with high-throughput sequencing data Bioinformatics. doi:10.1093/bioinformatics/btu638

36. Love MI, Huber W, Anders S (2014) Moderated estimation of fold change and dispersion for RNA-seq data with DESeq2. Genome Biol 15 (12). doi:ARTN 550 10.1186/s13059-014-0550-8

37. Tannu NS, Hemby SE (2006) Methods for proteomics in neuroscience. Prog Brain Res 158:41-82. doi:10.1016/S0079-6123(06)58003-3

38. Antonov AV, Schmidt T, Wang Y, Mewes HW (2008) ProfCom: a web tool for profiling the complex functionality of gene groups identified from high-throughput data. Nucleic Acids Res 36:W347-W351. doi:10.1093/nar/gkn239

39. Antonov AV et al. (2010) R spider: a network-based analysis of gene lists by combining signaling and metabolic pathways from Reactome and KEGG databases. Nucleic Acids Res 38:W78-W83. doi:10.1093/nar/gkq482

40. Lazar IM, Hoeschele I, de Morais J, Tenga MJ (2017) Cell Cycle Model System for Advancing Cancer Biomarker Research. Sci Rep 7 (1):17989. doi:10.1038/s41598-017-17845-6

41. Buzsaki G, Anastassiou CA, Koch C (2012) The origin of extracellular fields and currents - EEG, ECoG, LFP and spikes. Nat Rev Neurosci 13 (6):407-420. doi:10.1038/nrn3241

42. Rajasekaran K, Zanelli SA, Goodkin HP (2010) Lessons From the Laboratory: The Pathophysiology, and Consequences of Status Epilepticus. Semin Pediatr Neurol 17 (3):136-143. doi:10.1016/j.spen.2010.06.002

43. Huang TN, Chang HP, Hsueh YP (2010) CASK phosphorylation by PKA regulates the protein-protein interactions of CASK and expression of the NMDAR2b gene. J Neurochem 112 (6):1562-1573. doi:10.1111/j.1471-4159.2010.06569.x

44. Ghazalpour A et al. (2011) Comparative Analysis of Proteome and Transcriptome Variation in Mouse. Plos Genet 7 (6). doi:ARTN e1001393 10.1371/journal.pgen.1001393

45. Haider S, Pal R (2013) Integrated Analysis of Transcriptomic and Proteomic Data. Curr Genomics 14 (2):91-110. doi:Doi 10.2174/1389202911314020003

46. Farzi A et al. (2018) Arcuate nucleus and lateral hypothalamic CART neurons in the mouse brain exert opposing effects on energy expenditure. Elife 7. doi:ARTN e36494 10.7554/eLife.36494

47. Zhang J et al. (2012) Neuron-restrictive Silencer Factor (NRSF) Represses Cocaine- and Amphetamine-regulated Transcript (CART) Transcription and Antagonizes cAMP-response Element-binding Protein Signaling through a Dual NRSE Mechanism. Journal of Biological Chemistry 287 (51):42574-42587. doi:10.1074/jbc.M112.376590

48. Wang GS et al. (2004) Transcriptional modification by a CASK-interacting nucleosome assembly protein. Neuron 42 (1):113-128

49. Slawson JB et al. (2011) Central regulation of locomotor behavior of Drosophila melanogaster depends on a CASK isoform containing CaMK-like and L27 domains. Genetics 187 (1):171-184. doi:10.1534/genetics.110.123406 genetics.110.123406 [pii]

50. LaConte LE, Chavan V, Mukherjee K (2014) Identification and glycerol-induced correction of misfolding mutations in the X-linked mental retardation gene CASK. PLoS One 9 (2):e88276. doi:10.1371/journal.pone.0088276

51. Szklarczyk D et al. (2015) STRING v10: protein-protein interaction networks, integrated over the tree of life. Nucleic Acids Res 43 (D1):D447-D452. doi:10.1093/nar/gku1003

52. Crino PB, Miyata H, Vinters HV (2002) Neurodevelopmental disorders as a cause of seizures: Neuropathologic, genetic, and mechanistic considerations. Brain Pathol 12 (2):212-233

53. DeLuca SC, Wallace DA, Trucks MR, Mukherjee K (2017) A clinical series using intensive neurorehabilitation to promote functional motor and cognitive skills in three girls with CASK mutation. BMC Res Notes 10 (1):743. doi:10.1186/s13104-017-3065-z

54. Kerr A et al. (2019) Non-Cell Autonomous Roles for CASK in Optic Nerve Hypoplasia. Invest Ophthalmol Vis Sci 60 (10):3584-3594. doi:10.1167/iovs.19-27197

55. Staley K (2015) Molecular mechanisms of epilepsy. Nat Neurosci 18 (3):367-372. doi:10.1038/nn.3947

56. Gokce O, Sudhof TC (2013) Membrane-Tethered Monomeric Neurexin LNS-Domain Triggers Synapse Formation. Journal of Neuroscience 33 (36):14617-14628. doi:10.1523/Jneurosci.1232-13.2013

57. Tabuchi K, Biederer T, Butz S, Sudhof TC (2002) CASK participates in alternative tripartite complexes in which Mint 1 competes for binding with caskin 1, a novel CASK-binding protein. J Neurosci 22 (11):4264-4273. doi:20026421

58. Olsen O et al. (2005) Neurotransmitter release regulated by a MALS-liprin-alpha presynaptic complex. J Cell Biol 170 (7):1127-1134. doi:jcb.200503011 [pii]
10.1083/jcb.200503011
59. Zhang Y, Luan Z, Liu A, Hu G (2001) The scaffolding protein CASK mediates the interaction between rabphilin3a and beta-neurexins. FEBS Lett 497 (2-3):99-102. doi:S0014-5793(01)02450-4 [pii]
60. Spangler SA et al. (2013) Liprin-alpha2 promotes the presynaptic recruitment and turnover of RIM1/CASK to facilitate synaptic transmission. J Cell Biol 201 (6):915-928. doi:10.1083/jcb.201301011
61. Mukherjee K et al. (2010) Piccolo and bassoon maintain synaptic vesicle clustering without directly participating in vesicle exocytosis. Proc Natl Acad Sci U S A 107 (14):6504-6509. doi:10.1073/pnas.1002307107
1002307107 [pii]
62. Kaeser PS et al. (2011) RIM Proteins Tether Ca2+ Channels to Presynaptic Active Zones via a Direct PDZ-Domain Interaction. Cell 144 (2):282-295. doi:10.1016/j.cell.2010.12.029
63. Castillo PE et al. (2002) RIM1 alpha is required for presynaptic long-term potentiation. Nature 415 (6869):327-330. doi:DOI 10.1038/415327a
64. Ashery U et al. (2000) Munc13-1 acts as a priming factor for large dense-core vesicles in bovine chromaffin cells. Embo J 19 (14):3586-3596. doi:DOI 10.1093/emboj/19.14.3586

65. Rhee JS et al. (2002) beta phorbol ester- and diacylglycerol-induced augmentation of transmitter release is mediated by Munc13s and not by PKCs. Cell 108 (1):121-133. doi:Doi 10.1016/S0092-8674(01)00635-3

66. Kaufmann N et al. (2002) Drosophila liprin-alpha and the receptor phosphatase Dlar control synapse morphogenesis. Neuron 34 (1):27-38. doi:Doi 10.1016/S0896-6273(02)00643-8

67. Dai Y et al. (2006) SYD-2 Liprin-alpha organizes presynaptic active zone formation through ELKS. Nat Neurosci 9 (12):1479-1487. doi:10.1038/nn1808

68. Hata Y, Slaughter CA, Sudhof TC (1993) Synaptic Vesicle Fusion Complex Contains Unc-18 Homolog Bound to Syntaxin. Nature 366 (6453):347-351. doi:DOI 10.1038/366347a0

69. Tang J et al. (2006) A complexin/synaptotagmin 1 switch controls fast synaptic vesicle exocytosis. Cell 126 (6):1175-1187. doi:10.1016/j.cell.2006.08.030

70. Deak F et al. (2006) Rabphilin regulates SNARE-dependent re-priming of synaptic vesicles for fusion. Embo J 25 (12):2856-2866. doi:10.1038/sj.embjol.7601165

71. Maximov A, Shin OH, Liu XR, Sudhof TC (2007) Synaptotagmin-12, a synaptic vesicle phosphoprotein that modulates spontaneous neurotransmitter release. Journal of Cell Biology 176 (1):113-124. doi:10.1083/jcb.200607021

72. Hatsuzawa K et al. (2003) The R-SNARE motif of tomosyn forms SNARE core complexes with syntaxin 1 and SNAP-25 and down-regulates exocytosis. Journal of Biological Chemistry 278 (33):31159-31166. doi:10.1074/jbc.M305500200

73. Schoch S et al. (2002) RIM1 alpha forms a protein scaffold for regulating neurotransmitter release at the active zone. Nature 415 (6869):321-326. doi:DOI 10.1038/415321a

74. Clarkson C, Antunes FM, Rubio ME (2016) Conductive Hearing Loss Has Long-Lasting Structural and Molecular Effects on Presynaptic and Postsynaptic Structures of Auditory Nerve Synapses in the Cochlear Nucleus. Journal of Neuroscience 36 (39):10214-10227. doi:10.1523/Jneurosci.0226-16.2016

75. Guldner FH, Ingham CA (1980) Increase in Postsynaptic Density Material in Optic Target Neurons of the Rat Suprachiasmatic Nucleus after Bilateral Enucleation. Neurosci Lett 17 (1-2):27-31. doi:Doi 10.1016/0304-3940(80)90056-7

76. Chowdhury D, Hell JW (2018) Homeostatic synaptic scaling: molecular regulators of synaptic AMPA-type glutamate receptors. F1000Res 7:234. doi:10.12688/f1000research.13561.1

77. Turrigiano G (2012) Homeostatic Synaptic Plasticity: Local and Global Mechanisms for Stabilizing Neuronal Function. Csh Perspect Biol 4 (1). doi:ARTN a005736 10.1101/cshperspect.a005736

78. Aoto J et al. (2013) Presynaptic Neurexin-3 Alternative Splicing trans-Synaptically Controls Postsynaptic AMPA Receptor Trafficking. Cell 154 (1):75-88. doi:10.1016/j.cell.2013.05.060

79. Dai J, Aoto J, Sudhof TC (2019) Alternative Splicing of Presynaptic Neurexins Differentially Controls Postsynaptic NMDA and AMPA Receptor Responses. Neuron 102 (5):993-+. doi:10.1016/j.neuron.2019.03.032

80. Trotter JH et al. (2019) Synaptic neurexin-1 assembles into dynamically regulated active zone nanoclusters. Journal of Cell Biology 218 (8):2677-2698. doi:10.1083/jcb.201812076

81. Sanford JL, Mays TA, Rafael-Fortney JA (2004) CASK and Dlg form a PDZ protein complex at the mammalian neuromuscular junction. Muscle Nerve 30 (2):164-171. doi:10.1002/mus.20073

82. Hodge JJ, Mullasseril P, Griffith LC (2006) Activity-dependent gating of CaMKII autonomous activity by Drosophila CASK. Neuron 51 (3):327-337. doi:10.1016/j.neuron.2006.06.020

83. Lu CS et al. (2003) Regulation of the Ca2+/CaM-responsive pool of CaMKII by scaffold-dependent autophosphorylation. Neuron 40 (6):1185-1197. doi:Doi 10.1016/S0896-6273(03)00786-4

84. Jeyifous O et al. (2009) SAP97 and CASK mediate sorting of NMDA receptors through a previously unknown secretory pathway. Nat Neurosci 12 (8):1011-1019. doi:10.1038/nn.2362

nn.2362 [pii]

85. Omkumar RV et al. (1996) Identification of a phosphorylation site for calcium/calmodulindependent protein kinase II in the NR2B subunit of the N-methyl-D-aspartate receptor. J Biol Chem 271 (49):31670-31678. doi:10.1074/jbc.271.49.31670

86. Bayer KU, De Koninck P, Leonard AS, Hell JW, Schulman H (2001) Interaction with the NMDA receptor locks CaMKII in an active conformation. Nature 411 (6839):801-805. doi:Doi 10.1038/35081080

87. Hoskins R, Hajnal AF, Harp SA, Kim SK (1996) The C. elegans vulval induction gene lin-2 encodes a member of the MAGUK family of cell junction proteins. Development 122 (1):97-111

88. Kaech SM, Whitfield CW, Kim SK (1998) The LIN-2/LIN-7/LIN-10 complex mediates basolateral membrane localization of the C. elegans EGF receptor LET-23 in vulval epithelial cells. Cell 94 (6):761-771

89. Horvitz HR, Sulston JE (1980) Isolation and genetic characterization of cell-lineage mutants of the nematode Caenorhabditis elegans. Genetics 96 (2):435-454

90. Ferguson EL, Horvitz HR (1985) Identification and characterization of 22 genes that affect the vulval cell lineages of the nematode Caenorhabditis elegans. Genetics 110 (1):17-72

91. Alewine C, Kim BY, Hegde V, Welling PA (2007) Lin-7 targets the Kir 2.3 channel on the basolateral membrane via a L27 domain interaction with CASK. Am J Physiol Cell Physiol 293 (6):C1733-1741. doi:10.1152/ajpcell.00323.2007

92. Gross GG et al. (2013) X11/Mint genes control polarized localization of axonal membrane proteins in vivo. J Neurosci 33 (19):8575-8586. doi:10.1523/JNEUROSCI.5749-12.2013

93. Hansen KG et al. (2018) An ER surface retrieval pathway safeguards the import of mitochondrial membrane proteins in yeast. Science 361 (6407):1118-+. doi:10.1126/science.aar8174

94. Ferrari I, Crespi A, Fornasari D, Pietrini G (2016) Novel localisation and possible function of LIN7 and IRSp53 in mitochondria of HeLa cells. Eur J Cell Biol 95 (8):285-293. doi:10.1016/j.ejcb.2016.05.001

95. Poston CN, Krishnan SC, Bazemore-Walker CR (2013) In-depth proteomic analysis of mammalian mitochondria-associated membranes (MAM). J Proteomics 79:219-230. doi:10.1016/j.jprot.2012.12.018

96. Hung V et al. (2017) Proteomic mapping of cytosol-facing outer mitochondrial and ER membranes in living human cells by proximity biotinylation. Elife 6. doi:ARTN e24463 10.7554/eLife.24463

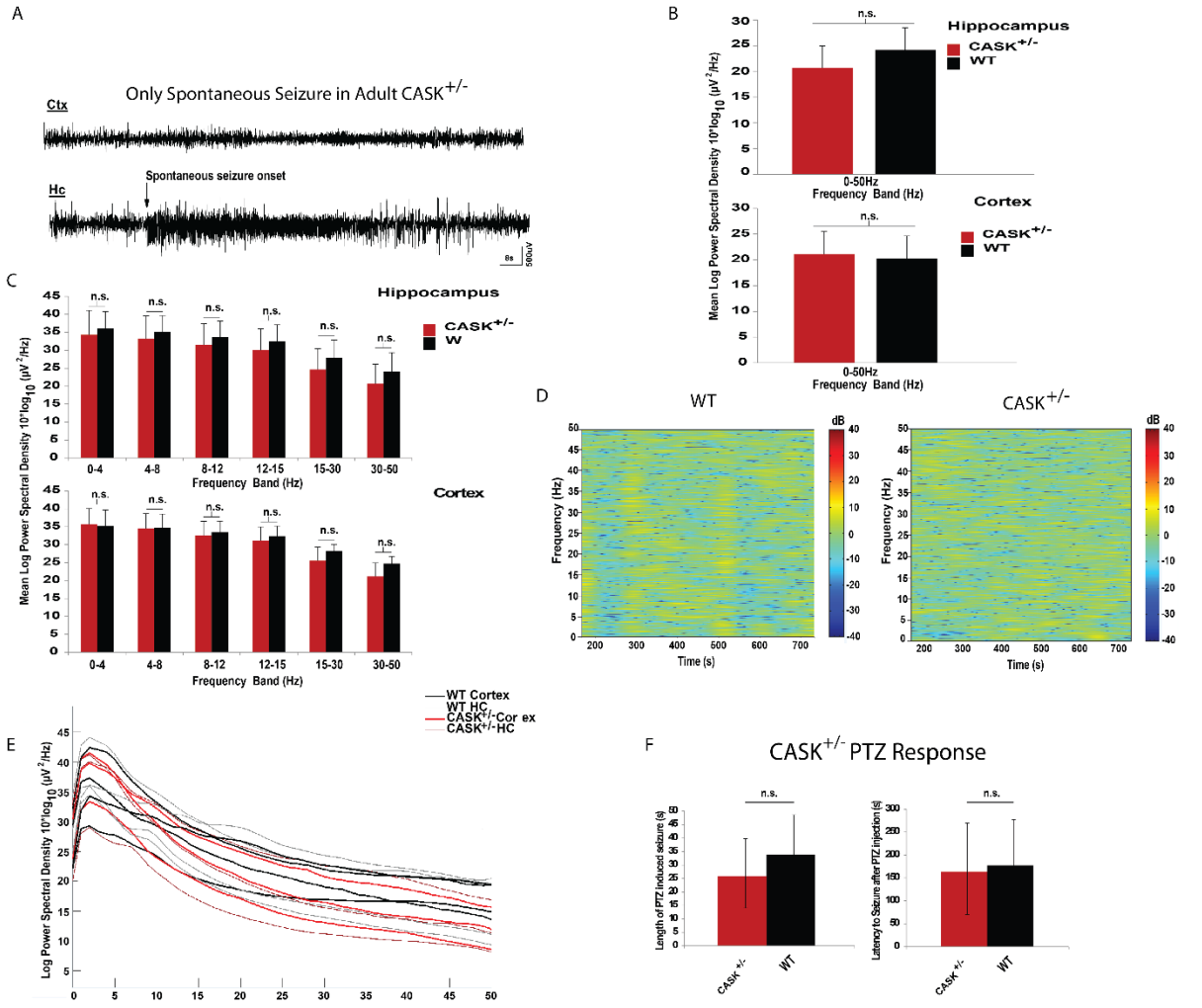

Figure 1: Electroencephalographic analysis of *Cask*$^{+/-}$ mice. A) The only spontaneous hippocampal (Hc) seizure recorded with vEEG, with corresponding cortical (Ctx) recording. B) Mean power in the 0-50Hz frequency range for cortical and hippocampal electrode placements. C) Mean power binned into biologically relevant frequency bands including delta, theta, alpha, beta, and gamma. D) Qualitative power spectral density over 15 minutes comparing a single *Cask*$^{+/-}$ and WT mouse. E) Shape of power spectral density versus frequency curve for each individual mouse (n=4 wild-type, 3 *Cask*$^{+/-}$ for B, C, and E). F) Latency to PTZ-induced seizure and length of PTZ-induced seizures for

each genotype (n=3 wild-type, 5 *Cask*$^{+/-}$). Comparisons for B, C, and F were made using a two-tailed Student's t-test for each frequency band; data represent mean±SEM.

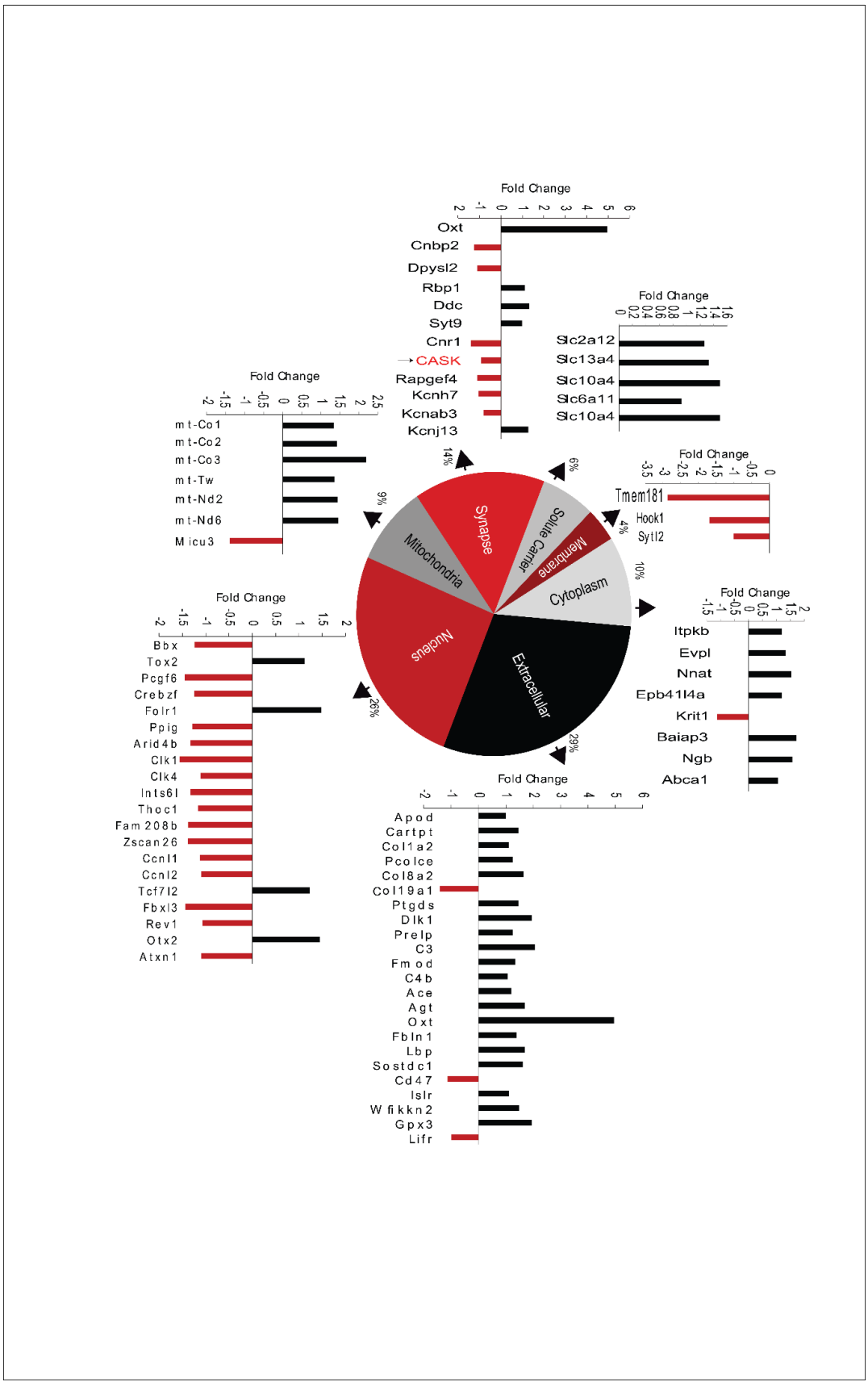
Fold Change
Oxt
Cnbp2
Dpysl2
Rbp1
Ddc
Syt9
Cnr1
CASK
Rapgef4
Kcnh7
Kcnab3
Kcnj13
Fold Change
Slc2a12
Slc13a4
Slc10a4
Slc6a11
Slc10a4
Fold Change
mt-Co1
mt-Co2
mt-Co3
mt-Tw
mt-Nd2
mt-Nd6
Micu3
Fold Change
Tmem181
Hook1
Sytl2
14%
6%
9%
4%
10%
26%
29%
Synapse
Solute Carrier
Membrane
Cytoplasm
Mitochondria
Nucleus
Extracellular
Fold Change
Bbx
Tox2
Pcgf6
Crebzf
Folr1
Ppig
Arid4b
Clk1
Clk4
Ints6l
Thoc1
Fam208b
Zscan26
Ccnl1
Ccnl2
Tcf7l2
Fbxl3
Rev1
Otx2
Atxn1
Fold Change
Itpkb
Evpl
Nnat
Epb41l4a
Krit1
Baiap3
Ngb
Abca1
Fold Change
Apod
Cartpt
Col1a2
Pcolce
Col8a2
Col19a1
Ptgds
Dlk1
Prelp
C3
Fmod
C4b
Ace
Agt
Oxt
Fbln1
Lbp
Sostdc1
Cd47
Islr
Wfikkn2
Gpx3
Lifr

Figure 2: Transcriptomic changes in brains of *Cask*$^{+/-}$ mice. Results from RNAseq were analyzed. 105 genes with $p<0.05$ were observed. A pie chart depicts enrichment in particular pathways and relative contribution to total changes. Redness indicates negative-fold change and blackness reflects positive-fold change. The fold change of genes in individual groups has been plotted as indicated by arrows. Comparisons were made using the false discovery rate (FDR) (Benjamini-Hochberg) corrected Likelihood Ratio Test (LRT) in the R-package DESeq2. Note that the GO:0005737 classification "cytoplasm" includes all genes which do not fall under nuclear, transmembrane, or extracellular; therefore, we manually curated genes into their respective subcellular compartments with the "cytoplasm" category in figure 2 containing only those transcripts which could not be otherwise grouped.

#	GO term help	Description	I^A	I^B	odds ratio help	p-value
1	GO:0005737	CYTOPLASM	115 (259)	3957 (29877)	3.35	4.02e-32
2	GO:0005515	PROTEIN BINDING	86 (259)	3804 (29877)	2.61	5.43e-15
3	GO:0003779	ACTIN BINDING	21 (259)	264 (29877)	9.18	1.70e-11
4	GO:0005886	PLASMA MEMBRANE	54 (259)	2255 (29877)	2.76	5.35e-09
5	GO:0045202	SYNAPSE	19 (259)	297 (29877)	7.38	1.43e-08
6	GO:0016020	MEMBRANE	92 (259)	5600 (29877)	1.90	9.85e-08
7	GO:0005856	CYTOSKELETON	25 (259)	664 (29877)	4.34	7.88e-07
8	GO:0043025	NEURONAL CELL BODY	16 (259)	262 (29877)	7.04	1.15e-06
9	GO:0000502	PROTEASOME COMPLEX	8 (259)	58 (29877)	15.91	3.07e-05

A

10	GO:0005516	CALMODULIN BINDING	10 (259)	116 (29877)	9.94	5.97e-05
11	GO:0000166	NUCLEOTIDE BINDING	38 (259)	1792 (29877)	2.45	0.00025
12	GO:0005839	PROTEASOME CORE COMPLEX	5 (259)	19 (29877)	30.36	0.0004

B

pathway ID	Description	Number of input genes	p-value
GO:0051603	PROTEOLYSIS INVOLVED IN CELLULAR PROTEIN CATABOLIC PROCESS	5	0.035
GO:0006904	VESICLE DOCKING INVOLVED IN EXOCYTOSIS	3	0.045
GO:0048168	REGULATION OF NEURONAL SYNAPTIC PLASTICITY	3	0.055
GO:0060048	CARDIAC MUSCLE CONTRACTION	3	0.075
GO:0051693	ACTIN FILAMENT CAPPING	3	0.075
GO:0007416	SYNAPSE ASSEMBLY	3	0.075

GO:0006520	CELLULAR AMINO ACID METABOLIC PROCESS	3	0.095
GO:0050885	NEUROMUSCULAR PROCESS CONTROLLING BALANCE	4	0.115
RN00260	GLYCINE, SERINE AND THREONINE METABOLISM	4	0.135
GO:0015031	PROTEIN TRANSPORT	17	0.195
GO:0007399	NERVOUS SYSTEM DEVELOPMENT	11	0.235
GO:0010976	POSITIVE REGULATION OF NEURON PROJECTION DEVELOPMENT	3	0.255
GO:0048169	REGULATION OF LONG-TERM NEURONAL SYNAPTIC PLASTICITY	3	0.255
GO:0016337	CELL-CELL ADHESION	5	0.265

#	GO term help	Description	I^A	I^B	odds ratio help	p-value
1	GO:0005739	MITOCHONDRION	54 (225)	1354 (29876)	5.30	1.69e-21
2	GO:0005737	CYTOPLASM	82 (225)	3957 (29876)	2.75	5.77e-16
3	GO:0006810	TRANSPORT	47 (225)	1618 (29876)	3.86	8.30e-13
4	GO:0005743	MITOCHONDRIAL INNER MEMBRANE	19 (225)	303 (29876)	8.33	1.71e-09
5	GO:0000166	NUCLEOTIDE BINDING	44 (225)	1792 (29876)	3.26	2.53e-09
6	GO:0070469	RESPIRATORY CHAIN	10 (225)	55 (29876)	24.14	8.50e-09
7	GO:0022900	ELECTRON TRANSPORT CHAIN	11 (225)	98 (29876)	14.90	1.77e-07
8	GO:0005525	GTP BINDING	17 (225)	322 (29876)	7.01	3.71e-07
9	GO:0003723	RNA BINDING	21 (225)	528 (29876)	5.28	5.68e-07
10	GO:0015031	PROTEIN TRANSPORT	20 (225)	478 (29876)	5.56	6.17e-07
11	GO:0045202	SYNAPSE	15 (225)	297 (29876)	6.71	7.34e-06

C

12	GO:0005515	PROTEIN BINDING	60 (225)	3804 (29876)	2.09	1.10e-05

D

pathway ID	Description	Number of input genes	p-value
GO:0006122	MITOCHONDRIAL ELECTRON TRANSPORT, UBIQUINOL TO CYTOCHROME C	3	0.01
GO:0022900	ELECTRON TRANSPORT CHAIN	11	0.01
GO:0006734	NADH METABOLIC PROCESS	3	0.01
GO:0006107	OXALOACETATE METABOLIC PROCESS	3	0.025
GO:0015031	PROTEIN TRANSPORT	20	0.035
GO:0006886	INTRACELLULAR PROTEIN TRANSPORT	10	0.055
GO:0008380	RNA SPLICING	11	0.055
RN00020	CITRATE CYCLE (TCA CYCLE)	4	0.075
GO:0006397	MRNA PROCESSING	12	0.135
GO:0006096	GLYCOLYSIS	4	0.155
GO:0006184	GTP CATABOLIC PROCESS	6	0.175
GO:0007017	MICROTUBULE-BASED PROCESS	3	0.215

Figure 3: Protein changes in *Cask*$^{+/-}$ mouse brain. iTraq proteomic results were analyzed using bioprofiling.de web interface for ProfCom and R spider analysis (Antonov, Schmidt et al. 2008, Antonov, Schmidt et al. 2010). A) Top 12 GO changes noted upon analysis of the proteins that were found at increased levels in CASK+/- mouse brain. B) Top 12 functional changes noted upon analysis of the proteins that were found at increased levels in *Cask*$^{+/-}$ mouse brain. C) Top 12 GO changes in proteins that were found at decreased levels in *Cask*$^{+/-}$ mouse brain. D) Top 12 top functional changes in proteins that were found to be decreased in *Cask*$^{+/-}$ mouse brain. IA is the ratio of changes within the particular GO group to total changes (enrichment observed). IB is the ratio of the total number of proteins in that GO group in the database to the total number of proteins in the database (enrichment by chance). The odds ratio strength of association is calculated as IA/ IB.

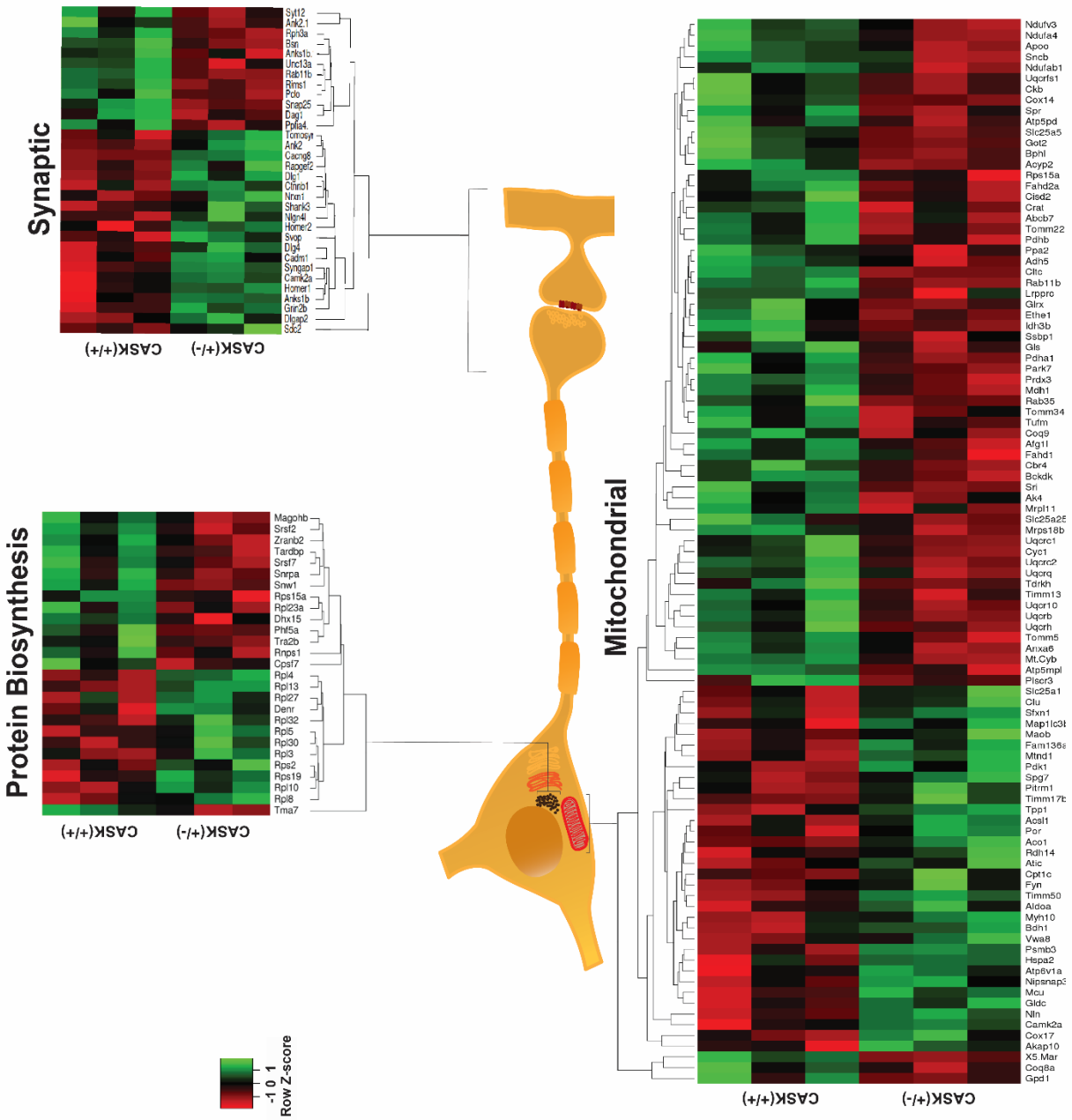
Synaptic
Syt12
Ank2.1
Rph3a
Rsn
Arhgap1b
Unc13a
Rab11b
Rims1
Pclo
Snap25
Dag1
Ppfia4
Tomosyn
Ank2
Cacng8
Rapgef2
Dlg1
Cfinio1
Nrxn1
Shank3
Nlgn4l
Homer2
Svop
Dlg4
Cadm1
Syngap1
Camk2a
Homer1
Arhgap1b
Grin2b
Dlgap2
Sdc2
CASK(+/+)
CASK(-/-)
Protein Biosynthesis
Magohb
Srsf2
Zranb2
Tardbp
Srsf7
Snrpa
Snw1
Rps15a
Rpl23a
Dhx15
Phf5a
Tra2b
Rnps1
Cpsf7
Rpl4
Rpl13
Rpl27
Denr
Rpl32
Rpl5
Rpl30
Rpl3
Rps2
Rps19
Rpl10
Rpl8
Tma7
CASK(+/+)
CASK(-/-)
Mitochondrial
Ndufv3
Ndufa4
Apoo
Sncb
Ndufab1
Uqcrfs1
Ckb
Cox14
Spr
Atp5pd
Slc25a5
Got2
Bphl
Acyp2
Rps15a
Fahd2a
Cisd2
Crat
Abcb7
Tomm22
Pdhb
Ppa2
Adh5
Cltc
Rab11b
Lrpprc
Glrx
Ethe1
Idh3b
Ssbp1
Gls
Pdha1
Park7
Prdx3
Mdh1
Rab35
Tomm34
Tufm
Coq9
Afg1l
Fahd1
Cbr4
Bckdk
Sri
Ak4
Mrpl11
Slc25a25
Mrps18b
Uqcrc1
Cyc1
Uqcrc2
Uqcrq
Tdrkh
Timm13
Uqcr10
Uqcrb
Uqcrh
Tomm5
Anxa6
Mt.Cyb
Atp5mpl
Plscr3
Slc25a1
Clu
Sfxn1
Map1lc3b
Maob
Fam136a
Mtnd1
Pdk1
Spg7
Pitrm1
Timm17b
Tpp1
Acsl1
Por
Aco1
Rdh14
Atic
Cpt1c
Fyn
Timm50
Aldoa
Myh10
Bdh1
Vwa8
Psmb3
Hspa2
Atp6v1a
Nipsnap3
Mcu
Gldc
Nln
Camk2a
Cox17
Akap10
X5.Mar
Coq8a
Gpd1
CASK(+/+)
CASK(-/-)
Row Z-score
-1 0 1

Figure 4. Protein changes encompassing protein synthetic, synaptic and mitochondrial pathways in *Cask*$^{+/-}$ mouse brain. iTraq proteomic results from Figure 3 were analyzed and subdivided into subcellular compartments using NIH DAVID and manual curation. 526 proteins, including CASK, are altered. Pathways altered were identified using NIH DAVID functional annotation database. Heat maps of three major pathways were plotted using heatmapper.ca. Neuron and organelle diagrams are for stylistic purposes only, subcellular proteomics was not conducted.

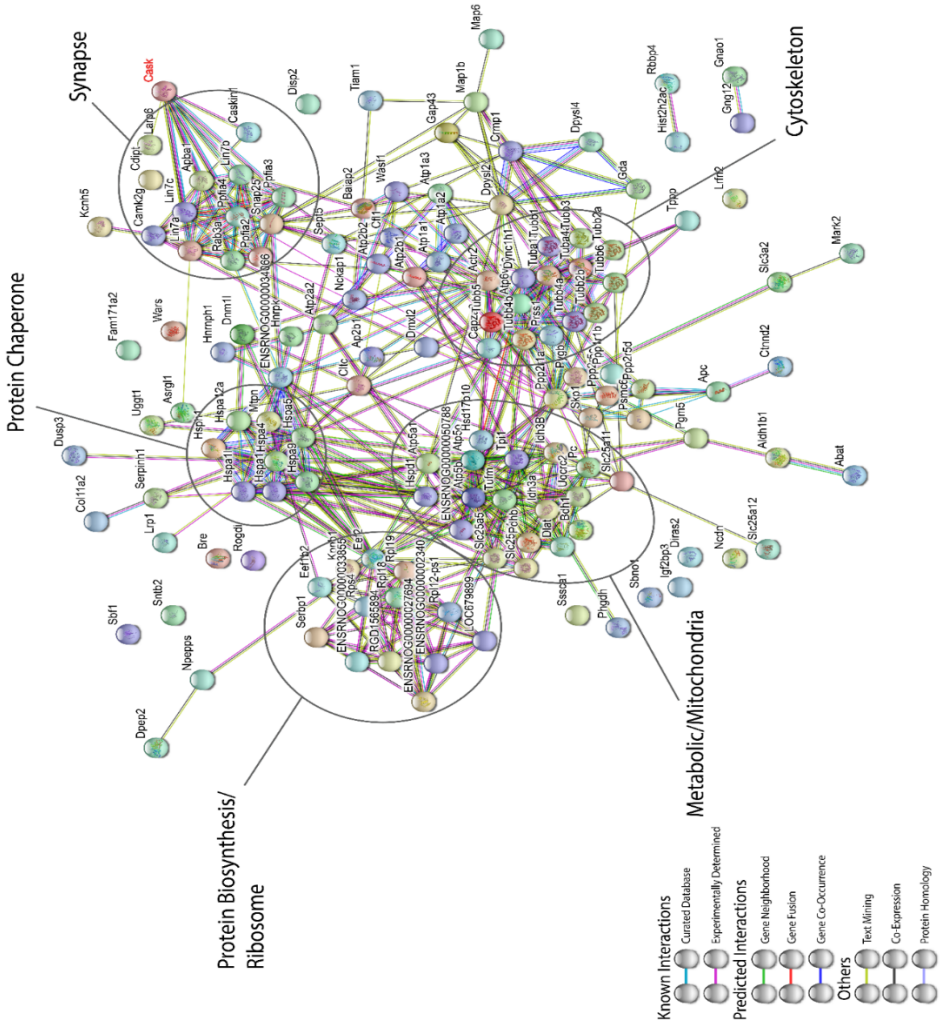

Figure 5. Brain proteins identified to be interacting with GFP-CASK through GFP-Trap mass spectrometry analysis are plotted using the STRING database interface. Protein clusters belonging to a specific pathway are indicated with ellipses. Color of strings between proteins indicates whether an interaction is experimentally determined or predicted as per the legend. Solved structures are indicated within each sphere for a given protein.

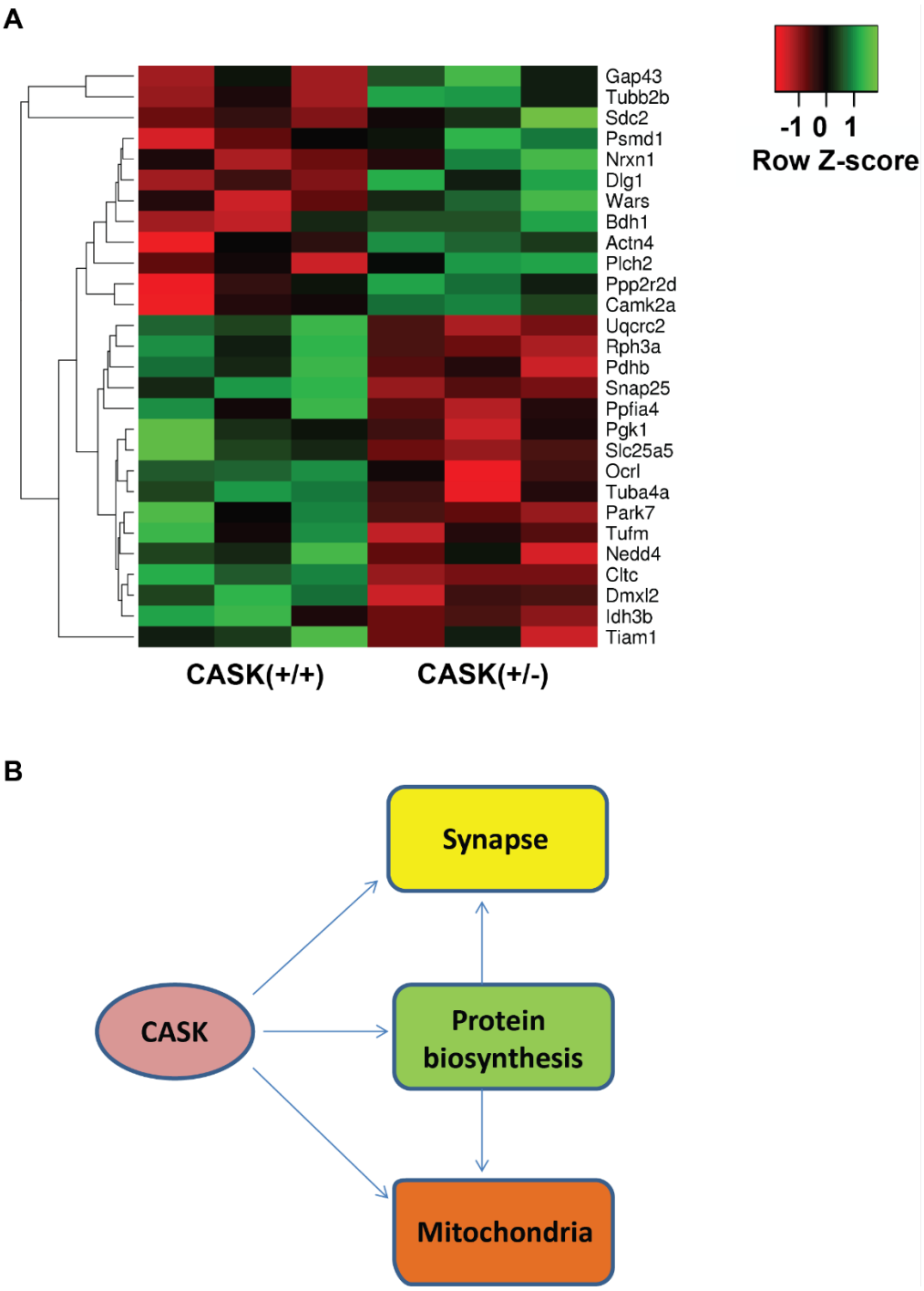

Figure 6. CASK interacting proteins exhibit both increase and decrease in *Cask*$^{+/-}$ mouse brain. A) Heat map of proteins found to interact with CASK that are also significantly changed in the iTRAQ proteomics data. B) A model indicating three cellular pathways that are likely to be altered by CASK haploinsufficiency. Our model highlights the

likelihood that changes seen in mRNA processing and ribosomal proteins themselves impact other pathways.

Preface: Chapter 3.3 outlines a case report describing the first indication we had that CASK-linked disorders may have a more complex pathological trajectory than initially hypothesized. The case outlines a human with an early truncation in the CASK protein that precludes any functional protein products and so allows for a description of phenotypes present in a human without CASK. This work was published in *Molecular Genetics and Genomic Medicine* in 2020.

3.3 Survival of a male patient harboring CASK Arg27Ter mutation to adolescence

Konark Mukherjee[1*], Paras A Patel[1], Deepa S Rajan[2], Leslie E. W. LaConte[1], and Sarika Srivastava[1*]

[1]Fralin Biomedical Research Institute at Virginia Tech Carilion, 2 Riverside Circle, Roanoke, VA, 24016, USA

[2]Children's Hospital of Pittsburgh of UPMC, University of Pittsburgh, Pittsburgh, PA, 15213, USA

* Corresponding Authors: Konark Mukherjee and Sarika Srivastava

Email: konark@vtc.vt.edu; Sarika_Srivastava@vtc.vt.edu

Running Title: CASK R27* mutation

Key words: CASK, microcephaly, cerebellar hypoplasia, epileptic encephalopathy, electroencephalogram

Abstract

Background: *CASK* is an X-linked gene in mammals and its deletion in males is incompatible with life. *CASK* heterozygous mutations in female patients associate with intellectual disability, microcephaly, pontocerebellar hypoplasia, and optic nerve hypoplasia, whereas *CASK* hemizygous mutations in males manifest as early infantile epileptic encephalopathy with a grim prognosis. Here, we report a rare case of survival of a male patient harboring a *CASK* null mutation to adolescent age.

Methods: Trio-whole-exome sequencing analysis was performed from blood genomic DNA. Magnetic resonance imaging (MRI), magnetic resonance spectroscopy (MRS), and electroencephalogram (EEG) analyses were performed to determine anomalies in brain development, metabolite concentrations, and electrical activity, respectively.

Results: Trio-WES analysis identified a de novo c.79C>T (p.Arginine27Ter) mutation in *CASK* causing a premature translation termination at the very N-terminus of the protein. The 17-year, 11-months-old male patient displays a profound intellectual disability, microcephaly, dysmorphism, ponto-cerebellar hypoplasia, and intractable epilepsy. His systemic symptoms include overall reduced somatic growth, dysautonomia, ventilator and G-tube dependence, and severe osteopenia. Brain MRI revealed a severe cerebellar and brain stem hypoplasia with progressive cerebral atrophy. EEG spectral analysis revealed a global functional defect with generalized background slowing and delta waves dominating even in the awake state.

Conclusion: This case study is the first to report the survival of a male patient carrying a *CASK* loss-of-function mutation to adolescence and highlights that improved palliative

care could extend survival. Moreover, multiple independent occurrences of the p.Arginine27Ter mutation suggest that the genomic position encoding Arginine27 in *CASK* may exhibit increased susceptibility to mutations.

Introduction

Mutations in the X-linked gene *CASK* (OMIM: 300172) are associated with intellectual disability, microcephaly and pontocerebellar hypoplasia (Najm, Horn et al. 2008, Moog, Kutsche et al. 2011, Burglen, Chantot-Bastaraud et al. 2012, Hayashi, Okamoto et al. 2012, LaConte, Chavan et al. 2018, LaConte, Chavan et al. 2019). *CASK* was found to be an essential gene for survival in mice, (Atasoy, Schoch et al. 2007, Srivastava, McMillan et al. 2016) and consistent with CASK's X-linked nature, the patient population predominantly consists of females harboring a single mutant allele. *CASK* mutations in human males have been described in literature and include missense mutations exhibiting partial loss-of-function, mosaicism due to somatic mutation in the developing embryo, as well as more profound mutations such as deletion of exon 2 and mutation in the start codon where no protein product has been detected (Hackett, Tarpey et al. 2010, Saitsu, Kato et al. 2012, Moog, Bierhals et al. 2015, Kerr, Patel et al. 2019). Patients with undetectable CASK protein exhibit prominent cerebellar hypoplasia and defects in the electroencephalogram (EEG) including multifocal epileptic discharges and burst-suppression and thus receive the diagnosis of Ohtahara syndrome (Saitsu, Kato et al. 2012). Other reports describe subjects with *CASK* null mutations that lack functional CASK protein, including a male patient with the CASK mutation p.Arg27Ter; this subject

exhibited pontocerebellar hypoplasia, hypotonia, ventricular septal defect, optic atrophy, and intractable seizures with burst-suppression pattern as observed by EEG (Moog, Bierhals et al. 2015). The CASK (p.Arg27Ter) mutation has also been described in females with severe pontocerebellar hypoplasia but no seizures were found (Hayashi, Uehara et al. 2017). Notably, loss-of-function mutations in the *CASK* gene are reported to be associated with reduced viability in females and lethality in males either *in utero* or during infancy (Najm, Horn et al. 2008, Moog, Bierhals et al. 2015, Hayashi, Uehara et al. 2017, Rama Devi, Lingappa et al. 2019). Here, we report a clinical case of a male patient at 17 years and 11 months of age who harbors the CASK (p.Arg27Ter) null mutation and exhibits extended survival to adolescence, raising the possibility that palliative care (Boersma, Miyasaki et al. 2014, Dallara and Tolchin 2014, Oliver 2018) could extend survival of male patients even in the absence of a functional CASK protein.

Methods

Ethical Compliance: The Virginia Tech Institutional Review Board approved the collection and use of data from the subject. Informed consent was obtained from the family prior to participation.

The genomic DNA was extracted from peripheral blood cells and exons from the *CASK* gene (NM_003688.3) were captured using the Agilent SureSelect V5 enrichment kit followed by sequencing on an Illumina HiSeq 2000, as previously described (Aldinger, Timms et al. 2019). Quantitative analysis of the EEG was done by manually binning each channel into biologically relevant frequency bands, calculating the mean power spectral density of each band, and plotting the average from each band.

Case Report and Results

We report a male patient at 17 years and 11 months of age who presented with severe intellectual disability, microcephaly, and seizures. He was first evaluated at birth in the NICU (neonatal intensive care unit) due to concerns about dysmorphism and microcephaly. Neuroimaging at that time revealed severe cerebellar hypoplasia, ventriculomegaly, and brain stem atrophy/hypoplasia. A three-generation pedigree revealed no known family history of neurological disorders or epilepsy (Figure 1A). The patient has been followed by neurology since first appearance. Given the profound hypotonia and poor feeding, he underwent G tube placement and Nissen fundoplication prior to discharge from the NICU at 8 weeks of age. He was subsequently noted to have severe hypotonia, profound developmental delay, microcephaly, and growth retardation in early childhood. Given a history of recurrent respiratory infections and chronic aspiration, he underwent tracheostomy around age 3 and has been ventilator-dependent since then. He is currently non-ambulatory with severe central hypotonia and increased appendicular tone. Secondary complications have included recurrent respiratory infections requiring hospitalization, severe osteopenia with pathologic fractures, deep vein thrombosis and autonomic instability (fluctuating body temperature, flushing, heart rate variability). Examinations of other organ systems are mostly unremarkable. Brain magnetic resonance imaging (MRI) revealed severe hypoplasia of the cerebellum and the brain stem (Figure 1B). A progressive atrophy of the supratentorial compartment is also observed, a feature that is shared by the previously described male. Magnetic resonance

(MR) spectroscopy indicated a moderate decrease in n-acetyl aspartate and an increase in choline peaks.

At birth in the NICU, the patient was noted to have a severely abnormal EEG with marked disorganized background and a hypsarrhythmia pattern. Initial seizure semiology was felt to be consistent with myoclonic seizures. The EEG eventually evolved into a burst-suppression pattern reminiscent of the infantile Ohtahara syndrome (Figure 2A). Subsequently, his seizure semiology has included tonic seizures, myoclonic seizures, and complex partial seizures. Currently, his seizures are intractable, with daily seizures despite multiple antiepileptic medications including Clobazam, Lamotrigine, Clonazepam, and Levetiracetam. He was noted to have a severe bone marrow suppression with Carbamezepine, and hyperammonemia with Valproic acid. Epileptiform activity in the form of spikes are easily observed in EEG and in 2 hours of recording a single electroclinical seizure of indeterminate onset was observed. Spectral analysis of the EEG traces confirmed an overall slowing with delta waves dominating even in the awake condition (Figure 2B).

The family underwent a diagnostic odyssey with multiple clinical diagnoses considered since birth until the trio whole exome sequencing (Trio-WES) test recently established his molecular diagnosis. Trio-WES analysis revealed that the patient has a *de novo CASK* (RefSeq NM_003688.3); c.79C>T (p.Arg27Ter) mutation in the second exon of the gene which introduces a nonsense mutation leading to premature translation termination at the arginine in 27th position (i.e. R27*). The R27 residue is present at the beginning of the N-terminal canonical protein kinase domain of CASK (Mukherjee,

Sharma et al. 2008). Based on the genotype, it is unlikely that the brain can express any functional CASK protein from different transcript isoforms.

4 DISCUSSION

This case report describes for the first time an extended clinical course of a male patient harboring the *CASK* p.Arg27Ter mutation. Because CASK is essential for survival, it has not been possible to study the phenotypic consequences caused by constitutive *CASK* deletion in mice as it leads to neonatal death (Atasoy, Schoch et al. 2007). The subject described here likely survived due to palliative care involving early tracheostomy and G-tube insertion (Chan and Devaiah 2009, Oliver 2018) in the NICU, as well as administration and adjustment of anti-epileptic drugs, which provided an opportunity to gain insights into the consequences of *CASK* null mutation beyond the neonatal period and on into adolescence.

Although *CASK* mutations are rare, multiple independent mutations arising at the same locus of a gene suggest that the specific locus may possess a higher susceptibility to mutation. We previously reported pathogenic genetic mutations in *CASK* that produce MICPCH (e.g. L209P and M519T) which arose independently in different individuals (LaConte, Chavan et al. 2018, LaConte, Chavan et al. 2019). The CASK p.Arg27Ter mutation has been previously described in two girls and two boys (Yang, Muzny et al. 2014, Moog, Bierhals et al. 2015, Hayashi, Uehara et al. 2017). Intriguingly, we are aware of a two-year-old boy with the p.Arg28Ter mutation exhibiting infantile spasm, dystonia, and developmental delay. The p.Arg28Ter mutation was also previously reported in a girl with intellectual disability, pontine and cerebellar atrophy who developed spasms at 3

years of age, but the seizures were controlled with antiepileptic drugs (Michaud, Lachance et al. 2014). Finally, the variant p.Arg28Leu has been described in a male patient presenting with FG syndrome (Piluso, D'Amico et al. 2009). Thus, the clustering of mutations at these two arginine residues (i.e. R27 and R28) at the beginning of the N-terminal kinase domain of CASK suggests that this region may constitute a mutational hotspot. In fact, the arginine codon 'CGA' is known to be a hotspot for conversion into a stop codon due to a C-to-T transition (Cowell, Smith et al. 1994, Cooper, Mort et al. 2010). Premature stop codons not only truncate the protein but also activate machinery for the nonsense-mediated decay of RNA (Romanov and Sukhoverov 2017).

Although haploinsufficiency of the *CASK* gene in females might present with seizures with incomplete penetrance (~40%) (Moog, Uyanik et al. 1993), hemizygous *CASK* mutations in males produces catastrophic neurodevastation and epileptic encephalopathy (Saitsu, Kato et al. 2012, Moog, Bierhals et al. 2015). *CASK* is an X-linked gene and is thus subject to random inactivation in females. *CASK* mutations therefore generate mosaicism in female brains, with only 50% of cells expressing the mutant version of CASK; this may explain the diminished severity of phenotypes in girls. In fact, both of the girls reported to have the heterozygous CASK p.Arg27Ter mutation exhibited microcephaly, pontocerebellar hypoplasia, and profound intellectual disability, but no seizures (Hayashi, Uehara et al. 2017). Surprisingly, in murine models, no secondary selection of CASK-positive cells has been noted, and to some extent, the function of CASK seems to be non-cell autonomous (Srivastava, McMillan et al. 2016, Kerr, Patel et al. 2019).

The subject described here, a male with CASK p.Arg27Ter mutation, shares similarities with the previously reported case (Moog, Bierhals et al. 2015) in having short stature, seizures with EEG abnormalities, severe pontocerebellar hypoplasia, and microcephaly. Although the previous case manifested with a relevant ventricular septal defect (VSD) and cardiac insufficiency, cardiac functioning is normal in our patient. Strikingly, in both reported cases of CASK p.Arg27Ter mutation in males, a progressive cerebral atrophy has been noted (Yang, Muzny et al. 2014, Moog, Bierhals et al. 2015). The precise mechanisms by which CASK loss produces a profound neurodevelopmental/degenerative defect or seizures remains uncertain. It has been suggested that CASK may act via its interaction with Tbr1 (Hsueh, Wang et al. 2000), but in a murine model, disruption of the CASK-Tbr1 interaction did not produce any structural defects or epilepsy (Huang 2016). CASK is also a presynaptic scaffolding molecule (Butz, Okamoto et al. 1998, Mukherjee, Sharma et al. 2008), and thus lack of CASK could produce synaptic defects. However, in a murine model of constitutive *CASK* deletion, it was reported that CASK loss did not affect the core neuronal functions of excitability, calcium-dependent presynaptic release, or postsynaptic receptor arrangement (Atasoy, Schoch et al. 2007). The only changes observed in the constitutive *CASK* deletion murine model were in action potential-independent spontaneous release (Atasoy, Schoch et al. 2007). It is unlikely that a minor electrophysiological change alone would manifest as such a profound neurodevelopmental condition. Recent work suggests that CASK may play critical roles in regulating mitochondrial, cytoskeletal, and protein biosynthetic functions (Mukherjee, Slawson et al. 2014, Srivastava, McMillan et al. 2016, Patel, Liang et al.

2020), but how these diverse functions of CASK relate to the observed disorder remains to be investigated.

Finally, boys with *CASK* mutations may present with Ohtahara syndrome, a type of epileptic encephalopathy displaying a burst-suppression EEG pattern (Saitsu, Kato et al. 2012, Moog, Bierhals et al. 2015). Epileptic encephalopathies are a heterogeneous group of epileptic disorders accompanied by a progressive encephalopathy (Khan and Al Baradie 2012). It has been argued that refractory seizures in epileptic encephalopathies may contribute to this progression (Howell, Harvey et al. 2016). The patient described here exhibited infantile spasms, which is also a type of epileptic encephalopathy that is often accompanied by a hypsarrhythmia pattern in the interictal EEG. Over time, the patient's EEG pattern evolved to display a burst-suppression pattern mimicking Ohtahara syndrome and subsequently evolved into tonic and myoclonic seizures. It is possible that with a genetic etiology of epileptic encephalopathy such as *CASK* mutation, the epileptic seizures may be a part of progressive encephalopathy, rather than a primary event, and hence evolve over time (encephalopathy with epilepsy) (Khan and Al Baradie 2012, Helbig, von Deimling et al. 2017). Notably, a more general analysis of the patient's EEG at the age of 17 years indicated an overall slowing, as well as pronounced attenuation.

In conclusion, with early clinical management and interventions that assist with respiration and nutrient delivery (palliative care), subjects born without functional CASK protein may develop beyond infancy, albeit with profound neurodevelopmental disability. Future studies are warranted to examine the underlying pathogenic mechanisms and associated diverse functions of CASK.

Acknowledgments: KM and PP are supported by R01EY024712 from the NIH's National Eye Institute to KM.

Conflict of Interest

The authors declare no potential conflict of interest.

References

Aldinger, K. A. et al. (2019). Redefining the Etiologic Landscape of Cerebellar Malformations. *Am J Hum Genet, 105*(3), 606-615. doi:10.1016/j.ajhg.2019.07.019

Atasoy, D. et al. (2007). Deletion of CASK in mice is lethal and impairs synaptic function. *Proc Natl Acad Sci U S A, 104*(7), 2525-2530. doi:0611003104 [pii]10.1073/pnas.0611003104

Boersma, I., Miyasaki, J., Kutner, J., & Kluger, B. (2014). Palliative care and neurology: time for a paradigm shift. *Neurology, 83*(6), 561-567. doi:10.1212/WNL.0000000000000674

Burglen, L. et al. (2012). Spectrum of pontocerebellar hypoplasia in 13 girls and boys with CASK mutations: confirmation of a recognizable phenotype and first description of a male mosaic patient. *Orphanet Journal of Rare Diseases, 7*, 18. doi:1750-1172-7-18 [pii]10.1186/1750-1172-7-18

Butz, S., Okamoto, M., & Sudhof, T. C. (1998). A tripartite protein complex with the potential to couple synaptic vesicle exocytosis to cell adhesion in brain. *Cell, 94*(6), 773-782.

Chan, T., & Devaiah, A. K. (2009). Tracheostomy in palliative care. *Otolaryngol Clin North Am, 42*(1), 133-141, x. doi:10.1016/j.otc.2008.09.002

Cooper, D. N. et al. (2010). Methylation-mediated deamination of 5-methylcytosine appears to give rise to mutations causing human inherited disease in CpNpG trinucleotides, as well as in CpG dinucleotides. *Human Genomics, 4*(6), 406. doi:10.1186/1479-7364-4-6-406

Cowell, J. K., Smith, T., & Bia, B. (1994). Frequent constitutional C to T mutations in CGA-arginine codons in the RB1 gene produce premature stop codons in patients with bilateral (hereditary) retinoblastoma. *Eur J Hum Genet, 2*(4), 281-290. doi:10.1159/000472372

Dallara, A., & Tolchin, D. W. (2014). Emerging subspecialties in neurology: palliative care. *Neurology, 82*(7), 640-642. doi:10.1212/WNL.0000000000000121

Hackett, A. et al. (2010). CASK mutations are frequent in males and cause X-linked nystagmus and variable XLMR phenotypes. *Eur J Hum Genet, 18*(5), 544-552. doi:ejhg2009220 [pii]10.1038/ejhg.2009.220

Hayashi, S. et al. (2012). Novel intragenic duplications and mutations of CASK in patients with mental retardation and microcephaly with pontine and cerebellar hypoplasia (MICPCH). *Hum Genet, 131*(1), 99-110. doi:10.1007/s00439-011-1047-0

Hayashi, S. et al. (2017). Comprehensive investigation of CASK mutations and other genetic etiologies in 41 patients with intellectual disability and microcephaly with pontine and cerebellar hypoplasia (MICPCH). *PLoS One, 12*(8). doi:ARTN e018179110.1371/journal.pone.0181791

Helbig, I., von Deimling, M., & Marsh, E. D. (2017). Epileptic Encephalopathies as Neurodegenerative Disorders. *Neurodegenerative Diseases: Pathology, Mechanisms, and Potential Therapeutic Targets, 15*, 295-315. doi:10.1007/978-3-319-57193-5_11

Howell, K. B., Harvey, A. S., & Archer, J. S. (2016). Epileptic encephalopathy: Use and misuse of a clinically and conceptually important concept. *Epilepsia, 57*(3), 343-347. doi:10.1111/epi.13306

Hsueh, Y. P., Wang, T. F., Yang, F. C., & Sheng, M. (2000). Nuclear translocation and transcription regulation by the membrane-associated guanylate kinase CASK/LIN-2. *Nature, 404*(6775), 298-302. doi:10.1038/35005118

Huang, T. N. a. H., Y.P. . (2016). Calcium/calmodulin-dependent serine protein kinase (CASK), a protein implicated in mental retardation and autism-spectrum disorders, interacts with T-Brain-1 (TBR1) to control extinction of associative memory in male mice. *Journal of Psychiatry and Neuroscience*. doi: 10.1503/jpn.150359

Kerr, A. et al. (2019). Non-Cell Autonomous Roles for CASK in Optic Nerve Hypoplasia. *Invest Ophthalmol Vis Sci, 60*(10), 3584-3594. doi:10.1167/iovs.19-27197

Khan, S., & Al Baradie, R. (2012). Epileptic encephalopathies: an overview. *Epilepsy Res Treat, 2012*, 403592. doi:10.1155/2012/403592

LaConte, L. E. W. et al. (2019). An N-terminal heterozygous missense CASK mutation is associated with microcephaly and bilateral retinal dystrophy plus optic nerve atrophy. *American Journal of Medical Genetics Part A, 179*(1), 94-103. doi:10.1002/ajmg.a.60687

LaConte, L. E. W. et al. (2018). Two microcephaly-associated novel missense mutations in CASK specifically disrupt the CASK-neurexin interaction. *Hum Genet, 137*(3), 231-246. doi:10.1007/s00439-018-1874-3

Michaud, J. L. et al. (2014). The genetic landscape of infantile spasms. *Hum Mol Genet, 23*(18), 4846-4858. doi:10.1093/hmg/ddu199

Moog, U. et al. (2015). Phenotypic and molecular insights into CASK-related disorders in males. *Orphanet Journal of Rare Diseases, 10*, 44. doi:10.1186/s13023-015-0256-3

Moog, U. et al. (2011). Phenotypic spectrum associated with CASK loss-of-function mutations. *J Med Genet, 48*(11), 741-751. doi:jmedgenet-2011-100218 [pii]10.1136/jmedgenet-2011-100218

Moog, U., Uyanik, G., & Kutsche, K. (1993). CASK-Related Disorders. In M. P. Adam, H. H. Ardinger, R. A. Pagon, S. E. Wallace, L. J. H. Bean, K. Stephens, & A. Amemiya (Eds.), *GeneReviews((R))*. Seattle (WA).

Mukherjee, K. et al. (2008). CASK Functions as a Mg2+-independent neurexin kinase. *Cell, 133*(2), 328-339. doi:10.1016/j.cell.2008.02.036S0092-8674(08)00287-0 [pii]

Mukherjee, K., Slawson, J. B., Christmann, B. L., & Griffith, L. C. (2014). Neuron-specific protein interactions of Drosophila CASK-beta are revealed by mass spectrometry. *Front Mol Neurosci, 7*, 58. doi:10.3389/fnmol.2014.00058

Najm, J. et al. (2008). Mutations of CASK cause an X-linked brain malformation phenotype with microcephaly and hypoplasia of the brainstem and cerebellum. *Nat Genet, 40*(9), 1065-1067. doi:10.1038/ng.194

Oliver, D. (2018). Improving patient outcomes through palliative care integration in other specialised health services: what we have learned so far and how can we improve? *Annals of Palliative Medicine*, S219-S230.

Patel, P. A. et al. (2020). Haploinsufficiency of X-linked intellectual disability gene CASK induces post-transcriptional changes in synaptic and cellular metabolic pathways. *Exp Neurol, 329*, 113319. doi:10.1016/j.expneurol.2020.113319

Piluso, G. et al. (2009). A missense mutation in CASK causes FG syndrome in an Italian family. *Am J Hum Genet, 84*(2), 162-177. doi:S0002-9297(09)00009-3 [pii]10.1016/j.ajhg.2008.12.018

Rama Devi, A. R., Lingappa, L., & Naushad, S. M. (2019). Identification and in Silico Characterization of a Novel CASK c.2546T>C (p.V849A) Mutation in a Male Infant with Pontocerebellar Hypoplasia. *Ann Indian Acad Neurol, 22*(4), 523-524. doi:10.4103/aian.AIAN_2_19

Romanov, G. A., & Sukhoverov, V. S. (2017). Arginine CGA codons as a source of nonsense mutations: a possible role in multivariant gene expression, control of mRNA quality, and aging. *Molecular Genetics and Genomics, 292*(5), 1013-1026. doi:10.1007/s00438-017-1328-y

Saitsu, H. et al. (2012). CASK aberrations in male patients with Ohtahara syndrome and cerebellar hypoplasia. *Epilepsia, 53*(8), 1441-1449. doi:10.1111/j.1528-1167.2012.03548.x

Srivastava, S. et al. (2016). X-linked intellectual disability gene CASK regulates postnatal brain growth in a non-cell autonomous manner. *Acta Neuropathol Commun, 4*, 30. doi:10.1186/s40478-016-0295-6

Yang, Y. P. et al. (2014). Molecular Findings Among Patients Referred for Clinical Whole-Exome Sequencing. *Jama-Journal of the American Medical Association, 312*(18), 1870-1879. doi:10.1001/jama.2014.14601

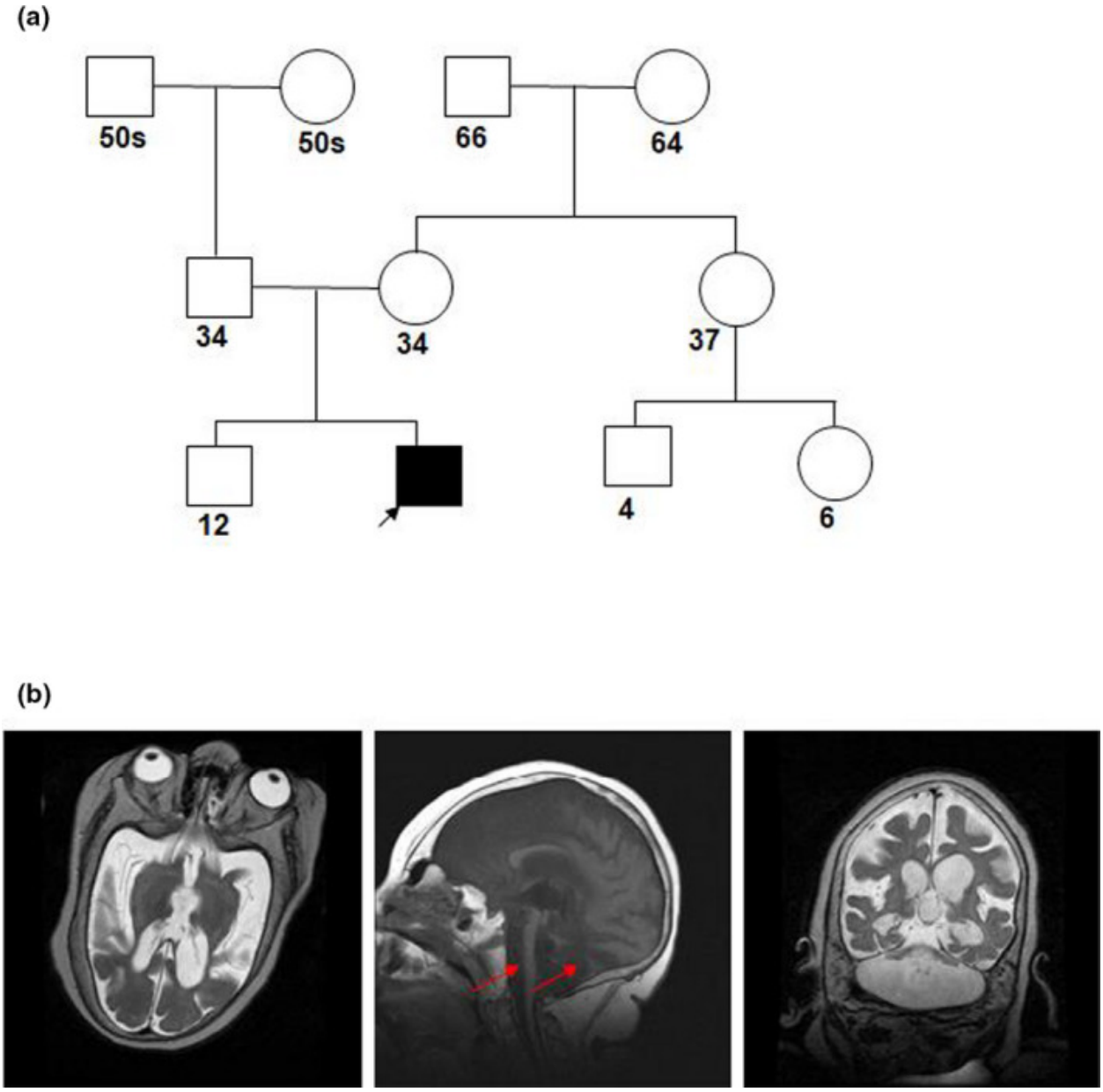

Figure 1 Pedigree chart and brain magnetic resonance imaging of the patient. A) Represents a three-generation pedigree chart demonstrating the non-inherited nature of the disorder. There is no remarkable history of the neurological disorder in the family. The numbers represent age in years and blackened square represent the proband. B) MRI scan of the patient obtained at 5 years of age revealed severe hypoplasia of the cerebellum and brain stem (represented by red arrowheads) along with a supratentorial

volume loss. The left, middle, and right panels depict the transverse, sagittal, and coronal planes, respectively.

(a)

(b)

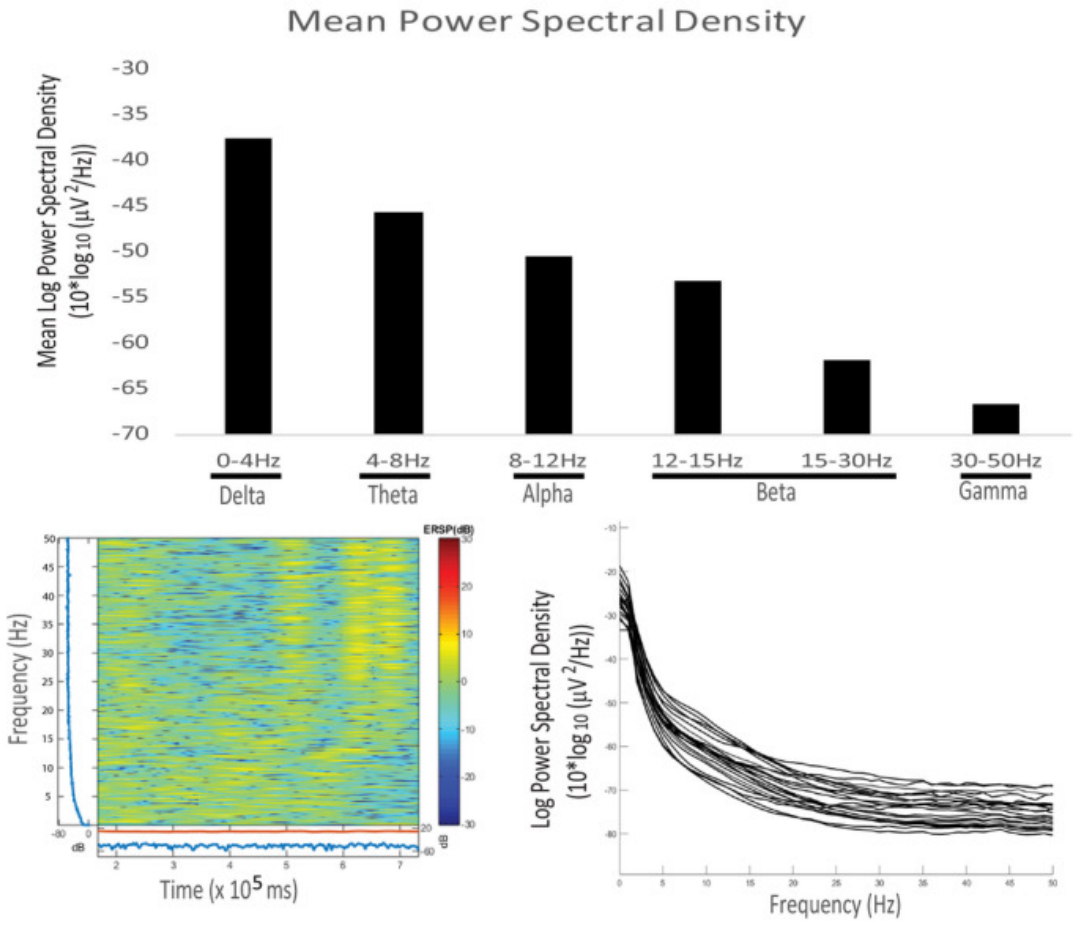
Mean Power Spectral Density
Mean Log Power Spectral Density (10*log10 (μV2/Hz))
-30
-35
-40
-45
-50
-55
-60
-65
-70
0-4Hz
Delta
4-8Hz
Theta
8-12Hz
Alpha
12-15Hz
15-30Hz
Beta
30-50Hz
Gamma
Frequency (Hz)
Time (x 10^5 ms)
ERSP(dB)
Log Power Spectral Density (10*log10 (μV2/Hz))
Frequency (Hz)

Figure 2 Electroencephalogram analysis of the patient. A) The EEG showing prolonged periods of attenuation and burst-suppression along with a disorganized background and multifocal spikes. B) Spectral analysis of the EEG at 17 years of age indicating generalized slowing. Qualitative power spectral density over 15 minutes is shown on the bottom left and the power spectral density for each channel over the entire recording is shown on the bottom right.

Preface: Chapter 3.4 describes the culmination of investigations into CASK-linked pathologies as outlined herein utilizing a human case of early truncation similar to that described in chapter 3.3. Leveraging another human case of arginine 27 to STOP, we identified molecular signatures of cell death and extended that into a novel murine model wherein CASK is deleted from cerebellar cells post-development to make findings illuminating the pathological trajectory of brain morphological abnormalities in the absence of CASK in human and mouse at different points in the lifespan. This work was published in the *Journal of Medical Genetics* in 2022.

3.4 Complete loss of X-linked gene CASK causes severe cerebellar degeneration

Paras A Patel[1,2], Julia Hegert[5], Ingrid Cristian[5], Alicia Kerr[2,3], Leslie EW LaConte[2,6], Michael A Fox[3,4], Sarika Srivastava[2,7] and Konark Mukherjee[2,,8*]

[1]Translational Biology, Medicine, and Health Graduate Program, Fralin Biomedical Research Institute, Roanoke, VA 24016, USA

[2]Center for Neurobiology Research, Fralin Biomedical Research Institute, Roanoke, VA 24016, USA

[3]Virginia Tech, Department of Biological Sciences, Blacksburg, VA 24060, USA

[4]Virginia Tech, School of Neuroscience, Blacksburg, VA, 24060, USA

[5]Orlando Health, APH, MP 331, USA

[6] Virginia Tech Carilion School of Medicine, Department of Basic Science Education, Roanoke, VA 24016, USA.

[7] Department of Internal Medicine, Virginia Tech Carilion School of Medicine, Roanoke, VA 24016, USA.

[8]Department of Psychiatry, Virginia Tech Carilion School of Medicine, Roanoke, VA 24016, USA.

* Corresponding Author, Konark Mukherjee,

FBRI, 2 Riverside Cir., Roanoke, VA 24014

Fax: 540-985-3373

Telephone: 540-526-2035

Email: konark@vtc.vt.edu,

One sentence summary of study: CASK loss causes cerebellar degeneration.

Abstract

Background: Heterozygous loss of X-linked genes like CASK and MeCP2 (Rett syndrome) causes developmental delay in girls, while in boys loss of the only allele of these genes leads to epileptic encephalopathy. The mechanism for these disorders remains unknown. CASK-linked cerebellar hypoplasia is presumed to result from defects in Tbr1-reelin-mediated neuronal migration.

Method: Here we report clinical and histopathological analyses of a deceased 2-month-old boy with a CASK-null mutation. We next generated a mouse line where CASK is completely deleted (hemizygous and homozygous) from post-migratory neurons in the cerebellum.

Result: The CASK-null human brain was smaller in size but exhibited normal lamination without defective neuronal differentiation, migration, or axonal guidance. The hypoplastic cerebellum instead displayed astrogliosis and microgliosis, markers for neuronal loss. We therefore hypothesize that CASK loss-induced cerebellar hypoplasia is the result of early neurodegeneration. Data from the murine model confirmed that in CASK loss, a small cerebellum results from post-developmental degeneration of cerebellar granule neurons. Further, at least in the cerebellum, functional loss from CASK deletion is secondary to degeneration of granule cells and not due to an acute molecular functional loss of CASK. Intriguingly, female mice with heterozygous deletion of CASK in the cerebellum do not display neurodegeneration.

Conclusion: We suggest that X-linked neurodevelopmental disorders like CASK mutation and Rett syndrome are pathologically neurodegenerative; random X-chromosome

inactivation in heterozygous mutant girls, however, results in 50% of cells expressing the functional gene, resulting in a non-progressive pathology, whereas complete loss of the only allele in boys leads to unconstrained degeneration and encephalopathy.

Word count=250 (excluding headings)

Keywords: CASK, MICPCH, neurodegeneration, X-linked, X-inactivation, cerebellum, ataxia

Introduction

Heterozygous mutations in certain X-linked genes (e.g., CDKL5, MeCP2 in Rett syndrome, and CASK in MICPCH (mental retardation and microcephaly with pontine and cerebellar hypoplasia (OMIM: 300749)) are linked to postnatal microcephaly in girls (Seltzer and Paciorkowski 2014). Hemizygous mutations in these same genes give rise to progressive epileptic encephalopathy and lethality in boys (Kankirawatana, Leonard et al. 2006, Saitsu, Kato et al. 2012, Jakimiec, Paprocka et al. 2020). Rett syndrome was the first such disorder to be reported; it was described as a cerebral atrophic syndrome by Andreas Rett in 1966 (Rett 1966). Until the 1990s, Rett syndrome was considered a neurodegenerative disorder (FitzGerald, Jankovic et al. 1990). With the discovery, however, of the MeCP2 gene association, postmortem autopsy observations, and the development of preclinical models, focus shifted to dendritic morphology and synapse development and dysfunction, resulting in the re-classification of Rett syndrome as a neurodevelopmental disorder (Neul and Zoghbi 2004) (Zoghbi 2003). Studies of the cellular pathology associated with MeCP2 loss in boys with epileptic encephalopathies have, however, been limited (Schule, Armstrong et al. 2008).

MICPCH is also considered a neurodevelopmental disorder that occurs due to heterozygous mutations in the X-linked gene CASK (calcium/calmodulin-dependent serine protein kinase) in girls. Despite the microcephaly associated with CASK mutation being described as postnatal and progressive, females with MICPCH grow into adulthood, often with intellectual disability that is non-progressive (Najm, Horn et al. 2008, Moog, Kutsche et al. 2011, Burglen, Chantot-Bastaraud et al. 2012, Takanashi, Okamoto et al.

2012, LaConte, Chavan et al. 2018). Such mutations in hemizygous males are, however, lethal. These boys exhibit epileptic encephalopathy with pronounced cerebellar hypoplasia and progressive supratentorial atrophy (Saitsu, Kato et al. 2012, Moog, Bierhals et al. 2015, Mukherjee, Patel et al. 2020). Regression of motor skills has also been noted in a girl with MICPCH in adolescence (Nishio, Kidokoro et al. 2020). The cellular pathology of CASK-linked disorders remains uncertain. This problem is exacerbated by the fact that CASK-null mice die within hours of birth and do not exhibit a difference in brain size or morphology from their wild type littermates at birth (Atasoy, Schoch et al. 2007). Based on the standard Theiler developmental staging of mice (Xue, Cai et al. 2013), the immediate postnatal period of mice best parallels the third trimester of human fetal development (Carnegie staging; (O'Rahilly and Muller 2010)), making any interpretation of postnatal brain pathology difficult.

Although often considered to be a component of presynaptic terminals, CASK in fact is ubiquitously expressed in the body (Hata, Butz et al. 1996, Stevenson, Laverty et al. 2000) and has been implicated in a variety of functions outside the brain, including cell polarization (Caruana 2002), renal development, and cardiac conductivity (Ahn, Kim et al. 2013, Beaudreuil, Zhang et al. 2019), (Eichel, Beuriot et al. 2016, Beuriot, Eichel et al. 2020). CASK is proposed to be involved in axonal branching (Kuo, Hong et al. 2010), dendritic arborization (Gao, Piguel et al. 2018), dendrite spinogenesis (Chao, Hong et al. 2008), and synaptogenesis (Samuels, Hsueh et al. 2007). Thus, many hypotheses as to why loss of CASK leads to defects in brain development can be proposed. CASK null mice, however, fail to exhibit any defects in synaptogenesis or neuronal morphology. The

only detectable phenotype is a change in action potential-independent neurotransmission (Atasoy, Schoch et al. 2007).

CASK also has a function in regulating gene transcription (Hsueh, Wang et al. 2000, Wang, Hong et al. 2004, Wang, Ding et al. 2004). It has been suggested that CASK translocates to the nucleus, where it regulates the function of T-box transcription factor (Tbr-1) (Bredt 2000, Hsueh, Wang et al. 2000). It is proposed that CASK forms a ternary complex with CINAP (CASK-interacting nucleosome assembly protein) and Tbr-1 to induce expression of molecules such as reelin that play a crucial role in brain development (Wang, Hong et al. 2004). Reelin is a secreted extracellular molecule critical for neuronal migration (Hirotsune, Takahara et al. 1995). Indeed, both in the reeler mice and Tbr-1 knockout mice, defects in proper lamination of cortex are seen (Hamburgh 1963, Hevner, Shi et al. 2001). In addition to the cortex defects, reeler mice also display a hypoplastic disorganized cerebellum with defects in neuronal migration and suppressed neurogenesis (Hamburgh 1963). The neurodevelopmental function of CASK has been specifically attributed to CASK's interaction with Tbr-1 and its presumed regulation of reelin expression (Najm, Horn et al. 2008, Takanashi, Arai et al. 2010, Namavar, Barth et al. 2012). Although the molecular role of CASK has been attributed to Tbr-1 binding or synaptic function, Tbr-1 null mice themselves show no difference in size of other brain regions including the cortex and cerebellum other than a smaller olfactory bulb (Hevner, Shi et al. 2001). Further, complete abrogation of the CASK-Tbr1 interaction fails to induce any structural defect in the brain or cerebellum (Huang and Hsueh 2017). Similarly, abolishing synaptic function does not seem to affect brain development in embryonic mice

or brain structure in postnatal mice (Verhage, Maia et al. 2000, Sando, Bushong et al. 2017). Thus it is unlikely that these purported functions of CASK can account for the changes seen in MICPCH. Using a murine model, we previously demonstrated that the histopathology of cerebellar hypoplasia in MICPCH involves a reduction in the number of cells in the internal granular layer (IGL) (Srivastava, McMillan et al. 2016). This could either be due to changes in the development of granule cells or the loss of granule cells after formation (degeneration), as seen in the weaver mouse (Cendelin 2014).

Here, we report a detailed clinical description and autopsy findings from a 2-month-old boy harboring the CASK null mutation R27* (R27Ter). Although the brain is small, the clear presence of tertiary gyri that form near term, as well as proper cortical and cerebellar lamination, argue against defects in neuronal migration; instead, we uncover evidence of neuronal damage and loss (degeneration) suggested by reactive astrogliosis and microgliosis in the cerebellum. We then design and execute a genetic experiment in mice that provides conclusive evidence that loss of CASK indeed produces neurodegeneration (loss of developed neurons) in the cerebellum. Most pontocerebellar hypoplasias (PCH) are progressive, but based on the postnatal brain growth pattern, it has been hypothesized that MICPCH has a distinct pathogenic mechanism (van Dijk, Barth et al. 2020). We instead provide evidence that mechanistically, MICPCH in girls with heterozygous CASK mutations is also degenerative, and the non-progressive course of MICPCH is dictated by the unique X-linked inheritance pattern in which 50% of brain cells express the normal gene.

Materials and Methods

Statement of Ethics

All studies described herein were approved by the Virginia Tech Institutional Animal Care and Use Committee and Institutional Review Board.

Statistics

A two-tailed Student's t-test was used when comparing two genotypes in each experiment to compute significance with an alpha of 0.05.

Clinical History, EKG (Supplemental Figure 1) and EEG spectral analysis method

Please see Supplemental file.

Generation of Mouse Lines

Calb2-Cre mice (strain 010774) were obtained from Jackson Laboratory, *Cask*^{floxed} mice (strain 006382) were a kind gift from Prof. Thomas Südhof. *Cask*^{floxed} females were bred with *Calb2*-Cre positive males to generate the F1 cross *Cask*^{floxed}::*Calb2*-Cre. F1 mice were bred to Ai14-LSL-tdTomato-positive males obtained from Jackson Laboratory (strain 007914) to generate fluorescent reporter mice. F1 mice were genotyped by PCR using primers targeted at either LoxP elements, a sequence within the Cre gene, or a sequence within the tdTomato gene. All lines were from a C57BL/6J background backcrossed for at least 25 generations.

Antibodies and Material Reagents

Bassoon monoclonal antibodies were obtained from Enzo Lifescience, GFAP (glial fibrillary acidic protein) monoclonal antibodies were obtained from Invitrogen, calbindin (D28K) polyclonal antibody from Invitrogen, synaptophysin, NeuN and S100β antibodies were obtained from Sigma and Iba1 antibody was obtained from FUJIFILM Wako.

Secondary antibodies conjugated with AlexaFluor 488, 550 and 633 were obtained from Thermofisher. Hardset Vectashield™ with DAPI was obtained from Vector Laboratories.

Immunostaining of Mouse Tissue

For all immunostaining, mice were sacrificed by trans-cardiac perfusion first with phosphate buffered saline (PBS) for exsanguination and subsequently with 4% paraformaldehyde for fixation of tissues. Brains were dissected and post-fixed for at least 24 hours in 4% paraformaldehyde. After post-fixation, brains were hemisected along the longitudinal fissure and 50μm sagittal sections were cut using a ThermoScientific™ Microm HM650V Vibratome. Sections were submerged in permeabilization/blocking solution composed of 10% fetal bovine serum and 1% Triton-X 100 in PBS overnight at +4°C.

Rabbit anti-calbindin was diluted at 1:50 in blocking solution and mouse anti-bassoon was diluted at 1:200 in blocking solution. Rabbit anti-NeuN antibody was diluted at 1:50. For glial immunostaining, mouse anti-GFAP was diluted at 1:200 in blocking solution and mouse anti-S100B was diluted at 1:1000. After blocking/permeabilization overnight, free-floating sections were incubated for 3 hours in dilute primary antibody at room temperature. After incubation in primary antibody, sections were washed 3 times for 5 minutes in PBS before being incubated in secondary antibody for the respective host species for 1 hour at room temperature. Sections were again washed and mounted on slides using VECTASHIELD® anti-fade medium. Synapse quantification was performed using the automated SynQuant algorithm (Wang, Wang et al. 2020).

Immunostaining of Human Tissue

Human tissue obtained during autopsy was post-fixed in 10% formalin overnight, embedded in paraffin, and subsequently sectioned into 20μm sections onto charged slides. Slides were deparaffinized with 3 changes of poly-xylenes for 10 minutes each time and rehydrated using an ethanol gradient from 100%-95%-70%-50%-H_2O for 5 minutes in each condition. Antigen retrieval was conducted by boiling slides in 10mM sodium citrate buffer with 0.1% Tween-20 for 10 minutes in a domestic microwave followed by running the slides under cold tap water for 10 minutes. Immunostaining for GFAP, calbindin, synaptophysin, S100B, and Iba1 (rabbit polyclonal antibody diluted at 1:500) was then conducted using the same procedure described for mouse tissue. Control tissue was obtained from a female born at 30 post conception weeks and died at 6 PNW.

Motor Behavioral Assays

Accelerating Rotarod experiments were conducted by placing 4 *Cask*$^{(floxed)}$::*Calb2*-Cre mice at P100 (post-ataxia onset), at P48 (pre-ataxia onset), and age-matched *Cask*$^{(floxed)}$ control mice on an accelerating Rotarod, beginning at 2 cycles/minute and accelerating at a rate of 5 cycles/minute until mice fell off the platform. Three trials were conducted in succession for each mouse, with 5 minutes of rest between trials.

Results

Complete CASK loss in humans causes encephalopathy and cerebellar atrophy

MICPCH subjects with heterozygous CASK mutations are known to live past their 30s. *Cask*$^{+/-}$ female mice are fertile beyond 6 months. We have allowed four *Cask*$^{+/-}$ mice to age more than two years (considered to be old for mice). All four mice survived to that

age without adverse events. We did not observe any obvious phenotypes in these aged mice compared to wild-type littermates. The cerebellum displayed the typical layers and configuration without severe deterioration, indicating that the disorder is non-progressive (Supplemental Figure 2).

Null mutation of *CASK* in mice is, however, lethal and in boys, produces progressive encephalopathy. Due to the early lethality of *Cask* null mice, the postnatal pathology of complete *Cask* loss has been difficult to study to date. Here we describe detailed clinical findings and autopsy results from a 2-month-old boy with a *CASK* null mutation who expired due to hypoventilation and neurogenic respiratory failure. A copy number variation study was unremarkable, but next generation sequencing of genes revealed a de novo c.79C>T (p.Arginine27Ter) *CASK* mutation in exon 2 (Figure 1A). This *CASK* mutation introduces a stop codon in the very N-terminus of the CASK protein, precluding expression of any splice variant of CASK (Supplemental Figure 3). Magnetic resonance imaging (MRI) indicated normal lateral and third ventricles with an elongated fourth ventricle. The cerebellum appeared markedly hypoplastic without a vermis. The small posterior fossa was filled with fluid (Figure 1B). The corpus callosum was thin but present without any midline shift, and myelination was delayed for age. The cavum septum pellucidum seemed to be more prominent. No heterotopic cells were noted in any area, but there was some degree of smoothening, particularly of the frontal cortex. The brain stem appeared to be extremely thin.

Video electroencephalographic (vEEG) monitoring was done both during awake and sleeping states. Awake-state background EEG displayed a burst-suppression

pattern with variable amounts of bursts and suppressions (Figure 1F and Supplemental Figure 4). This EEG pattern is typical of Ohtahara syndrome, a devastating epileptic encephalopathy that usually co-occurs with *CASK*-null mutations (Saitsu, Kato et al. 2012, Moog, Bierhals et al. 2015, Mukherjee, Patel et al. 2020). The burst phase was dominated by a mixture of theta and delta waves. Overall, the EEG retained its symmetry in both hemispheres but was discontinuous. No electroclinical seizures were observed during the two hours period of recording, although intermittent and independent sharp waves were observed, predominantly in the right temporal and occipital region. The sleep EEG was similar to the waking EEG and included burst-suppression signals. A spectral analysis of the entire epoch revealed skewing towards lower frequency with delta and alpha power dominating the spectra (Figure 1D-G).

At autopsy, head circumference was 32.7 cm, with a 37.0 cm crown-rump length and crown-heel length of 51.0 cm. The decedent was small for his age, and the brain weight was 300.8 grams, which is 60% of what is expected at this age (Supplemental Figure 5). Except for lung, heart, and spleen, most other organs were smaller than expected but had an overall normal gross appearance (autopsy report). The brain was well formed with normal gyrification in the cerebral hemispheres. Tertiary gyri were present, and there was no evidence of polymicrogyria or other abnormal configuration. The Sylvian fissure was well formed, and the leptomeninges were clear (Figure 2A). Vascularization, including the circle of Willis, was normally formed. The central part of the cerebral hemispheres was edematous, and the septum cavum pellucidum was present (0.9 cm in vertical length). The basal ganglia displayed a normal architecture bilaterally. The left

hippocampus was also architecturally normal with a serpiginous appearance. The right hippocampus had a blurred appearance (Supplemental Figure 6 and autopsy report). The thalamus was normally formed and firm. The lateral ventricles were not dilated; the midbrain was very small with a patent but pinpoint cerebral aqueduct, and the fourth ventricle was slit-like. The cerebellum and the pons were markedly hypoplastic (Figure 2A, Supplemental Figure 6). The cerebellum, despite hypoplasia, had a normal configuration but did not exhibit the usual folia. There was no evidence for heterotopia of cells. Although the cerebellum had grown both laterally and in length, it remained a very thin, leaf-like structure (Figure 2A). The anterior vermis was not identifiable and appeared to be membrane-like; cerebellar hemispheres were thin, flattened and firm (Supplemental Figure 7). The spinal cord was of uniform caliber and had no obvious pathology (autopsy report).

Absence of CASK does not affect neuronal migration, axonal guidance, or lamination in humans but may promote neuronal loss

Histologically, the cerebellum itself displayed proper cellular organization, with a defined external granular layer (EGL), molecular layer, and internal granular layer (IGL). The two-dimensional growth of the cerebellum, which is mediated by the formation of the Purkinje cell plate (Tissir and Goffinet 2003), remained unperturbed as described above, and there was a uniform single layer of developed Purkinje cells between the molecular layer and the internal granular layer. The dendritic arbors of Purkinje cells are clearly visible in the molecular layer (Figure 2B). Overall, the migration of Purkinje cells, which requires reelin (Tissir and Goffinet 2003), is largely unaffected. The R27ter subject's age

was 10 postnatal weeks (PNW), and comparisons were made with a cerebellum from a PNW 6 pre-term infant who died of a non-neurological cause around the same date. The migratory pattern of granule cells was visible and appropriate for age in the R27ter cerebellum, but the IGL appears hypocellular (Figure 2B,M and Supplemental Figure 7G,H). The dentate nucleus was absent, and the anterior vermis displayed very few granule cells (Supplemental Figure 7D and 8). Inferior olivary nuclei were poorly formed and did not display pseudohypertrophy. The midbrain consisted of astrocytic cells with pink cytoplasm and some neuronal cells, but no organized substantia nigra was noted (Supplemental Figure 9A). Sections of the cortex indicated orderly and proper neuronal migration; the germinal matrix was appropriately thinned for this age (Supplemental Figure 9B). The white matter tracts were discreet and adequate for the decedent's age (Supplemental Figure 6). The basal ganglia and hippocampi were properly organized and unremarkable. The midbrain and pons displayed corticospinal tracts. The cerebral aqueduct was patent and dilated. Within the pons, the pontine decussation was seen and the locus coeruleus properly formed (Supplemental Figure 9C). The medullary olives were poorly formed, and the fourth ventricle was widely patent. The spinal cord was unremarkable with adequate anterior horn cells and uniform radiating column. The central canal was patent throughout (Supplemental Figure 6 and official autopsy report).

Histologically, almost all organs including the bone marrow, heart, and intestines were unremarkable. The endocrine glands also appeared normal, except for the adrenal cortex, which was thinned out. The kidneys had appropriate and orderly glomerular and tubular development (Supplemental Figure 10C,D).

Data clearly indicate that although CASK loss affects the size of the brain globally, the cerebellum and brainstem are disproportionately affected. Both in murine models and the human subject, early lethality is likely linked with the dysfunction of the brainstem leading to respiratory failure. *Cask* null mice display hypoventilation and die within hours of birth although the brain is of normal size and properly laminated at death (Atasoy, Schoch et al. 2007).

The normal lamination and configuration of the brain in both CASK null humans and mice suggests that the histological pathology related to CASK loss is likely to be degenerative, with neuronal loss. Two common hallmarks of neuronal damage and neuronal loss are loss of synapses and reactive gliosis. We therefore next evaluated the cerebellum of the decedent for evidence of synapses and of gliosis (Figure 2C-J). Previous studies in the murine model have shown that CASK loss-of-function does not negatively impact synapse formation (Atasoy, Schoch et al. 2007, Srivastava, McMillan et al. 2016), and in the human cerebellum evaluated here, immunostaining revealed that levels of the synaptic marker synaptophysin in the decedent's cerebellar cortex were similar to levels observed in a control cerebellum (Figure 2C,E). Strikingly, the synaptophysin staining appeared to be mostly perisomatic for Purkinje cells, although punctae are also clearly visible in dendrites of the molecular layer (ML). This staining pattern is different than would be expected for the age; in typical development, the most prominent synaptophysin staining from 34 weeks onward is in the ML (Sarnat, Flores-Sarnat et al. 2013). Early in development, perisomatic synapses are mostly formed by climbing fibers which translocate postnatally to dendrites in the ML (Ichikawa, Yamasaki et al. 2011). Parallel

fibers (the axons of granule cells) also form synapses on Purkinje cell dendrites in the ML. The lack of synaptophysin staining in the ML is most likely attributable to the loss of abundant parallel fibers and incomplete translocation of the climbing fibers in the early postnatal phase. We next examined the cerebellum for the presence of gliosis; GFAP and S100β staining was done for astrocytes and Bergmann glia, and Iba1 staining was done for microglia, the resident immune cells of the brain critical for clearing dead cells and debris which often accumulate in regions of neurodegeneration (Figure 2 C,D) (Perry, Nicoll et al. 2010). Data indicate that, compared to the control, the decedent exhibits ~5-fold higher amounts of GFAP immunoreactivity, specifically in the IGL (Figure 2C,F). In fact, large reactive astrocytes in the IGL were readily observed only in the CASK null cerebellum (and Supplemental Figure 11). The CASK null brain also exhibited more microglia in the IGL (Figure 2 D,G). Finally we observed increased S100β immunoreactivity both in the ML and the IGL, with an increased number of S100β positive cells (Figure 2D,H-J). Together these data suggest that loss of CASK produces early neurodegenerative changes, causing the CASK-linked phenotype to typically manifest postnatally. Finally, we investigated myelination within the cerebellar cortex using FluoroMyelin lipid staining (Figure 2K) and observed that although the myelination pattern exhibited a disturbed arrangement within the IGL of the 10 PNW R27Ter subject, discrete myelinated tracts were noted, in contrast to the near-absent staining observed in the 6 PNW control subject, indicating progress of myelination with maturity (Figure 2 K,L). The number of cells in the IGL, however, was low (Figure 2M). The histological findings thus indicate that the disorganized white matter may be secondary to ongoing cerebellar grey

matter degeneration. In fact, the development and synaptogenesis of the fetal and neonatal cerebellum and its connections in humans are well described (Sarnat, Flores-Sarnat et al. 2013, Sarnat, Flores-Sarnat et al. 2013), and our study suggests that this process is not delayed or stalled; instead, the structures that develop earlier, such as the dentate nucleus, are earlier to degenerate. This same trend is seen in the cerebellar cortex, where the vermis, which develops earlier than the cerebellar hemispheres, appears to be highly atrophied and rudimentary (Sarnat, Flores-Sarnat et al. 2013, Sarnat, Flores-Sarnat et al. 2013). Based on our histological observations, we hypothesize that loss of CASK induces cerebellar cortical degeneration, specifically after migration of cerebellar glutamatergic cells such as granule cells or neurons of the dentate nucleus. To test this idea, we next employed murine genetic experiments, where CASK is deleted in a temporally and spatially specified manner using Cre-LoxP-mediated gene excision.

Calb2-Cre targets post-migratory granule cells and a subset of Purkinje cells in the cerebellum

Previous neuroimaging data and the comprehensive CASK null brain histological autopsy results presented here clearly indicate that within the brain, loss of CASK is likely to disproportionately affect the hindbrain including the brainstem and cerebellum. In particular, CASK-linked lethality most likely results from effects on the brain stem. To avoid any lethality, our focus, therefore, is to evaluate the long-term effect of CASK loss only in the cerebellum. We have previously demonstrated that CASK loss does not affect cerebellar development (Srivastava, McMillan et al. 2016). In order to test our hypothesis,

we needed to disassociate CASK loss from developmental migration of cerebellar neurons. To do so, we chose a mouse line in which Cre-recombinase is driven by an endogenous promoter of the signaling molecule *Calb2* (calretinin/calbindin2), reported earlier (Kerr, Patel et al. 2019). It has been shown that *Calb2* expresses in nearly all granule cells in the cerebellum (Schiffmann, Cheron et al. 1999, Bearzatto, Servais et al. 2006), but the exact timing of initiation of *Calb2*-Cre gene recombination in granule cells was not known. There have also been conflicting reports about the expression of *Calb2* in the Purkinje cells within the cerebellum (Schiffmann, Cheron et al. 1999, Bearzatto, Servais et al. 2006). We therefore first tested the recombination specificity of *Calb2*-Cre in mice at ages when the cerebellum is still developing and displays both the EGL and IGL (P8 and P15). We crossed *Calb2*-Cre mice with Cre-recombination indicator mice (LSL-tdTomato) (Figure 3A). The distribution of the tdTomato-expressing neurons serves as a proxy for CASK deletion when *Calb2*-Cre mice are crossed with *Cask*^{floxed} mice in parallel (Figure 3B). Our data indicate that *Calb2*-Cre is active in the cerebellum as early as P8. By P8, recombination was observed in granule cells but only after migration into the IGL; recombination was also observed in many post-migratory Purkinje cells (Figure 3C). By P15, Calb2-Cre already exhibited robust recombination in many parts of the brain and in the entirety of post-migratory granule cells. Dense cellular distribution with recombination was seen in the cerebellum, hippocampus, striatum and olfactory bulb. Sparsely distributed cells were observed throughout the brain, including the cortex (Figure 3D, E). The brainstem displayed minimal recombination, with sparsely tdTomato-labeled cells. Within the cerebellum, all granular cells in the IGL and a subset of post-migratory

Purkinje cells were positive for recombination at P15. Cells in the EGL, however, did not display any recombination, indicating that *Calb2*-Cre-driven recombination occurs only after migration of granule cells (Figure 3E). Our data thus indicate that *Calb2*-Cre specifically leads to deletion of CASK both in a subset of Purkinje cells and in granule cells after migration by P15 and is not likely to affect the brainstem or its function. Thus crossing *Calb2*-Cre with *Cask*^{floxed} line generates mice where CASK deletion is naturally synchronized to migration within different cerebellar neurons.

Deletion of CASK from cerebellar neurons results in later-onset progressive degeneration of the cerebellum and severe ataxia

We therefore next examined mice from crosses of the *Calb2*-Cre and *Cask*^{floxed} lines. It has been shown previously that the *Cask*^{floxed} mouse is a hypomorph that expresses ~40% CASK, likely due to a phenomenon known as selection cassette interference (Atasoy, Schoch et al. 2007). *Cask*^{floxed} mice are smaller than wild type mice and exhibit cerebellar hypoplasia (Atasoy, Schoch et al. 2007, Najm, Horn et al. 2008, Srivastava, McMillan et al. 2016). *Cask*^{floxed};*Calb2*-Cre F1 mice were genotyped by PCR.

Cask^{floxed};*Calb2*-Cre mice remain indistinguishable from the *Cask*^{floxed} mice well into adulthood (~40 days), indicating that acute deletion of *Cask* does not have significant effects on cerebellar development, motor learning, or locomotor function. Past two months of age, however, *Cask*^{floxed};*Calb2*-Cre mice begin displaying obvious locomotor incoordination and ataxia which are rapidly progressive. By approximately P100, these mice are profoundly ataxic, are unable to keep their balance and repeatedly fall over with an inability to walk forward (supplemental video). Despite profound motor coordination

deficits, the *Cask*^{floxed};*Calb2*-Cre mice are otherwise healthy and display a slick coat, good body condition score, and are bright, alert and responsive. Compared to littermate *Cask*^{floxed} controls, the cerebellum of the *Cask*^{floxed};*Calb2*-Cre mouse is extremely diminished in volume at P100 when the motor phenotype has reached maximum (Figure 4A,B). Comparing the histology of the *Cask*^{floxed};*Calb2*-Cre cerebellum at P30 (well before onset of ataxia) and P100 (after onset of ataxia), our results indicate that at P30, the cerebellum of *Cask*^{floxed};*Calb2*-Cre mice is populated with well-placed granule and Purkinje cells. At P100, however, we observe profound loss of granule cells, whereas Purkinje cells remain visible as a standard single layer of cells (Figure 4C). The molecular layer of the cerebellum is thin and collapsed, most likely due to loss of parallel fibers arising from the granular cells and loss of synaptic connections between granule cells and Purkinje cells (Figure 4D-G). We therefore next quantified synaptic connections within the cerebellar layers using bassoon as a pre-synaptic marker. As seen in Supplemental Figure 12, our data indicate that synapse density is unaltered, although the absolute number of synapses is reduced due to the shrunken volume of the molecular layer. The large number of remaining synapses are likely derived from the climbing fibers. Notably, in our previous studies, we did not observe degeneration of retinal ganglion cells, which are also positive for *Calb2*-Cre (Kerr, Patel et al. 2019). Our data here thus indicate that loss of CASK results in the disproportionate degeneration of a specific vulnerable neuronal population, cerebellar granule cells, leading to cerebellar hypoplasia.

A decrease in grey matter creates an impression of increased white matter area. We therefore quantified myelin in the *Cask*^{floxed};*Calb2*-Cre mice using FluoroMyelin^{TM}

staining. As seen in Figure 4H-I, the myelin appears to be disorganized in the white matter of folia from the *Cask*^{floxed};*Calb2*-Cre mouse cerebellum, which is most obvious in the region immediately distal to Purkinje cells. We also observed extremely limited myelinated axons in the anterior-most folium (Figure 4H). Quantification of pixels displayed a strong trend towards a decrease in fluoromyelin staining which did not reach statistical significance (Figure 4I). The degeneration of cerebellar grey matter thus is also associated with disorganization of the white matter in the *Cask*^{floxed};*Calb2*-Cre mouse cerebellum, and the broadened white matter layer is likely to be filled only with acellular matrix. Because the *Cask*^{floxed};*Calb2*-Cre mouse represents a targeted deletion of CASK in cerebellar neuronal cells, it is reasonable to conclude that the observed disordered white matter is a property of the underlying neuronal pathology rather than an oligodendrocyte-mediated pathology, confirming our observations from the human subject.

Neuronal loss or damage is typically associated with gliosis, as seen in the human subject, so we next immunostained mouse cerebella with a marker for reactive gliosis, glial acidic fibrillary protein (GFAP) (Figure 5A). Although *Cask*^{floxed} mice display some GFAP positivity, *Cask*^{floxed};*Calb2*-Cre mice displayed an almost 2-fold higher level of astrogliosis compared to age-matched control *Cask*^{floxed} mice (Figure 5B). Most of the GFAP in these cerebella was associated with Bergmann glia, since the IGL was extremely hypocellular. On staining the Bergmann glia with S100β, we did not see increased immunoreactivity in Bergmann glia or proliferation of Bergmann glia (Figure 5C,F), but we did observe a strong trend of increased S100β reactivity in the IGL extracellular space

(Figure 5D, E). S100β is known to be secreted during metabolic stress and functions via binding to a receptor of advanced glycation end products (Gerlach, Demel et al. 2006, Zglejc-Waszak, Mukherjee et al. 2021). Overall, this finding suggests that CASK loss-of-function produces protracted neuronal loss in the cerebellum, explaining why MICPCH in humans typically becomes obvious a few months after birth. The cerebellar hypoplasia associated with loss of CASK represents disproportionate neuronal loss in the cerebellum.

Finally, we examined the functional loss associated with the cerebellar degeneration in *Cask*^{floxed};Calb2-Cre mice. By P100, the mouse's hindlimbs can no longer maintain normal righting, and the mice display hindlimb clasping with no obvious dystonic movement (Figure 5G). Accelerating rotarod balance experiments suggest that even at P48, the mutant mice have a trend to underperform on a rotarod, indicating that the process of cerebellar degeneration and consequent functional degradation may be ongoing even before obvious locomotor defects are visually noticed within the cage. At P70 the mice are unable to perform on the rotarod at all, demonstrating a rapid degradation of locomotor coordination within a short span of 3 weeks (Figure 5H). Additionally, the cerebellar degeneration and accompanying motor phenotype only manifest in the homozygous knockout of CASK from cerebellar cells and not in the heterozygous deletion (Figure 5G,H and Supplemental Figure 13), despite CASK being absent from approximately half the cells in the heterozygous deletion due to its X-linked nature. This indicates that cerebellar degeneration requires total deletion of CASK in the cerebellum to produce degeneration in a non-cell autonomous fashion (Srivastava,

McMillan et al. 2016, Kerr, Patel et al. 2019). Our data additionally suggest that CASK haploinsufficiency is not sufficient to affect the cerebellum after postnatal development. Overall, our data indicate that deletion of CASK does not affect brain development, and the brain phenotype is unlikely due to defects of reelin function. Further, CASK loss leads to degeneration of cerebellar neurons, causing pronounced cerebellar atrophy that results in a progressive cerebellar ataxia.

Discussion

Developmental disorders are defined based on their clinical course rather than cellular pathology. Presentation of a severe, chronic disability (mental and/or physical impairment) in three or more areas of major life activity by the age of 22 that is likely to continue through the individual's lifetime is classified as a developmental disorder (*Developmental Disabilities Assistance and Bill of Rights Act of 2000*). Strategies for molecular therapeutic intervention, however, are more likely to be dependent on cellular pathology rather than the clinical course of a given disorder. Conditions associated with mutations in the human *CASK* gene have been described as developmental disorders (Moog, Kutsche et al. 2011, Burglen, Chantot-Bastaraud et al. 2012). *CASK* is a ubiquitously expressed gene and has been proposed to have a function in a variety of organs including the intestine, kidney, heart and brain (Hata, Butz et al. 1996, Stevenson, Laverty et al. 2000), and mutations in *CASK* produce microcephaly as well as somatic growth retardation (Moog, Kutsche et al. 2011, Burglen, Chantot-Bastaraud et al. 2012). In boys who do not express *CASK,* a clear picture has emerged consisting of neurological devastation, microcephaly, pontocerebellar hypoplasia (PCH), and a consistently

abnormal EEG pattern characterized by disorganization, low frequency, attenuation and discontinuity. *CASK* null boys are thus likely to be diagnosed with epileptic encephalopathies such as Ohtahara syndrome and West syndrome. Despite uniform neurological findings in these subjects, findings involving other organ systems remain inconsistent and often unremarkable. Our analysis of *CASK* null mutations in boys indicates that the function/s of CASK that are critical for survival are brain-specific; all other organ systems can function within the normal range without CASK (Mukherjee, Patel et al. 2020). In fact, we have previously demonstrated that deletion of *CASK* in neurons is sufficient to produce somatic and brain size reduction in mice (Srivastava, McMillan et al. 2016). The thinning and dysfunction of the brain stem manifests as aberrant respiratory, deglutition and cardiovascular reflexes, and it is this dysfunction that underlies the lethality associated with CASK loss in mammals (Atasoy, Schoch et al. 2007, Mukherjee, Patel et al. 2020).

Neurodevelopment could be stalled at several steps of brain development. This includes cell proliferation, neuronal differentiation and polarization, neuronal migration and final neuronal maturation including axonal and dendritic growth and synaptogenesis. At a molecular level CASK has been proposed to play a role in all these processes. Evidence exists to suggest that CASK participates in mitotic spindle orientation and cell proliferation (Porter, White et al. 2019), in cell polarization (Caruana 2002), and in axonal and dendritic maturation and synaptogenesis (Samuels, Hsueh et al. 2007, Kuo, Hong et al. 2010, Gao, Piguel et al. 2018). Within the synapse, CASK can be found in molecular complexes that include other important molecules like Mint1, Caskin, liprin-α and the adhesion molecule

neurexin (Hata, Butz et al. 1996, Butz, Okamoto et al. 1998, Tabuchi, Biederer et al. 2002, LaConte, Chavan et al. 2016). CASK is a kinase that phosphorylates neurexin and is likely to regulate this complex formation (Mukherjee, Sharma et al. 2008, Mukherjee, Sharma et al. 2010, Cortese, Zhu et al. 2016, LaConte, Chavan et al. 2016). The most accepted notion of CASK in neurodevelopment has, however, been the role of CASK in neuronal migration via its interaction with CINAP and Tbr-1, resulting in the upregulation of reelin transcription (Hsueh, Wang et al. 2000, Wang, Hong et al. 2004, Najm, Horn et al. 2008, Mori, Kasem et al. 2019). Surprisingly, our analysis of the CASK-null human brain does not support any of these putative roles of CASK in neurodevelopment.

Genetic manipulation of *Cask* in murine models has demonstrated that CASK-linked murine brain pathology is postnatal and not likely to be a developmental defect (Srivastava, McMillan et al. 2016, Kerr, Patel et al. 2019). Although the delivery of the decedent described here was late preterm, Apgar scores were normal, and the infant was released from the hospital without concern. Rapid regression within days to weeks has been noted in this and other boys with *CASK*-null mutations, indicating that although degeneration may begin in the third trimester, it continues rapidly throughout infancy. Despite a smaller size, the gross and histological findings in a brain without CASK are minimal. Overall, the brain configuration, vasculature, ventricular system, meninges, brain lamination, and neuronal migration all remained unaltered. The decrease in foliation noted in the decedent's cerebellum is likely explained by the rapid loss of granule cells after migration that precludes the formation of a densely packed IGL, a critical step for inducing foliation (Sudarov and Joyner 2007; Takeda, Kameo et al. 2021), although we cannot

strictly exclude specific developmental disruptions in the formation of 'anchoring centers' required for foliation (Sudarov and Joyner 2007). Overall our data indicate that in the presence of *CASK* mutation, embryonic brain development appears unchanged, with no defect in neuronal differentiation and migration. The findings from neuroimaging and histological studies of human cases are consistent with findings from CASK knockout mice where brain size, lamination, and synapse formation are all normal at birth (Atasoy, Schoch et al. 2007). In fact, the absence of an acute locomotor effect in *Cask*^{floxed};*Calb2*-Cre mice excludes a synaptic role of CASK in cerebellar function. Importantly, our study here strongly suggests that CASK does not play a role in neurodevelopment via the purported Tbr-1-reelin pathway. This interpretation is in line with the observation that in the mouse model, abrogation of the CASK-Tbr-1 interaction does not affect brain size or lamination (Huang and Hsueh 2017). A number of CASK missense mutations have been identified that are associated with intellectual disability and MICPCH. Recent studies on these missense mutations have also indicated that the CASK-Tbr-1 interaction does not play a role in MICPCH (LaConte, Chavan et al. 2018, Pan, Tibbe et al. 2021).

In girls with heterozygous *CASK* mutations, the predominant manifestations are also brain-related (Moog, Kutsche et al. 2011, Burglen, Chantot-Bastaraud et al. 2012). Our data presented here demonstrate that although *Cask*$^{+/-}$ mice have cerebellar hypoplasia, they do not significantly degenerate further in old age, which agrees with the clinical definition of a neurodevelopmental disease. In girls with MICPCH and in *Cask*$^{+/-}$ mice, however, ~50% of cells still express CASK (Srivastava, McMillan et al. 2016, Mori, Kasem et al. 2019), confounding the study of neuropathology and making it difficult to draw firm

conclusions. Conditional genetic animal model experimentation allows us to overcome the difficulties presented by this X-linked condition and also helps separate the neurodegenerative pathology of CASK loss from developmental contributions.

CASK deletion in mice is lethal, making postnatal developmental studies in a whole-body knockout model impossible. We have, however, previously demonstrated that CASK does not play a role in maturation and migration of cerebellar neurons by deleting CASK specifically in a distributed subpopulation of granule cells and maturing Purkinje cells (Srivastava, McMillan et al. 2016) . In the current work, we have generated otherwise healthy mice that do not express *Cask* in many parts of the brain, including the post-migratory cerebellar neurons, allowing us to clearly demonstrate that lack of CASK produces cerebellar atrophy through granule cell degeneration. This granule cell degeneration likely underlies MICPCH. CASK has previously been identified as a biomarker for several neurodegenerative disorders (Strand, Aragaki et al. 2005, Arefin, Mathieson et al. 2012, George, Singh et al. 2018, Morello, Guarnaccia et al. 2019); our study thus explains these previous unbiased findings. CASK loss, however, does not uniformly produce neurodegeneration; for example, loss of CASK is also associated with optic nerve hypoplasia, but unexpectedly, CASK deletion from retinal ganglion cells (whose axons form the optic nerve) does not negatively affect optic nerve pathology in mice of the same genotype (Kerr, Patel et al. 2019). Similarly, *Calb2* is present in many cortical interneurons and neurons of the olfactory bulb, hippocampus and striatum, but we do not observe severe atrophy of these regions in the *Cask*^{floxed};*Calb2*-Cre mice (Figure 4A). In fact, a closer look within the cerebellum suggests that cerebellar

degeneration may be primarily due to granule cell death, making this condition most similar to Norman-type cerebellar atrophy (OMIM: 213200). Many Purkinje cells, which are among the first cerebellar cells to express *Calb2*-Cre, do not die off but rather persist throughout the lifespan, even following the appearance of ataxia. Thus CASK loss apparently affects neurons differentially.

PCH pathologies are typically thought to be neurodegenerative beginning antenatally (van Dijk, Barth et al. 2020). Defects in both energy production and protein metabolism (specifically, protein synthesis) are known to disproportionately affect the cerebellum and are likely causes of PCH (Kasher, Namavar et al. 2011). In the case of CASK mutation, PCH has been described as neurodevelopmental, mostly due to the non-progressive course seen in females (van Dijk, Baas et al. 2018). In contrast to hemizygous and homozygous *Cask*^{floxed};*Calb2*-Cre mice, the heterozygous *Cask*^{floxed};*Calb2*-Cre mice fail to exhibit cerebellar degeneration (Supplemental Figure 13). Our findings here thus suggest that CASK-linked PCH is also neurodegenerative, and the arrest of neurodegeneration in girls most likely arises from mosaicism of the defective X-linked gene, which guarantees that ~50% of brain cells retain a normally functioning *CASK* gene (Figure 6). Mechanistically, our findings demonstrate that CASK is also likely to function in pathways associated with energy production and protein metabolism (Srivastava, McMillan et al. 2016, Patel, Liang et al. 2020), confirming that MICPCH shares not only the pathogenic mechanism, but also a common molecular pathway, with other types of PCH.

Heterozygous mutations in X-linked genes other than *CASK*, such as MeCP2 and CDKL5, are associated with postnatal microcephaly in girls (Seltzer and Paciorkowski 2014). Intriguingly, subjects with mutations in these genes show an initial normal developmental trajectory followed by developmental arrest and delay (regression) (Hagberg, Aicardi et al. 1983, Fehr, Wilson et al. 2013). Mutational analysis of orthologous genes in murine models also reveal phenotypes which are clearly post-developmental, presenting only in adulthood (Guy, Hendrich et al. 2001) (Montgomery, Louis Sam Titus et al. 2018). Incidentally, just like CASK mutations, CDKL5 and MeCP2 mutations in males are associated with epileptic encephalopathy (Kankirawatana, Leonard et al. 2006, Jakimiec, Paprocka et al. 2020). These data raise the possibility that even in disorders such as Rett syndrome (MeCP2 mutation) and CDKL5 deficiency, the pathology may be neurodegenerative, as originally suggested by Andreas Rett (Rett 1966), but the clinical course may not be progressive in females due to the mosaic expression of the normal gene under heterozygous conditions.

Acknowledgements

We thank Drs. Thomas Südhof and Alexei Morozov for providing CASK^{floxed} mice and Ai14-LSL-tdTomato mice, respectively.

Funding

The work was supported with funding from the NIH National Eye Institute (R01EY024712) and Angelina CASK Neurological Research Foundation to KM, and from NIH National Institute of Neurological Disorders and Stroke grant (R01NS117698) to S.S.

Author contribution

Experiments were conceived by KM, PP, MF, IC. Data analyzed by KM, MF, PP, JH, LL, SS. Experiments conducted by PP, AK, JH. Paper written by KM, PP, MF, LL, SS, IC, JH. All authors read and approved the final manuscript.

Declarations

Ethics Approval and Consent to Participate

All studies described herein were approved by the Virginia Tech Institutional Animal Care and Use Committee and Virginia Tech Institutional Review Board.

Competing Interests

The authors have declared that no conflict of interest exists.

References

Ahn, S. Y. et al. (2013). "Scaffolding proteins DLG1 and CASK cooperate to maintain the nephron progenitor population during kidney development." J Am Soc Nephrol **24**(7): 1127-1138.

Aldinger, K. A. et al. (2019). "Redefining the Etiologic Landscape of Cerebellar Malformations." Am J Hum Genet **105**(3): 606-615.

Alewine, C., B. Y. Kim, V. Hegde and P. A. Welling (2007). "Lin-7 targets the Kir 2.3 channel on the basolateral membrane via a L27 domain interaction with CASK." Am J Physiol Cell Physiol **293**(6): C1733-1741.

Antonov, A. V. et al. (2010). "R spider: a network-based analysis of gene lists by combining signaling and metabolic pathways from Reactome and KEGG databases." Nucleic Acids Research **38**: W78-W83.

Antonov, A. V., T. Schmidt, Y. Wang and H. W. Mewes (2008). "ProfCom: a web tool for profiling the complex functionality of gene groups identified from high-throughput data." Nucleic Acids Research **36**: W347-W351.

Aoto, J. et al. (2013). "Presynaptic Neurexin-3 Alternative Splicing trans-Synaptically Controls Postsynaptic AMPA Receptor Trafficking." Cell **154**(1): 75-88.

Arefin, A. S. et al. (2012). "Unveiling clusters of RNA transcript pairs associated with markers of Alzheimer's disease progression." PLoS One **7**(9): e45535.

Aronesty, E. (2011). "ea-utils : "Command-line tools for processing biological sequencing data"."

Ashery, U. et al. (2000). "Munc13-1 acts as a priming factor for large dense-core vesicles in bovine chromaffin cells." Embo Journal **19**(14): 3586-3596.

Atasoy, D. et al. (2007). "Deletion of CASK in mice is lethal and impairs synaptic function." Proc Natl Acad Sci U S A **104**(7): 2525-2530.

Bayer, K. U. et al. (2001). "Interaction with the NMDA receptor locks CaMKII in an active conformation." Nature **411**(6839): 801-805.

Bearzatto, B. et al. (2006). "Targeted calretinin expression in granule cells of calretinin-null mice restores normal cerebellar functions." FASEB J **20**(2): 380-382.

Beaudreuil, S. et al. (2019). "Circulating CASK is associated with recurrent focal segmental glomerulosclerosis after transplantation." PLoS One **14**(7): e0219353.

Beuriot, A. et al. (2020). "Distinct calcium/calmodulin-dependent serine protein kinase domains control cardiac sodium channel membrane expression and focal adhesion anchoring." Heart Rhythm **17**(5 Pt A): 786-794.

Biederer, T. et al. (2002). "SynCAM, a synaptic adhesion molecule that drives synapse assembly." Science **297**(5586): 1525-1531.

Biederer, T. and T. C. Sudhof (2001). "CASK and protein 4.1 support F-actin nucleation on neurexins." J Biol Chem **276**(51): 47869-47876.

Boersma, I., J. Miyasaki, J. Kutner and B. Kluger (2014). "Palliative care and neurology: time for a paradigm shift." Neurology **83**(6): 561-567.

Bredt, D. S. (2000). "Cell biology. Reeling CASK into the nucleus." Nature **404**(6775): 241-242.

Brown, K. T. (1968). "Electroretinogram - Its Components and Their Origins." Vision Research **8**(6): 633-+.

Brown, N. L., S. Patel, J. Brzezinski and T. Glaser (2001). "Math5 is required for retinal ganglion cell and optic nerve formation." Development **128**(13): 2497-2508.

Burglen, L. et al. (2012). "Spectrum of pontocerebellar hypoplasia in 13 girls and boys with CASK mutations: confirmation of a recognizable phenotype and first description of a male mosaic patient." Orphanet J Rare Dis **7**: 18.

Butz, S., M. Okamoto and T. C. Sudhof (1998). "A tripartite protein complex with the potential to couple synaptic vesicle exocytosis to cell adhesion in brain." Cell **94**(6): 773-782.

Buzsaki, G., C. A. Anastassiou and C. Koch (2012). "The origin of extracellular fields and currents - EEG, ECoG, LFP and spikes." Nature Reviews Neuroscience **13**(6): 407-420.

Caruana, G. (2002). "Genetic studies define MAGUK proteins as regulators of epithelial cell polarity." Int J Dev Biol **46**(4): 511-518.

Caruana, G. (2002). "Genetic studies define MAGUK proteins as regulators of epithelial cell polarity." International Journal of Developmental Biology **46**(4): 511-518.

Castillo, P. E. et al. (2002). "RIM1 alpha is required for presynaptic long-term potentiation." Nature **415**(6869): 327-330.

Cendelin, J. (2014). "From mice to men: lessons from mutant ataxic mice." Cerebellum & ataxias **1**(1): 1-21.

Chan, T. and A. K. Devaiah (2009). "Tracheostomy in palliative care." Otolaryngol Clin North Am **42**(1): 133-141, x.

Chao, H. W. et al. (2008). "SUMOylation of the MAGUK protein CASK regulates dendritic spinogenesis." J Cell Biol **182**(1): 141-155.

Chen, C. A., J. Yin, R. A. Lewis and C. P. Schaaf (2017). "Genetic causes of optic nerve hypoplasia." J Med Genet **54**(7): 441-449.

Cheng, H. C., M. Y. Yen and A. G. Wang (2015). "Neuroimaging and clinical features of patients with optic nerve hypoplasia in Taiwan." Taiwan J Ophthalmol **5**(1): 15-18.

Chowdhury, D. and J. W. Hell (2018). "Homeostatic synaptic scaling: molecular regulators of synaptic AMPA-type glutamate receptors." F1000Res **7**: 234.

Clarkson, C., F. M. Antunes and M. E. Rubio (2016). "Conductive Hearing Loss Has Long-Lasting Structural and Molecular Effects on Presynaptic and Postsynaptic Structures of Auditory Nerve Synapses in the Cochlear Nucleus." Journal of Neuroscience **36**(39): 10214-10227.

Cohen, A. R. et al. (1998). "Human CASK/LIN-2 binds syndecan-2 and protein 4.1 and localizes to the basolateral membrane of epithelial cells." J Cell Biol **142**(1): 129-138.

Cooper, D. N. et al. (2010). "Methylation-mediated deamination of 5-methylcytosine appears to give rise to mutations causing human inherited disease in CpNpG trinucleotides, as well as in CpG dinucleotides." Human Genomics **4**(6): 406.

Cortese, G. P. et al. (2016). "Parkin Deficiency Reduces Hippocampal Glutamatergic Neurotransmission by Impairing AMPA Receptor Endocytosis." J Neurosci **36**(48): 12243-12258.

Cowell, J. K., T. Smith and B. Bia (1994). "Frequent constitutional C to T mutations in CGA-arginine codons in the RB1 gene produce premature stop codons in patients with bilateral (hereditary) retinoblastoma." Eur J Hum Genet **2**(4): 281-290.

Crino, P. B., H. Miyata and H. V. Vinters (2002). "Neurodevelopmental disorders as a cause of seizures: Neuropathologic, genetic, and mechanistic considerations." Brain Pathology **12**(2): 212-233.

Dai, J., J. Aoto and T. C. Sudhof (2019). "Alternative Splicing of Presynaptic Neurexins Differentially Controls Postsynaptic NMDA and AMPA Receptor Responses." Neuron **102**(5): 993-+.

Dai, Y. et al. (2006). "SYD-2 Liprin-alpha organizes presynaptic active zone formation through ELKS." Nature Neuroscience **9**(12): 1479-1487.

Dallara, A. and D. W. Tolchin (2014). "Emerging subspecialties in neurology: palliative care." Neurology **82**(7): 640-642.

Daniel, S. et al. (2019). "Effect of ocular hypertension on the pattern of retinal ganglion cell subtype loss in a mouse model of early-onset glaucoma." Exp Eye Res: 107703.

Deak, F. et al. (2006). "Rabphilin regulates SNARE-dependent re-priming of synaptic vesicles for fusion." Embo Journal **25**(12): 2856-2866.

DeLuca, S. C., D. A. Wallace, M. R. Trucks and K. Mukherjee (2017). "A clinical series using intensive neurorehabilitation to promote functional motor and cognitive skills in three girls with CASK mutation." BMC Res Notes **10**(1): 743.

Edvardson, S. et al. (2013). "Agenesis of corpus callosum and optic nerve hypoplasia due to mutations in SLC25A1 encoding the mitochondrial citrate transporter." Journal of Medical Genetics **50**(4): 240-245.

Eichel, C. A. et al. (2016). "Lateral Membrane-Specific MAGUK CASK Down-Regulates NaV1.5 Channel in Cardiac Myocytes." Circ Res **119**(4): 544-556.

Fairless, R. et al. (2008). "Polarized Targeting of Neurexins to Synapses Is Regulated by their C-Terminal Sequences." Journal of Neuroscience **28**(48): 12969-12981.

Fallon, L. et al. (2002). "Parkin and CASK/LIN-2 associate via a PDZ-mediated interaction and are co-localized in lipid rafts and postsynaptic densities in brain." J Biol Chem **277**(1): 486-491.

Farzi, A. et al. (2018). "Arcuate nucleus and lateral hypothalamic CART neurons in the mouse brain exert opposing effects on energy expenditure." Elife **7**.

Fehr, S. et al. (2013). "The CDKL5 disorder is an independent clinical entity associated with early-onset encephalopathy." Eur J Hum Genet **21**(3): 266-273.

Ferguson, E. L. and H. R. Horvitz (1985). "Identification and characterization of 22 genes that affect the vulval cell lineages of the nematode Caenorhabditis elegans." Genetics **110**(1): 17-72.

Ferrari, I., A. Crespi, D. Fornasari and G. Pietrini (2016). "Novel localisation and possible function of LIN7 and IRSp53 in mitochondria of HeLa cells." European Journal of Cell Biology **95**(8): 285-293.

FitzGerald, P. M. et al. (1990). "Extrapyramidal involvement in Rett's syndrome." Neurology **40**(2): 293-295.

Frisén, L. and L. Holmegaard (1978). "Spectrum of optic nerve hypoplasia." British Journal of Ophthalmology **62**(1): 7-15.

Gao, R. et al. (2018). "CNTNAP2 stabilizes interneuron dendritic arbors through CASK." Mol Psychiatry **23**(9): 1832-1850.

Garcia-Filion, P. and M. Borchert (2013). "Prenatal determinants of optic nerve hypoplasia: review of suggested correlates and future focus." Surv Ophthalmol **58**(6): 610-619.

George, G., S. Singh, S. B. Lokappa and J. Varkey (2018). "Gene co-expression network analysis for identifying genetic markers in Parkinson's disease - a three-way comparative approach." Genomics.

Gerlach, R. et al. (2006). "Active secretion of S100B from astrocytes during metabolic stress." Neuroscience **141**(4): 1697-1701.

Ghazalpour, A. et al. (2011). "Comparative Analysis of Proteome and Transcriptome Variation in Mouse." Plos Genetics **7**(6).

Gokce, O. and T. C. Sudhof (2013). "Membrane-Tethered Monomeric Neurexin LNS-Domain Triggers Synapse Formation." Journal of Neuroscience **33**(36): 14617-14628.

Gross, G. G. et al. (2013). "X11/Mint genes control polarized localization of axonal membrane proteins in vivo." J Neurosci **33**(19): 8575-8586.

Guldner, F. H. and C. A. Ingham (1980). "Increase in Postsynaptic Density Material in Optic Target Neurons of the Rat Suprachiasmatic Nucleus after Bilateral Enucleation." Neuroscience Letters **17**(1-2): 27-31.

Gurevich, L. and M. M. Slaughter (1993). "Comparison of the waveforms of the ON bipolar neuron and the b-wave of the electroretinogram." Vision Res **33**(17): 2431-2435.

Guy, J., B. Hendrich, M. Holmes, J. E. Martin and A. Bird (2001). "A mouse Mecp2-null mutation causes neurological symptoms that mimic Rett syndrome." Nat Genet **27**(3): 322-326.

Hackett, A. et al. (2010). "CASK mutations are frequent in males and cause X-linked nystagmus and variable XLMR phenotypes." Eur J Hum Genet **18**(5): 544-552.

Hagberg, B., J. Aicardi, K. Dias and O. Ramos (1983). "A progressive syndrome of autism, dementia, ataxia, and loss of purposeful hand use in girls: Rett's syndrome: report of 35 cases." Ann Neurol **14**(4): 471-479.

Haider, S. and R. Pal (2013). "Integrated Analysis of Transcriptomic and Proteomic Data." Current Genomics **14**(2): 91-110.

Hamburgh, M. (1963). "Analysis of the Postnatal Developmental Effects of "Reeler," a Neurological Mutation in Mice. A Study in Developmental Genetics." Dev Biol **8**: 165-185.

Hansen, K. G. et al. (2018). "An ER surface retrieval pathway safeguards the import of mitochondrial membrane proteins in yeast." Science **361**(6407): 1118-+.

Hata, Y., S. Butz and T. C. Sudhof (1996). "CASK: a novel dlg/PSD95 homolog with an N-terminal calmodulin-dependent protein kinase domain identified by interaction with neurexins." J Neurosci **16**(8): 2488-2494.

Hata, Y., C. A. Slaughter and T. C. Sudhof (1993). "Synaptic Vesicle Fusion Complex Contains Unc-18 Homolog Bound to Syntaxin." Nature **366**(6453): 347-351.

Hatsuzawa, K., T. Lang, D. Fasshauer, D. Bruns and R. Jahn (2003). "The R-SNARE motif of tomosyn forms SNARE core complexes with syntaxin 1 and SNAP-25 and down-regulates exocytosis." Journal of Biological Chemistry **278**(33): 31159-31166.

Hayashi, S. et al. (2012). "Novel intragenic duplications and mutations of CASK in patients with mental retardation and microcephaly with pontine and cerebellar hypoplasia (MICPCH)." Hum Genet **131**(1): 99-110.

Hayashi, S. et al. (2017). "Comprehensive investigation of CASK mutations and other genetic etiologies in 41 patients with intellectual disability and microcephaly with pontine and cerebellar hypoplasia (MICPCH)." Plos One **12**(8).

Helbig, I., M. von Deimling and E. D. Marsh (2017). "Epileptic Encephalopathies as Neurodegenerative Disorders." Neurodegenerative Diseases: Pathology, Mechanisms, and Potential Therapeutic Targets **15**: 295-315.

Hevner, R. F. et al. (2001). "Tbr1 regulates differentiation of the preplate and layer 6." Neuron **29**(2): 353-366.

Hirotsune, S. et al. (1995). "The reeler gene encodes a protein with an EGF-like motif expressed by pioneer neurons." Nat Genet **10**(1): 77-83.

Hodge, J. J., P. Mullasseril and L. C. Griffith (2006). "Activity-dependent gating of CaMKII autonomous activity by Drosophila CASK." Neuron **51**(3): 327-337.

Horng, S. et al. (2017). "Astrocytic tight junctions control inflammatory CNS lesion pathogenesis." Journal of Clinical Investigation **127**(8): 3136-3151.

Horvitz, H. R. and J. E. Sulston (1980). "Isolation and genetic characterization of cell-lineage mutants of the nematode Caenorhabditis elegans." Genetics **96**(2): 435-454.

Hoskins, R., A. F. Hajnal, S. A. Harp and S. K. Kim (1996). "The C. elegans vulval induction gene lin-2 encodes a member of the MAGUK family of cell junction proteins." Development **122**(1): 97-111.

Howell, K. B., A. S. Harvey and J. S. Archer (2016). "Epileptic encephalopathy: Use and misuse of a clinically and conceptually important concept." Epilepsia **57**(3): 343-347.

Hoyt, C. S. and F. A. Billson (1986). "Optic-Nerve Hypoplasia - Changing Perspectives." Australian and New Zealand Journal of Ophthalmology **14**(4): 325-331.

Hoyt, C. S. and W. V. Good (1992). "Do we really understand the difference between optic nerve hypoplasia and atrophy?" Eye (Lond) **6 (Pt 2)**: 201-204.

Hsueh, Y. P., T. F. Wang, F. C. Yang and M. Sheng (2000). "Nuclear translocation and transcription regulation by the membrane-associated guanylate kinase CASK/LIN-2." Nature **404**(6775): 298-302.

Huang, T. N., H. P. Chang and Y. P. Hsueh (2010). "CASK phosphorylation by PKA regulates the protein-protein interactions of CASK and expression of the NMDAR2b gene." J Neurochem **112**(6): 1562-1573.

Huang, T. N. and Y. P. Hsueh (2017). "Calcium/calmodulin-dependent serine protein kinase (CASK), a protein implicated in mental retardation and autism-spectrum disorders, interacts with T-Brain-1 (TBR1) to control extinction of associative memory in male mice." J Psychiatry Neurosci **42**(1): 37-47.

Huang, T. N. a. H., Y.P. (2016). "Calcium/calmodulin-dependent serine protein kinase (CASK), a protein implicated in mental retardation and autism-spectrum disorders,

interacts with T-Brain-1 (TBR1) to control extinction of associative memory in male mice." Journal of Psychiatry and Neuroscience.

Huberman, A. D. and C. M. Niell (2011). "What can mice tell us about how vision works?" Trends in Neurosciences **34**(9): 464-473.

Hung, V. et al. (2017). "Proteomic mapping of cytosol-facing outer mitochondrial and ER membranes in living human cells by proximity biotinylation." Elife **6**.

Ichikawa, R. et al. (2011). "Developmental switching of perisomatic innervation from climbing fibers to basket cell fibers in cerebellar Purkinje cells." J Neurosci **31**(47): 16916-16927.

Ivarsson, Y. et al. (2013). "Prevalence, Specificity and Determinants of Lipid-Interacting PDZ Domains from an In-Cell Screen and In Vitro Binding Experiments." Plos One **8**(2).

Jakimiec, M., J. Paprocka and R. Smigiel (2020). "CDKL5 Deficiency Disorder-A Complex Epileptic Encephalopathy." Brain Sci **10**(2).

Jeyifous, O. et al. (2009). "SAP97 and CASK mediate sorting of NMDA receptors through a previously unknown secretory pathway." Nat Neurosci **12**(8): 1011-1019.

Kaech, S. M., C. W. Whitfield and S. K. Kim (1998). "The LIN-2/LIN-7/LIN-10 complex mediates basolateral membrane localization of the C. elegans EGF receptor LET-23 in vulval epithelial cells." Cell **94**(6): 761-771.

Kaeser, P. S. et al. (2011). "RIM Proteins Tether Ca2+ Channels to Presynaptic Active Zones via a Direct PDZ-Domain Interaction." Cell **144**(2): 282-295.

Kankirawatana, P. et al. (2006). "Early progressive encephalopathy in boys and MECP2 mutations." Neurology **67**(1): 164-166.

Kasher, P. R. et al. (2011). "Impairment of the tRNA-splicing endonuclease subunit 54 (tsen54) gene causes neurological abnormalities and larval death in zebrafish models of pontocerebellar hypoplasia." Hum Mol Genet **20**(8): 1574-1584.

Katagiri, S. et al. (2017). "Retinal Structure and Function in Eyes with Optic Nerve Hypoplasia." Sci Rep **7**: 42480.

Kaufmann, N. et al. (2002). "Drosophila liprin-alpha and the receptor phosphatase Dlar control synapse morphogenesis." Neuron **34**(1): 27-38.

Kaur, S. et al. (2013). "Optic nerve hypoplasia." Oman J Ophthalmol **6**(2): 77-82.

Kerr, A. et al. (2019). "Non-Cell Autonomous Roles for CASK in Optic Nerve Hypoplasia." Invest Ophthalmol Vis Sci **60**(10): 3584-3594.

Khan, S. and R. Al Baradie (2012). "Epileptic encephalopathies: an overview." Epilepsy Res Treat **2012**: 403592.

Khaper, T. et al. (2017). "Increasing incidence of optic nerve hypoplasia/septo-optic dysplasia spectrum: Geographic clustering in Northern Canada." Paediatr Child Health **22**(8): 445-453.

Kim, D., B. Landmead and S. L. Salzberg (2015). "HISAT: a fast spliced aligner with low memory requirements." Nature Methods **12**(4): 357-U121.

Kong, L. et al. (2012). "An update on progress and the changing epidemiology of causes of childhood blindness worldwide." J AAPOS **16**(6): 501-507.

Kong, Y. (2011). "Btrim: A fast, lightweight adapter and quality trimming program for next-generation sequencing technologies." Genomics **98**(2): 152-153.

Kuo, T. Y., C. J. Hong, H. L. Chien and Y. P. Hsueh (2010). "X-linked mental retardation gene CASK interacts with Bcl11A/CTIP1 and regulates axon branching and outgrowth." J Neurosci Res **88**(11): 2364-2373.

LaConte, L. E. W. and K. Mukherjee (2013). "Structural constraints and functional divergences in CASK evolution." Biochem Soc Trans **41**(4): 1017-1022.

LaConte, L. E. W. et al. (2016). "CASK stabilizes neurexin and links it to liprin-alpha in a neuronal activity-dependent manner." Cell Mol Life Sci **73**(18): 3599-3621.

LaConte, L. E. W., V. Chavan and K. Mukherjee (2014). "Identification and glycerol-induced correction of misfolding mutations in the X-linked mental retardation gene CASK." PLoS One **9**(2): e88276.

LaConte, L. E. W. et al. (2019). "An N-terminal heterozygous missense CASK mutation is associated with microcephaly and bilateral retinal dystrophy plus optic nerve atrophy." American Journal of Medical Genetics Part A **179**(1): 94-103.

LaConte, L. E. W. et al. (2018). "Two microcephaly-associated novel missense mutations in CASK specifically disrupt the CASK-neurexin interaction." Hum Genet **137**(3): 231-246.

LaConte, L. E. W. et al. (2016). "CASK stabilizes neurexin and links it to liprin-alpha in a neuronal activity-dependent manner." Cellular and Molecular Life Sciences **73**(18): 3599-3621.

Lambert, S. R., C. S. Hoyt and M. H. Narahara (1987). "Optic-Nerve Hypoplasia." Survey of Ophthalmology **32**(1): 1-9.

Lazar, I. M., I. Hoeschele, J. de Morais and M. J. Tenga (2017). "Cell Cycle Model System for Advancing Cancer Biomarker Research." Sci Rep **7**(1): 17989.

Leonoudakis, D. et al. (2004). "A multiprotein trafficking complex composed of SAP97, CASK, Veli, and Mint1 is associated with inward rectifier Kir2 potassium channels." J Biol Chem **279**(18): 19051-19063.

Li, S. et al. (2005). "Rhodopsin-iCre transgenic mouse line for Cre-mediated rod-specific gene targeting." Genesis **41**(2): 73-80.

Liang, C. et al. (2017). "Optic Nerve Hypoplasia Is a Pervasive Subcortical Pathology of Visual System in Neonates." Invest Ophthalmol Vis Sci **58**(12): 5485-5496.

Love, M. I., W. Huber and S. Anders (2014). "Moderated estimation of fold change and dispersion for RNA-seq data with DESeq2." Genome Biology **15**(12).

Lozovatsky, L., N. Abayasekara, S. Piawah and Z. Walther (2009). "CASK deletion in intestinal epithelia causes mislocalization of LIN7C and the DLG1/Scrib polarity complex without affecting cell polarity." Mol Biol Cell **20**(21): 4489-4499.

Lu, C. S. et al. (2003). "Regulation of the Ca2+/CaM-responsive pool of CaMKII by scaffold-dependent autophosphorylation." Neuron **40**(6): 1185-1197.

Lu, P. F., K. Takai, V. M. Weaver and Z. Werb (2011). "Extracellular Matrix Degradation and Remodeling in Development and Disease." Cold Spring Harbor Perspectives in Biology **3**(12).

Maximov, A., O. H. Shin, X. R. Liu and T. C. Sudhof (2007). "Synaptotagmin-12, a synaptic vesicle phosphoprotein that modulates spontaneous neurotransmitter release." Journal of Cell Biology **176**(1): 113-124.

Michaud, J. L. et al. (2014). "The genetic landscape of infantile spasms." Hum Mol Genet **23**(18): 4846-4858.

Monavarfeshani, A. et al. (2018). "LRRTM1 underlies synaptic convergence in visual thalamus." Elife **7**.

Montgomery, K. R., A. S. C. Louis Sam Titus, L. Wang and S. R. D'Mello (2018). "Elevated MeCP2 in Mice Causes Neurodegeneration Involving Tau Dysregulation and Excitotoxicity: Implications for the Understanding and Treatment of MeCP2 Triplication Syndrome." Mol Neurobiol **55**(12): 9057-9074.

Moog, U. et al. (2015). "Phenotypic and molecular insights into CASK-related disorders in males." Orphanet Journal of Rare Diseases **10**.

Moog, U. et al. (2011). "Phenotypic spectrum associated with CASK loss-of-function mutations." J Med Genet **48**(11): 741-751.

Moog, U., G. Uyanik and K. Kutsche (1993). CASK-Related Disorders. GeneReviews((R)). M. P. Adam, H. H. Ardinger, R. A. Pagon et al. Seattle (WA).

Morello, G. et al. (2019). "Integrative multi-omic analysis identifies new drivers and pathways in molecularly distinct subtypes of ALS." Sci Rep **9**(1): 9968.

Mori, T. et al. (2019). "Deficiency of calcium/calmodulin-dependent serine protein kinase disrupts the excitatory-inhibitory balance of synapses by downregulating GluN2B (vol 24, pg 1079, 2019)." Molecular Psychiatry **24**(7): 1093-1093.

Mukherjee, K. et al. (2020). "Survival of a male patient harboring CASK Arg27Ter mutation to adolescence." Mol Genet Genomic Med: e1426.

Mukherjee, K. et al. (2010). "Evolution of CASK into a Mg2+-Sensitive Kinase." Science Signaling **3**(119).

Mukherjee, K. et al. (2008). "CASK Functions as a Mg2+-independent neurexin kinase." Cell **133**(2): 328-339.

Mukherjee, K., J. B. Slawson, B. L. Christmann and L. C. Griffith (2014). "Neuron-specific protein interactions of Drosophila CASK-beta are revealed by mass spectrometry." Front Mol Neurosci **7**: 58.

Mukherjee, K. et al. (2010). "Piccolo and bassoon maintain synaptic vesicle clustering without directly participating in vesicle exocytosis." Proc Natl Acad Sci U S A **107**(14): 6504-6509.

Najm, J. et al. (2008). "Mutations of CASK cause an X-linked brain malformation phenotype with microcephaly and hypoplasia of the brainstem and cerebellum." Nat Genet **40**(9): 1065-1067.

Namavar, Y., P. G. Barth, F. Baas and B. T. Poll-The (2012). "Reply: Mutations of TSEN and CASK genes are prevalent in pontocerebellar hypoplasias type 2 and 4." Brain **135**(1): e200-e200.

Neul, J. L. and H. Y. Zoghbi (2004). "Rett syndrome: a prototypical neurodevelopmental disorder." Neuroscientist **10**(2): 118-128.

Nishio, Y. et al. (2020). "The eldest case of MICPCH with CASK mutation exhibiting gross motor regression." Brain Dev.

O'Rahilly, R. and F. Muller (2010). "Developmental stages in human embryos: revised and new measurements." Cells Tissues Organs **192**(2): 73-84.

Oliver, D. (2018). "Improving patient outcomes through palliative care integration in other specialised health services: what we have learned so far and how can we improve?" Annals of Palliative Medicine: S219-S230.

Olsen, O. et al. (2002). "Basolateral membrane expression of the Kir 2.3 channel is coordinated by PDZ interaction with Lin-7/CASK complex." Am J Physiol Cell Physiol **282**(1): C183-195.

Olsen, O. et al. (2005). "Neurotransmitter release regulated by a MALS-liprin-alpha presynaptic complex." J Cell Biol **170**(7): 1127-1134.

Omkumar, R. V. et al. (1996). "Identification of a phosphorylation site for calcium/calmodulindependent protein kinase II in the NR2B subunit of the N-methyl-D-aspartate receptor." J Biol Chem **271**(49): 31670-31678.

Pak, C. et al. (2015). "Human Neuropsychiatric Disease Modeling using Conditional Deletion Reveals Synaptic Transmission Defects Caused by Heterozygous Mutations in NRXN1." Cell Stem Cell **17**(3): 316-328.

Pan, Y. E. et al. (2021). "Missense mutations in CASK, coding for the calcium-/calmodulin-dependent serine protein kinase, interfere with neurexin binding and neurexin-induced oligomerization." J Neurochem **157**(4): 1331-1350.

Patel, P. A. et al. (2020). "Haploinsufficiency of X-linked intellectual disability gene CASK induces post-transcriptional changes in synaptic and cellular metabolic pathways." Exp Neurol **329**: 113319.

Perry, V. H., J. A. Nicoll and C. Holmes (2010). "Microglia in neurodegenerative disease." Nat Rev Neurol **6**(4): 193-201.

Pfeifer, C. M. and C. A. Martinot (2017). "Zellweger syndrome: Depiction of MRI findings in early infancy at 3.0 Tesla." Neuroradiology Journal **30**(5): 442-444.

Piluso, G. et al. (2009). "A missense mutation in CASK causes FG syndrome in an Italian family." Am J Hum Genet **84**(2): 162-177.

Porter, A. P., G. R. M. White, N. A. Mack and A. Malliri (2019). "The interaction between CASK and the tumour suppressor Dlg1 regulates mitotic spindle orientation in mammalian epithelia." J Cell Sci **132**(14).

Poston, C. N., S. C. Krishnan and C. R. Bazemore-Walker (2013). "In-depth proteomic analysis of mammalian mitochondria-associated membranes (MAM)." Journal of Proteomics **79**: 219-230.

Prusky, G. T., P. W. R. West and R. M. Douglas (2000). "Behavioral assessment of visual acuity in mice and rats." Vision Research **40**(16): 2201-2209.

Puyang, Z., H. Chen and X. Liu (2015). "Subtype-dependent Morphological and Functional Degeneration of Retinal Ganglion Cells in Mouse Models of Experimental Glaucoma." J Nat Sci **1**(5): e103.

Rajasekaran, K., S. A. Zanelli and H. P. Goodkin (2010). "Lessons From the Laboratory: The Pathophysiology, and Consequences of Status Epilepticus." Seminars in Pediatric Neurology **17**(3): 136-143.

Rama Devi, A. R., L. Lingappa and S. M. Naushad (2019). "Identification and in Silico Characterization of a Novel CASK c.2546T>C (p.V849A) Mutation in a Male Infant with Pontocerebellar Hypoplasia." Ann Indian Acad Neurol **22**(4): 523-524.

Rett, A. (1966). "[On a unusual brain atrophy syndrome in hyperammonemia in childhood]." Wien Med Wochenschr **116**(37): 723-726.

Rhee, J. S. et al. (2002). "beta phorbol ester- and diacylglycerol-induced augmentation of transmitter release is mediated by Munc13s and not by PKCs." Cell **108**(1): 121-133.

Rodriguez, A. R., L. P. D. Muller and N. C. Brecha (2014). "The RNA binding protein RBPMS is a selective marker of ganglion cells in the mammalian retina." Journal of Comparative Neurology **522**(6): 1411-1443.

Romanov, G. A. and V. S. Sukhoverov (2017). "Arginine CGA codons as a source of nonsense mutations: a possible role in multivariant gene expression, control of mRNA quality, and aging." Molecular Genetics and Genomics **292**(5): 1013-1026.

Saitsu, H. et al. (2012). "CASK aberrations in male patients with Ohtahara syndrome and cerebellar hypoplasia." Epilepsia **53**(8): 1441-1449.

Samuels, B. A. et al. (2007). "Cdk5 promotes synaptogenesis by regulating the subcellular distribution of the MAGUK family member CASK." Neuron **56**(5): 823-837.

Sando, R. et al. (2017). "Assembly of Excitatory Synapses in the Absence of Glutamatergic Neurotransmission." Neuron **94**(2): 312-321 e313.

Sanford, J. L., T. A. Mays and J. A. Rafael-Fortney (2004). "CASK and Dlg form a PDZ protein complex at the mammalian neuromuscular junction." Muscle Nerve **30**(2): 164-171.

Sarnat, H. B., L. Flores-Sarnat and R. N. Auer (2013). "Sequence of synaptogenesis in the fetal and neonatal cerebellar system - part 1: Guillain-Mollaret triangle (dentato-rubro-olivo-cerebellar circuit)." Dev Neurosci **35**(1): 69-81.

Sarnat, H. B., L. Flores-Sarnat and R. N. Auer (2013). "Synaptogenesis in the foetal and neonatal cerebellar system. 2. Pontine nuclei and cerebellar cortex." Dev Neurosci **35**(4): 317-325.

Schiffmann, S. N. et al. (1999). "Impaired motor coordination and Purkinje cell excitability in mice lacking calretinin." Proc Natl Acad Sci U S A **96**(9): 5257-5262.

Schoch, S. et al. (2002). "RIM1 alpha forms a protein scaffold for regulating neurotransmitter release at the active zone." Nature **415**(6869): 321-326.

Schule, B. et al. (2008). "Severe congenital encephalopathy caused by MECP2 null mutations in males: central hypoxia and reduced neuronal dendritic structure." Clin Genet **74**(2): 116-126.

Seltzer, L. E. and A. R. Paciorkowski (2014). "Genetic disorders associated with postnatal microcephaly." Am J Med Genet C Semin Med Genet **166C**(2): 140-155.

Simon Anders, P. T. P., Wolfgang Huber (2014). "HTSeq — A Python framework to work with high-throughput sequencing data Bioinformatics."

Slawson, J. B. et al. (2011). "Central regulation of locomotor behavior of Drosophila melanogaster depends on a CASK isoform containing CaMK-like and L27 domains." Genetics **187**(1): 171-184.

Spangler, S. A. et al. (2013). "Liprin-alpha2 promotes the presynaptic recruitment and turnover of RIM1/CASK to facilitate synaptic transmission." J Cell Biol **201**(6): 915-928.

Srivastava, S. et al. (2016). "X-linked intellectual disability gene CASK regulates postnatal brain growth in a non-cell autonomous manner." Acta Neuropathologica Communications **4**.

Staley, K. (2015). "Molecular mechanisms of epilepsy." Nature Neuroscience **18**(3): 367-372.

Stevenson, D. et al. (2000). "Mapping and expression analysis of the human CASK gene." Mamm Genome **11**(10): 934-937.

Stockton, R. A. and M. M. Slaughter (1989). "B-Wave of the Electroretinogram - a Reflection of on Bipolar Cell-Activity." Journal of General Physiology **93**(1): 101-122.

Strand, A. D. et al. (2005). "Gene expression in Huntington's disease skeletal muscle: a potential biomarker." Hum Mol Genet **14**(13): 1863-1876.

Su, J. M. et al. (2016). "Collagen-derived matricryptins promote inhibitory nerve terminal formation in the developing neocortex." Journal of Cell Biology **212**(6): 721-736.

Su, J. M., K. Gorse, F. Ramirez and M. A. Fox (2010). "Collagen XIX Is Expressed by Interneurons and Contributes to the Formation of Hippocampal Synapses." Journal of Comparative Neurology **518**(2): 229-253.

Sudarov, A. and A. L. Joyner (2007). "Cerebellum morphogenesis: the foliation pattern is orchestrated by multi-cellular anchoring centers." Neural development **2**(1): 1-22.

Szklarczyk, D. et al. (2015). "STRING v10: protein-protein interaction networks, integrated over the tree of life." Nucleic Acids Research **43**(D1): D447-D452.

Taban, M., B. H. Cohen, A. David Rothner and E. I. Traboulsi (2006). "Association of optic nerve hypoplasia with mitochondrial cytopathies." J Child Neurol **21**(11): 956-960.

Tabuchi, K., T. Biederer, S. Butz and T. C. Sudhof (2002). "CASK participates in alternative tripartite complexes in which Mint 1 competes for binding with caskin 1, a novel CASK-binding protein." J Neurosci **22**(11): 4264-4273.

Takanashi, J. et al. (2010). "Neuroradiologic features of CASK mutations." AJNR Am J Neuroradiol **31**(9): 1619-1622.

Takanashi, J. et al. (2012). "Clinical and radiological features of Japanese patients with a severe phenotype due to CASK mutations." Am J Med Genet A **158A**(12): 3112-3118.

Takeda, H. et al. (2021). "Cerebellar foliation via non-uniform cell accumulation caused by fiber-guided migration of granular cells." Journal of Biomechanical Science and Engineering **16**(1): 20-00516-00520-00516.

Tang, J. et al. (2006). "A complexin/synaptotagmin 1 switch controls fast synaptic vesicle exocytosis." Cell **126**(6): 1175-1187.

Tannu, N. S. and S. E. Hemby (2006). "Methods for proteomics in neuroscience." Functional Genomics and Proteomics in the Clinical Neurosciences **158**: 41-82.

Taranova, O. V. et al. (2006). "SOX2 is a dose-dependent regulator of retinal neural progenitor competence." Genes Dev **20**(9): 1187-1202.

Tissir, F. and A. M. Goffinet (2003). "Reelin and brain development." Nature Reviews Neuroscience **4**(6): 496-505.

Tracy, C. M. et al. (2015). "Retinal Cone Photoreceptors Require Phosducin-Like Protein 1 for G Protein Complex Assembly and Signaling." Plos One **10**(2).

Trotter, J. H. et al. (2019). "Synaptic neurexin-1 assembles into dynamically regulated active zone nanoclusters." Journal of Cell Biology **218**(8): 2677-2698.

Turrigiano, G. (2012). "Homeostatic Synaptic Plasticity: Local and Global Mechanisms for Stabilizing Neuronal Function." Cold Spring Harbor Perspectives in Biology **4**(1).

van Dijk, T., F. Baas, P. G. Barth and B. T. Poll-The (2018). "What's new in pontocerebellar hypoplasia? An update on genes and subtypes." Orphanet J Rare Dis **13**(1): 92.

van Dijk, T. et al. (2020). "Postnatal Brain Growth Patterns in Pontocerebellar Hypoplasia." Neuropediatrics.

Verhage, M. et al. (2000). "Synaptic assembly of the brain in the absence of neurotransmitter secretion." Science **287**(5454): 864-869.

Wang, G. S. et al. (2004). "Transcriptional modification by a CASK-interacting nucleosome assembly protein." Neuron **42**(1): 113-128.

Wang, T. F. et al. (2004). "Identification of Tbr-1/CASK complex target genes in neurons." J Neurochem **91**(6): 1483-1492.

Wang, Y. et al. (2020). "SynQuant: an automatic tool to quantify synapses from microscopy images." Bioinformatics **36**(5): 1599-1606.

Weigand, J. E., J. N. Boeckel, P. Gellert and S. Dimmeler (2012). "Hypoxia-Induced Alternative Splicing in Endothelial Cells." Plos One **7**(8).

Xue, L. et al. (2013). "Global expression profiling reveals genetic programs underlying the developmental divergence between mouse and human embryogenesis." BMC Genomics **14**: 568.

Yang, Y. P. et al. (2014). "Molecular Findings Among Patients Referred for Clinical Whole-Exome Sequencing." Jama-Journal of the American Medical Association **312**(18): 1870-1879.

Zanelli, S., H. P. Goodkin, S. Kowalski and J. Kapur (2014). "Impact of transient acute hypoxia on the developing mouse EEG." Neurobiology of Disease **68**: 37-46.

Zeng, M. L., F. Ye, J. Xu and M. J. Zhang (2018). "PDZ Ligand Binding-Induced Conformational Coupling of the PDZ-SH3-GK Tandems in PSD-95 Family MAGUKs." Journal of Molecular Biology **430**(1): 69-86.

Zglejc-Waszak, K., K. Mukherjee and J. K. Juranek (2021). "The cross-talk between RAGE and DIAPH1 in neurological complications of diabetes: A review." Eur J Neurosci **54**(6): 5982-5999.

Zhang, J. et al. (2012). "Neuron-restrictive Silencer Factor (NRSF) Represses Cocaine- and Amphetamine-regulated Transcript (CART) Transcription and Antagonizes cAMP-response Element-binding Protein Signaling through a Dual NRSE Mechanism." Journal of Biological Chemistry **287**(51): 42574-42587.

Zhang, Y., Z. Luan, A. Liu and G. Hu (2001). "The scaffolding protein CASK mediates the interaction between rabphilin3a and beta-neurexins." FEBS Lett **497**(2-3): 99-102.

Zoghbi, H. Y. (2003). "Postnatal neurodevelopmental disorders: meeting at the synapse?" Science **302**(5646): 826-830.

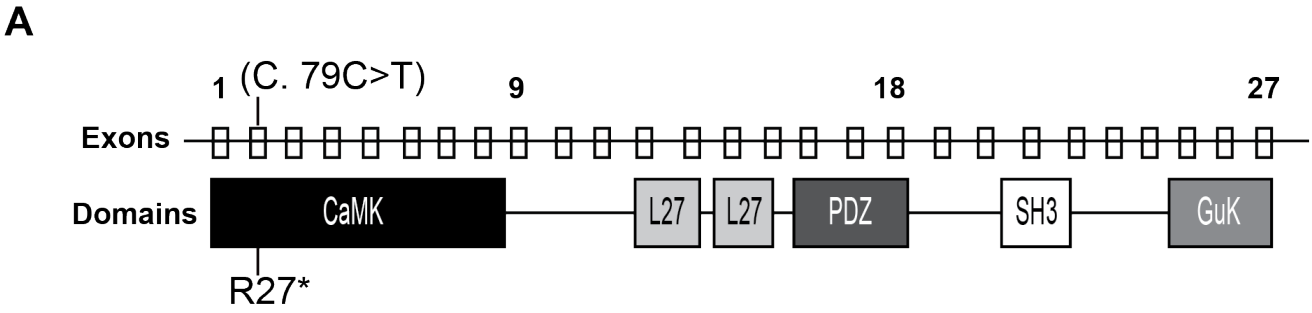
A
1 (C. 79C>T)
9
18
27
Exons
Domains
CaMK
L27
L27
PDZ
SH3
GuK
R27*

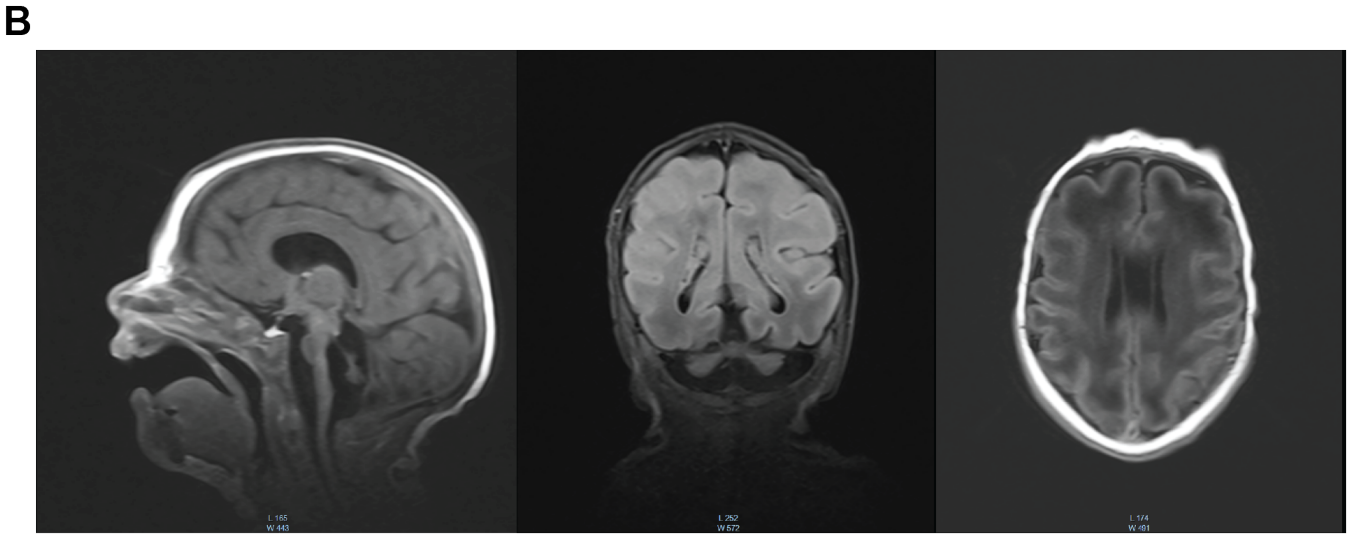
B

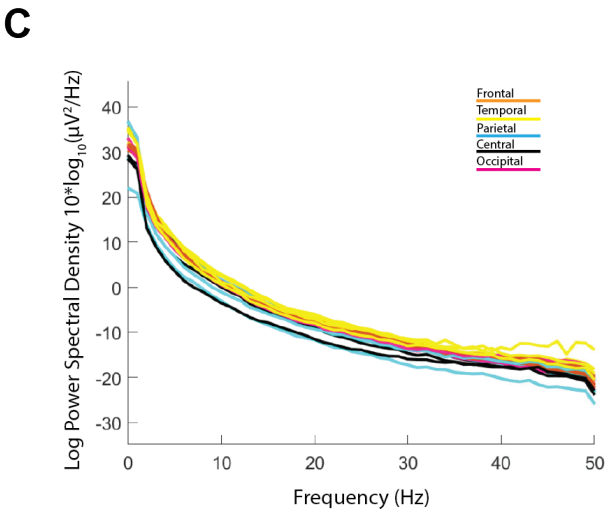
C
Log Power Spectral Density 10*log10(μV²/Hz)
Frequency (Hz)
Frontal
Temporal
Parietal
Central
Occipital

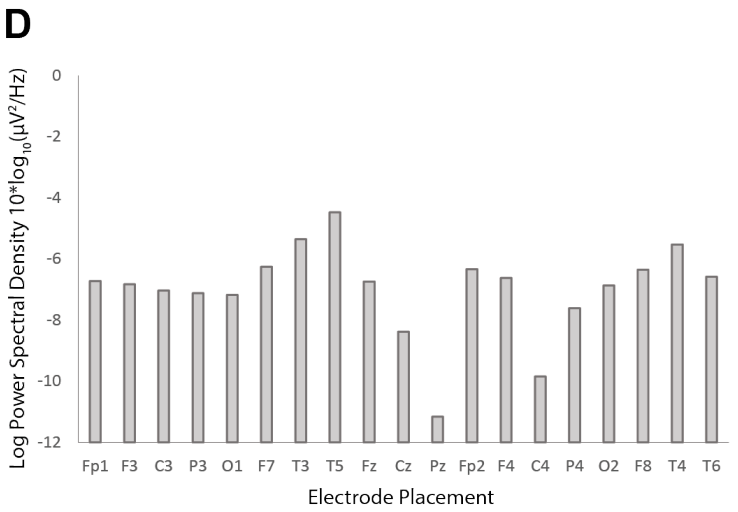
D
Log Power Spectral Density 10*log10(μV²/Hz)
Fp1 F3 C3 P3 O1 F7 T3 T5 Fz Cz Pz Fp2 F4 C4 P4 O2 F8 T4 T6
Electrode Placement

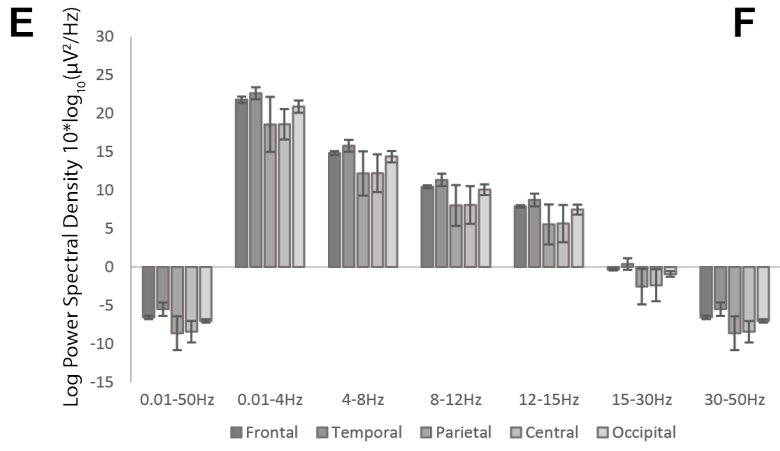
E
Log Power Spectral Density 10*log10(μV²/Hz)
0.01-50Hz
0.01-4Hz
4-8Hz
8-12Hz
12-15Hz
15-30Hz
30-50Hz
Frontal
Temporal
Parietal
Central
Occipital

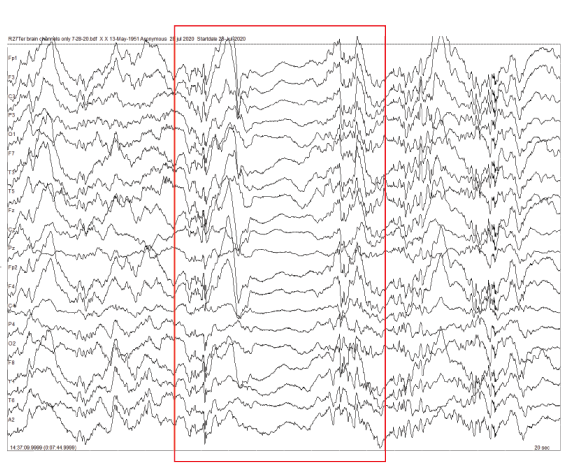
F

Figure 1. The R27Ter mutation results in early truncation of *CASK*, pontocerebellar hypoplasia, and slowed EEG in a human subject. A) Location of the R27Ter mutation in the male decedent; top row: exons of the human *CASK* gene; bottom row: corresponding CASK protein domains. B) Brain MRI scan obtained at 2 weeks revealed severely diminished cerebellar and pontine size with otherwise normal formation of cortical gyri; sagittal, coronal, and transverse planes can be seen from left to right, respectively. C) Power spectral density curves in the 0.01-50Hz range for each electrode independently; colors correspond to underlying cortical location of a given electrode. D) Quantification of mean power spectral density for each electrode in the entire 0.01-50Hz range. E) Mean power spectral density divided into biologically relevant frequency bands of delta, theta, alpha, beta, and low gamma divided by lobe; error bars represent standard deviation between electrodes within a given lobe. F) Example of a burst suppression pattern observed in the R27Ter EEG trace. Red box indicates the onset and duration of the burst suppression.

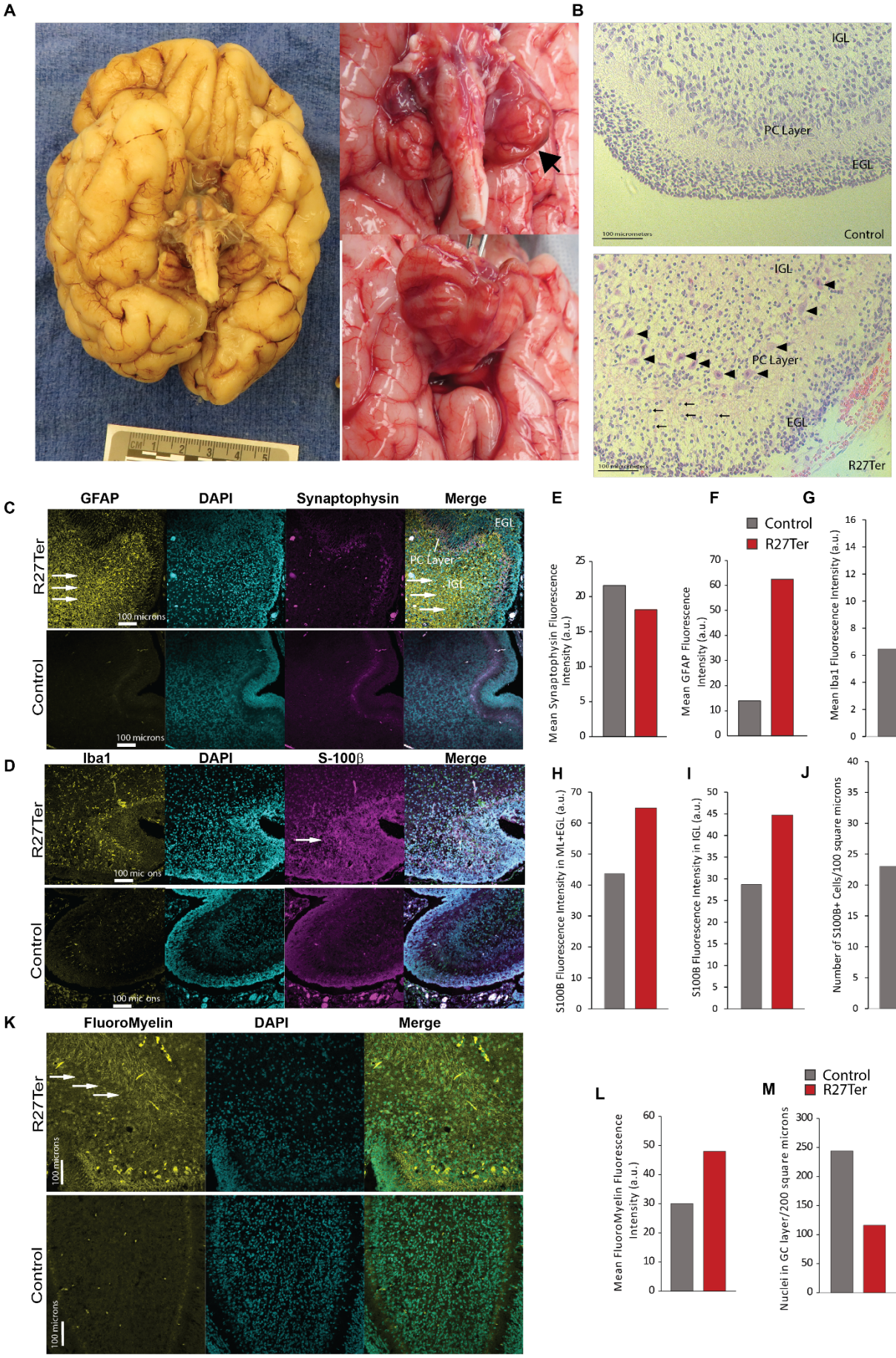
A
B
IGL
PC Layer
EGL
Control
IGL
PC Layer
EGL
R27Ter
C
GFAP
DAPI
Synaptophysin
Merge
R27Ter
Control
EGL
PC Layer
IGL
100 microns
100 microns
D
Iba1
DAPI
S-100β
Merge
R27Ter
Control
100 mic ons
100 mic ons
K
FluoroMyelin
DAPI
Merge
R27Ter
Control
100 microns
100 microns
E
Mean Synaptophysin Fluorescence Intensity (a.u.)
F
Control
R27Ter
Mean GFAP Fluorescence Intensity (a.u.)
G
Mean Iba1 Fluorescence Intensity (a.u.)
H
S100B Fluorescence Intensity in ML+EGL (a.u.)
I
S100B Fluorescence Intensity in IGL (a.u.)
J
Number of S100B+ Cells/100 square microns
L
Mean FluoroMyelin Fluorescence Intensity (a.u.)
M
Control
R27Ter
Nuclei in GC layer/200 square microns

Figure 2. Absence of CASK leads to smaller brain with normal gyrification and cellular migration but increase in gliosis within cerebellum. A) Gross image of the underside of the brain of the decedent showing normal gyri development with a severely diminished cerebellar volume. Proper neuronal migration is absolutely crucial for normal gyrification of cortex and appearance of the tertiary gyri as seen here. The cerebral hemispheres can be seen but the cerebellum is a thin leaf-like structure with a very rudimentary vermis (more details in Supplemental Figure 6, 7 and 8). B) H&E staining of the cerebellar cortex of a control (6 postnatal week (PNW)) female (died of unrelated cause on same day) and the R27Ter subject (10 PNW); the R27Ter mutation cerebellum exhibits proper lamination of the cerebellar cortex, with an external granular layer (EGL), internal granular layer (IGL), and Purkinje cell layer; arrowheads indicate properly aligned Purkinje cells. Compared to the 6 PNW normal cerebellum, the Purkinje cells in R27Ter cerebellum are already more developed with abundant cytoplasm and intricate dendritic arborization. The molecular layer in the R27Ter mutation cerebellum also exhibits a higher proportion of granule cells migrating from the EGL to the IGL (arrows), with thinning of the EGL compared to a normal 6 PNW cerebellum. However, the IGL still appears to be depleted. C) Representative images of GFAP and synaptophysin immunostaining in the R27Ter and a control human cerebellum; from left to right: GFAP, DAPI, synaptophysin, merge. Arrows indicate increased GFAP immunoreactivity. (D) Representative images of Iba1 and S100β immunostaining in control and R27Ter subjects, showing increased Iba1 immunoreactivity in the R27Ter cerebellum. (E) Quantification of synaptophysin immunostaining fluorescence intensity between R27Ter and control cerebella,

demonstrating that immunoreactivity for synaptophysin is unaltered in the absence of CASK. (F-I) Quantification of GFAP, S100β, and Iba1 fluorescence intensity, indicating increased immunoreactivity for GFAP, S100β, and Iba1 in the R27Ter cerebellum compared to control. (J) Quantification of S100β+ cells per 100 μm^2 in the R27Ter and control cerebella; a 100 μm^2 window, including the IGL and Purkinje cell layers, was used for quantification. (K) FluoroMyelin staining of R27Ter and control cerebella, indicating disorganized white matter in the R27Ter subject. (L) Quantification of FluoroMyelin fluorescence intensity. (M) Quantification of DAPI+ nuclei in the granular layer, indicating a decreased number of cells.

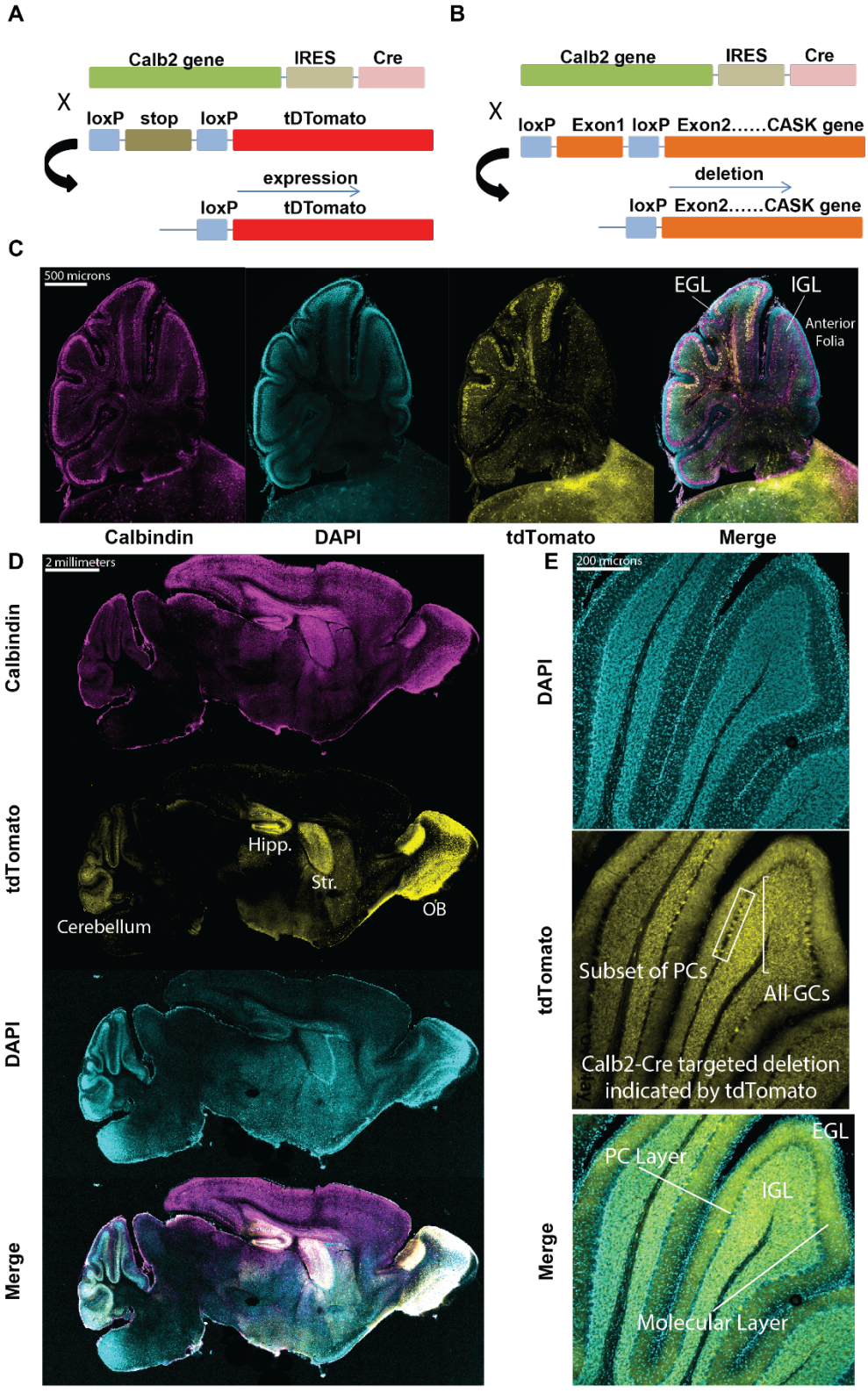
A
Calb2 gene
IRES
Cre
X
loxP
stop
loxP
tDTomato
expression
loxP
tDTomato
B
Calb2 gene
IRES
Cre
X
loxP
Exon1
loxP
Exon2.....CASK gene
deletion
loxP
Exon2.....CASK gene
C
500 microns
EGL
IGL
Anterior
Folia
Calbindin
DAPI
tdTomato
Merge
D
2 millimeters
Calbindin
tdTomato
Hipp.
Str.
OB
Cerebellum
DAPI
Merge
E
200 microns
DAPI
tdTomato
Subset of PCs
All GCs
Calb2-Cre targeted deletion
indicated by tdTomato
Merge
EGL
PC Layer
IGL
Molecular Layer

Figure 3. *Calb2*-Cre expresses only in post-migratory cerebellar granule cells and a subset of Purkinje cells in the anterior folia. (A) Employing the LoxP-STOP-LoxP tdTomato reporter mice for determination of cell-type and age-specific Cre-mediated recombination; tdTomato expression serves as a proxy for CASK deletion in subsequent panels. (B) Schematic of breeding strategy used to selectively delete *Cask* from cerebellar cells. (C) Sagittal section of cerebellum at P8, demonstrating recombination in a subset of Purkinje cells and cells in the internal granular layer, but not in granule cells of the external granular layer; from left to right: calbindin, DAPI, tdTomato, merge. (D) 20x images of a sagittal section of whole mouse brain at P15, demonstrating recombination in several brain regions, notably the cerebellum, olfactory bulb (OB), hippocampus (Hipp.), and striatum (Str.) after development; from top to bottom: calbindin, tdTomato, DAPI, merge. (E) Higher magnification images of cerebellar folia at P15, demonstrating recombination in virtually all cells in the granular layer but only in a small subset of Purkinje cells; box indicates a sample of the subpopulation of Purkinje cells expressing tdTomato reporter, and bracket indicates all granule cells observed expressing tdTomato. The Purkinje cell (PC) layer, molecular layer, IGL, and EGL are indicated for one folium for anatomical orientation.

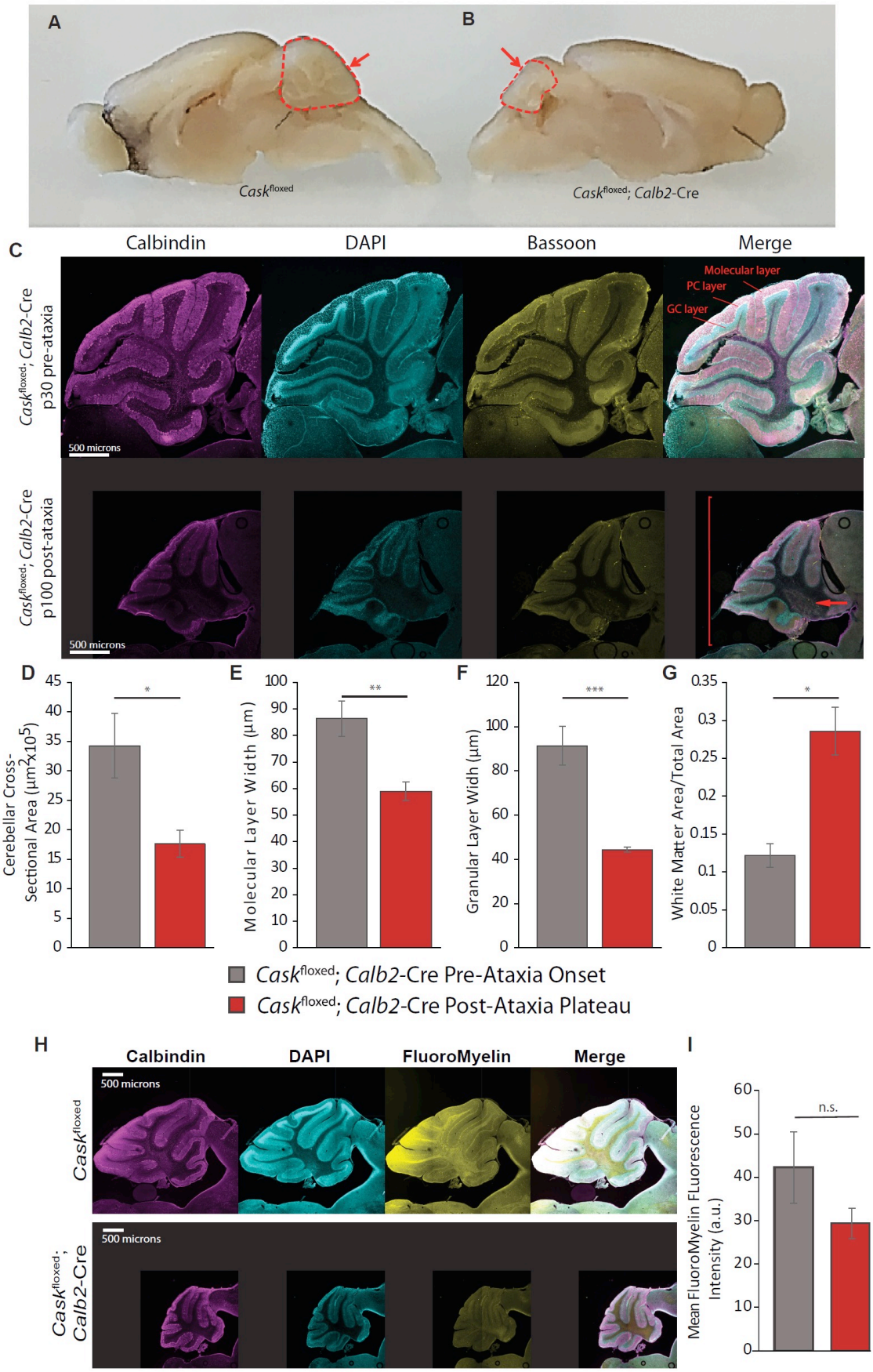
A
B
Cask floxed
Cask floxed; Calb2-Cre
C
Calbindin
DAPI
Bassoon
Merge
Molecular layer
PC layer
GC layer
Cask floxed; Calb2-Cre p30 pre-ataxia
Cask floxed; Calb2-Cre p100 post-ataxia
500 microns
D
Cerebellar Cross-Sectional Area (µm2x10^5)
E
Molecular Layer Width (µm)
F
Granular Layer Width (µm)
G
White Matter Area/Total Area
Cask floxed; Calb2-Cre Pre-Ataxia Onset
Cask floxed; Calb2-Cre Post-Ataxia Plateau
H
Calbindin
DAPI
FluoroMyelin
Merge
Cask floxed
Cask floxed; Calb2-Cre
I
Mean FluoroMyelin FLuorescence Intensity (a.u.)
n.s.

Figure 4. Deletion of *Cask* from post-migratory cerebellar cells results in profound cerebellar degeneration. (A) Gross images of age-matched *Cask*^{floxed} control and (B) *Cask*^{floxed};*Calb2*-Cre brains after plateau of ataxia; arrow indicates diminished volume of the cerebellum while the remainder of the brain remains similarly sized. (C) 10x image of *Cask*^{floxed};*Calb2*-Cre at P30 (top) and P100 (bottom), demonstrating severely reduced cross-sectional area, molecular layer width and granular layer width at P100; the arrow indicates expanded white matter; the bracket indicates diminished overall cerebellar size. (D-F) Quantification of the entire cross-sectional area pre- and post-ataxia, molecular layer width, and granular layer width. (G) Ratio of white matter area to total cross-sectional area pre- and post-ataxia. n=3 for (B-G). (H) Cerebella of adult *Cask*^{floxed};*Calb2*-Cre post-ataxia plateau and *Cask*^{floxed} controls were labeled for calbindin, DAPI and FluoroMyelin (white matter). The mice display disorganized white matter with loss of myelinated fibers in the anterior folia. (I) Quantification of pixel intensity of FluoroMyelin performed with n=4 mice of each genotype.

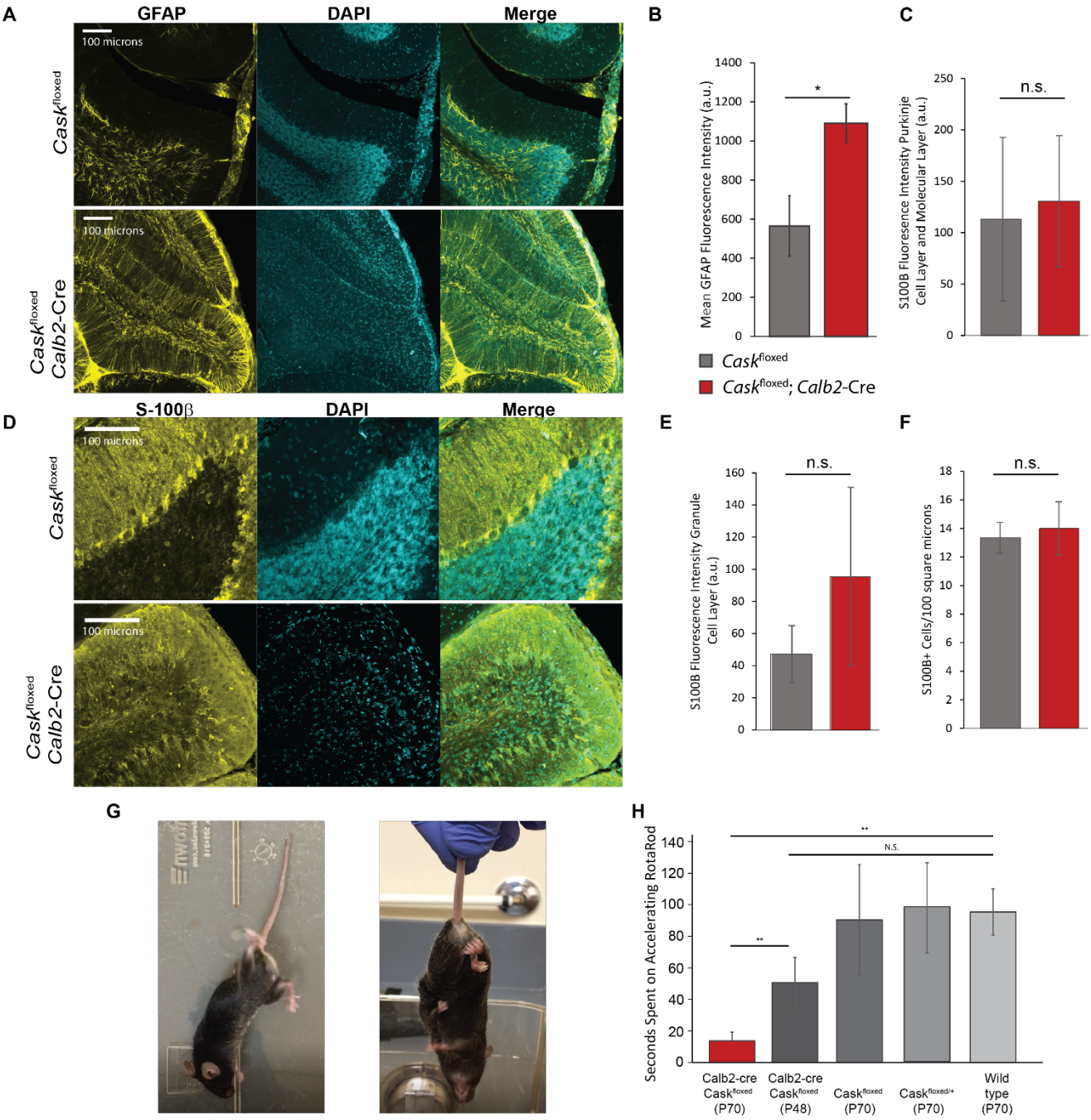

Figure 5. Reactive astrogliosis and locomotor incoordination resulting from cerebellar degeneration caused by CASK loss. (A) Representative images of GFAP immunostaining of anterior cerebellar folia in *Cask*^{floxed};*Calb2*-Cre post-ataxia plateau and age-matched *Cask*^{floxed} controls; from left to right: GFAP, DAPI, merge. (B) Quantification of

fluorescence intensity of GFAP staining by genotype; asterisk indicates $p<0.05$, n=3 mice of each genotype. (C-E) Representative images and quantification of S100β immunostaining in *Cask*^{floxed}; *Calb*-Cre compared to *Cask*^{floxed} controls. Fluorescence intensity was measured for the Purkinje cell layer and molecular layer (C) and the granule cell layer (E) separately due to the unique anatomical distribution of Bergmann glia. (F) Quantification of S100β+ cells in each genotype represented in (D). N=3 mice for each experiment; n.s. indicates $p>0.05$. (G) Example of aberrant locomotor behavior at rest (left) and hindlimb-clasping behavior in a *Cask*^{floxed};*Calb2*-Cre mouse (right). (H) Time spent on an accelerating rotarod in seconds by genotype from left to right: *Cask*^{floxed};*Calb2*-Cre post-ataxia onset (n=4); *Cask*^{floxed};*Calb2*-Cre pre-ataxia onset (n=5); age-matched *Cask*^{floxed} controls (n=4); age-matched heterozygous *Cask*$^{floxed/+}$ controls (n=3); and age-matched wild-type controls (n=4). * indicates $p < 0.05$ using a two-tailed Student's t-test. Results are plotted as mean±SEM for all panels.

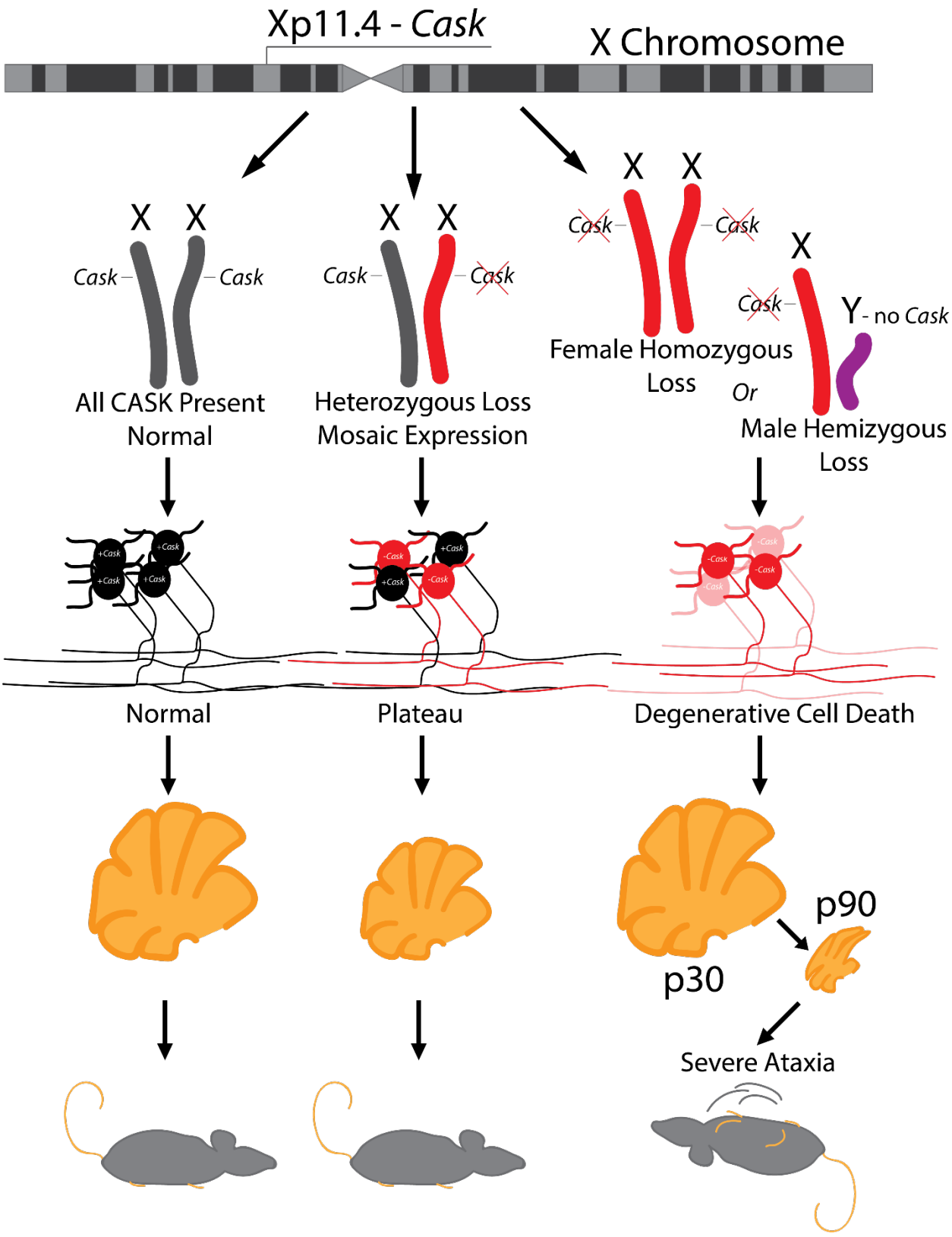

Figure 6. Model describing zygosity-based mechanism of a neurodevelopmental versus

neurodegenerative clinical course of CASK-linked phenotype based on random X-chromosome inactivation. CASK is an X-linked gene critical for maintenance of cerebellar neurons. Heterozygous mutation in CASK produces CASK loss-of-function in only 50% of neurons (red). In the heterozygous condition (red and gray), neurodegeneration thus plateaus (bottom middle), causing an apparent neurodevelopmental disorder, whereas hemizygous CASK mutations (red and purple) in male mice or homozygous CASK mutation (two reds) in female mice produce a progressive phenotype typical of neurodegeneration with severe ataxia (bottom right).

4. Discussion

Through a detailed investigation of a single molecule and its associated pathologies, I have herein described several important findings on the *CASK* gene, cerebellar function, as well as the difficulty in modeling monogenic neurological disorders. In summation: (1) the CASK protein may have multifarious roles within cells and cannot be easily ascribed a solely synaptic function; (2) loss of the CASK protein leads to a degenerative progressive pathology rather than a developmental failure as previously hypothesized; (3) ablation or loss-of-function of CASK results in specific death of cerebellar granule cells after migration has completed; (4) post-developmental death of granule cells results in a profound ataxia in a murine model; (5) progression of CASK-linked pathologies may not be correlated to a molecular function of the protein.

4.1 Multifarious Roles of the CASK Protein

While initially described as a protein involved in synaptic function (Hata et al. 1996; Atasoy et al. 2007), my work herein has demonstrated that CASK likely participates in various cellular activities outside of the synapse. The first indication can be seen simply in the whole brain cell-type specific RNA-sequencing database documented in Zhang et al. 2014, wherein RNA transcripts of the *Cask* gene can be found in approximately equal levels as in neurons in non-synapse forming cells such as astrocytes and at double levels

in oligodendrocyte progenitor cells (Zhang et al. 2014). Together with data from the NCBI gene expression database showing that *Cask* transcripts are present at high levels in organs outside of the nervous system such as the kidney (The NCBI Handbook), which is not particularly enriched in neuronal cell types, this is a first indication that CASK may not have an exclusively synaptic function. Herein, I have furthered this non-synaptic understanding of CASK. Our work in Patel, PA et al. (2020), demonstrates several important pieces of evidence.

Firstly, co-immunoprecipitation combined with tandem mass spectrometry demonstrates that CASK may complex with molecules outside of the synapse. Indeed, CASK's complexing partners include synaptic molecules and SNAREs such as liprins-alpha, Mint1, and syntaxin (Patel, PA et al. 2020 Figure 5), but extend to proteins which are classified by Gene Ontology as belonging to four other subcellular compartments and biological functions. These compartments and functions broadly cluster as belonging to the ribosomal subunits, protein-folding chaperones, cytoskeletal elements, and mitochondrial proteins (Patel, PA et al. 2020 Figure 5). The specific function of these complexes remains to be discovered as well as the functional utility (if any) of these complexes. An experiment such as the one described in figure 1 of Patel, PA et al. (2020) captures the total field of possible interactions while allowing for non-specific interactions and large complexes which may have been pulled down due to secondary, tertiary, or n-th order interactions.

We therefore then used a face- and contruct-validated murine model of *Cask* heterozygous deletion (*Cask*$^{+/-}$) to further elaborate the functional changes which may be

occurring. Bulk RNA-sequencing from whole brain homogenate in the *Cask*$^{+/-}$ model demonstrates that CASK ablation largely results in changes to nuclear transcripts, transcripts encoding extracellular matrix-associated proteins, and mitochondrial transcripts (Patel, PA et al. 2020 Figure 2). The changes in nuclear transcripts such as transcription factors may be attributable to a nuclear homeostatic response to the loss of a given gene while the changes in extracellular matrix-associated transcripts may be a response to necessary remodeling of the extracellular matrix in response to shrinking brain size and cell death. Changes in mitochondrial transcripts likewise could reflect an energetic compensation to the loss of an important gene in half of brain cells, especially in light of CASK's potential interacting partners in the mitochondria.

However, at the protein level, our results become more refined. Conducting a bulk proteomics from whole brain lysate in the *Cask*$^{+/-}$ model, three broad classes of changes become apparent (Patel, PA et al. 2020 Figure 4). Of course, synaptic changes are represented with pre-synaptic proteins being almost entirely downregulated while post-synaptic proteins are almost entirely upregulated. This could again reflect a homeostatic compensation to the loss of CASK's function at the pre-synapse: when CASK is not present in half of brain cells, pre-synaptic function in the form of vesicle clustering and fusion at appropriate intervals may be impaired leading to a haphazard upregulation of post-synaptic receptors to grasp at a survivable functionality.

Indeed, in the functional realm, the brain of the *Cask*$^{+/-}$ model appears to be relatively well *in vivo*. Electroencephalography using tungsten wires reveals that local field potential power spectral density is unchanged in the cortex and hippocampus of the *Cask*$^{+/-}$ mouse

as compared to wild-type littermate controls (Patel, PA et al. 2020 Figure 1). As well, only a single seizure event was observed in the hippocampus of the *Cask*$^{+/-}$ model. Together with the spectral analysis, these results indicate that, at the level of the local field potential, electrical activity is not changed in the heterozygous absence of CASK. This somewhat contrasts with previous work (Atasoy et al. 2007; Mori et al. 2019) demonstrating that absence of CASK induces an increase in miniature excitatory post-synaptic potentials relative to inhibitory post-synaptic potentials. This change has been posited as a mechanism explaining the Othahara Syndrome phenotype in humans wherein loss-of-function mutations in CASK lead to epileptic encephalopathy with burst suppression. However, taken with the molecular data in figures 2-4 of the paper, these changes may be compensated through up- or downregulation of related proteins that ultimately prevent catastrophic changes in the local field potential under heterozygous conditions. In total loss of CASK, epileptic encephalopathy persists.

Recent findings using induced neurons from cultured fibroblasts taken from human subjects with point mutations in *CASK* further exacerbate this issue. Two recent studies (Becker et al. 2020 and McSweeney et al. 2022) used induced neurons in culture to demonstrate that network activity is altered and an increase in the frequency of excitatory synaptic transmission is increased in these cultures. While these studies rely on the advantage of being human cells converted into neurons and being thus genomically comparable to the actual human subjects, they also have the disadvantages which come with two-dimensional culture systems. The physiology of a living brain cannot be fully recapitulated under such circumstances. Further, these differences have particular

salience in the case of CASK-linked disorders for several reasons. Predominantly, it has been demonstrated repeatedly that pathological progression in CASK-linked disorders is non-cell autonomous in nature (Kerr et al. 2019, Patel, PA et al. 2022) and preferentially affects certain cell types of the nervous system, but not others (e.g. granule cells) (Patel, PA et al. 2022). These studies have a utility for unmasking novel functions of CASK in human cells. However, the utility of drawing conclusions about the pathology based on culture systems, even though they recapitulate the genome of the human, is questionable.

4.2 Loss of CASK Leads to Degeneration

The nature of CASK-linked pathologies is complicated by several factors, including that complete ablation of CASK leads to early postnatal lethality as well as the large number of binding partners and molecular changes occurring as described above. The inability to generate a mouse model which survives beyond several days after birth and the appearance of symptoms in humans presenting weeks to months after birth has led to an entrenchment of the idea that loss of CASK function results from developmental abnormalities preventing adequate migration of neurons and lamination of brain tissue (Hsueh et al. 2000). However, in Patel, PA et al. 2022, we definitively show that loss of CASK protein leads to early degeneration of the brain resultant from neuronal cell death rather than developmental failure. The two sides of this coin have been difficult to disentangle precisely because of the timing of the onset of the pathology. Degeneration of this sort which occurs early post-natally may appear as a developmental failure.

Evidence from the visual system presented in Liang C et al. 2017 and Kerr et al. 2019 showed that the optic nerve hypoplasia associated with CASK loss only begins to manifest several days after birth, that retinal lamination and migration of retinal ganglion cells is unaffected, and that retinal ganglion cells specifically die out in a non cell-autonomous manner in the course of progression of the pathology. Likewise, evidence from Srivastava et al. 2016 showed that brain size is normal at birth in the *Cask*$^{+/-}$ murine model, but does not reach normal levels leading to a microcephaly phenotype. However, the brain of the *Cask*$^{+/-}$ mouse at postnatal day 0 is well formed and properly laminated (Srivastava et al. 2016). These results provide the first clues that loss of CASK does not lead to developmental abnormalities or affect cell migration or patterning.

In Mukherjee et al. 2020, we had the first opportunity to investigate a case of early truncation of CASK where the 27th arginine was mutated to a STOP codon; this mutation occurs in the second coding exon of CASK and precludes any functional protein production whatsoever. Several important features of this case shed light on CASK-linked disorders. Firstly, the subject, at the time of reporting, was 17 years of age. This indicates that complete absence of CASK protein in human does not necessarily result in death so long as respiratory and nutritional functions are maintained exogenously. Secondly, this case reports with microcephaly, ponto-cerebellar hypoplasia, and intractable epilepsy, confirming that, in the extreme case where no functional CASK is present, these are associated phenotypes. And finally, the subject demonstrated an abnormally slow EEG pattern, with delta waves dominating the power spectrum. This EEG pattern is consistent

with other cases of CASK loss in human and calls into question the over-excitation hypothesis presented for how CASK-loss manifests as epilepsy in humans.

Extending this observation with another case, in Patel, PA et al. 2022, we leverage another human case of early truncation in the *CASK* gene at the same site as that reported in Srivastava et al. 2020 (Arginine 27 to stop; Arg27Ter) wherein a stop codon is introduced via single-nucleotide polymorphism within the second exon of the human *CASK* gene to ablate any functional transcript of *CASK* in this human case (Patel, PA et al. 2022 Figure 1). Gross examination of the brain of this subject indicates properly formed tertiary gyri as well as adequate lamination of the cortex and cerebellum. *In vivo*, scalp electroencephalography revealed burst suppression patterns and a general slowing the electroencephalography pattern with delta frequencies predominating (Patel, PA et al. 2022 Figure 1), consistent with previous observations (Mukherjee et al. 2020).

However, the cerebellum of this subject in particular was vastly shrunken compared to a control who died of non-neurological causes at a similar age. Histopathological examination of the cerebellum revealed that, while lamination was normal, there was a depletion of cells in the internal granular layer of the cerebellum with no defects in Purkinje cells. Molecular examination using immunohistochemistry subsequently revealed an upregulation of glial fibrillary acidic protein (GFAP), which is often upregulated in astroglia following insults to the nervous system such as physical damage (reviewed in: Brenner et al. 2021) or degenerative processes (reviewed in Carter et al. 2019). This data from the human subject provided early evidence that complete loss of CASK leads to degeneration mediated by cell death which could be investigated in a murine model.

4.3 CASK Loss Causes Death of Granule Cells

Investigating the degenerative cell death further in a murine model required generated such a model which is not susceptible to the tractability problem of early post-natal death. Later in Patel, PA et al. 2022, we created such a model by specifically deleting *Cask* from the majority of cerebellar neurons via Cre recombinase expression driven by the *Calb2* promoter. The *Calb2* promotor enables expression of Cre in all granule cells observed as well as a subset of Purkinje cells in the anterior folia of the cerebellum. Further, Cre is only expressed after granule cells have completed migration into the internal granular layer as demonstrated by time-course tdTomato reporter experiments (Patel, PA et al. 2022 Figure 3).

Deleting *Cask* after migration has completed allowed us to provide the first evidence that, when development of the cerebellum is unaffected by lack of CASK, cell death and degeneration still proceed. In the cerebellar knockout, granule cells develop normally and successfully form connections onto Purkinje cells via their parallel fibers (Patel, PA et al. Supplemental Figure), however begin to die out starting at approximately post-natal day 60 in a progressive fashion until around post-natal day 100 when degeneration is complete (Patel, PA et al. 2022 Figure 4). This degeneration includes a massive loss of granule cells and depletion of the internal granular layer, as well as gross morphological changes including shrinkage of cerebellar volume by approximately two-thirds and decreases in rounding of the cerebellar folia, particularly anterior folia.

The actual time-course of the degeneration is an interesting feature to highlight as well. The variability observed in the onset and progression of degeneration signals the actual variability in a pathology and how this deviates from normal physiology (Mukherjee et al. 2022). It lends to a consideration of how disease modeling may not be as cleanly mechanistic as we hope in the lab, but mechanisms need still be unveiled.

4.4 Granule Cell Loss Leads to Ataxia

One critical finding coming out of the CASK-linked degeneration is the severe motor phenotype that accompanies the loss of cerebellar granule cells after migration has completed. The function of granule cells themselves is as yet unknown, though several hypotheses have been put forward regarding their function in motor learning and sparse coding of motor information (Galliano et al. 2013; Giovannucci et al. 2017; Marr 1969; Albus 1971; Schweighofer, 2001).

The primary function ascribed to granule cells thus far is that they participate in learning novel motor behaviors (Schweighofer, 2001). This is primarily evidenced by observations of spontaneously occurring mutations which lead to cerebellar dysfunction in mouse lines. One of the primary lines which has been investigated is the *Weaver* mouse in which granule cells form in their progenitor zone, but die before and during migration into the internal granular layer. This granule cell death is accompanied by an ataxic gait phenotype (Rakic, 1973; Patil et al. 1995; Hess et al. 1996). However, the complication to investigating granule cell function in this way is that the granule cells die during

development before forming parallel fiber synapses or receiving mossy fiber input. This precludes any ability to study their function in the developed cerebellum using the *Weaver* mouse.

To address these concerns, one study ablated P/Q type calcium channels in parallel fibers in the adult mouse (Galliano et al. 2013). Ablation of these channels will putatively block any synchronous synaptic release at parallel fiber pre-synaptic terminals and thus ablate information being transmitted to Purkinje cell dendrites via granule cells. Upon ablating the channels, the authors observed no ataxic phenotype. Instead, they noted that the mouse has deficits in learning novel motor tasks, but previously learned tasks remain unaffected (Galliano et al. 2013). Thus motor learning became a putative function of this cell type.

However, the findings presented herein demonstrate an obvious ataxia even during normal locomotion which precedes concurrently with specific death of granule cells. Additionally, due to the degenerative nature of the phenotype which only begins around postnatal day 60, one can observe that the mouse learns proper locomotion at the level of healthy age-matched controls, but then loses this ability (Patel, PA et al. 2022 Figure 5). It can therefore be posited that granule cells do play some role in maintaining already learned behaviors. However, in the degenerated cerebellum due to CASK loss, cerebellar gross morphology is also severely altered with collapsing of Purkinje cell dendrites and thinning of the molecular layer. Thus, it remains an open question whether the ataxia is resultant from loss of granule cell function or alterations in Purkinje cell morphology disallowing them to maintain normal physiology.

4.5 Molecular Function and Pathogenesis

To conclude, I will briefly discuss the peculiar relationship between genes, their proteins, and the progression of pathologies associated with them.

A holy grail (or white whale) of biology over the last 60 years since the molecular biology revolution with the discovery of DNA structure (Watson and Crick, 1953) has been to understand how genes give rise to biological functions. Enormous progress has been made on this front in understanding healthy physiology using genetic strategies such as generating knockout and knockin mice, conducting gain- and loss-of-function studies in animals and cell culture models, and other strategies. Indeed, since the genomics revolution of the early 2000s, it is now possible to interrogate gene networks and their dynamic functions in living organisms. Technologies like CRISPR promise to hasten the pace of these experiments and give even more power to the molecular biologist in playing the experimental keys of nature.

However, the test case of CASK-linked disorders demonstrates that a similar pace of progress may not be possible in the investigation of disorders. The precise molecular function of CASK is as yet unknown, though it may be tricky to find as a multi-domain scaffolding protein with potentially tens of interacting proteins. However, it becomes difficult to imagine how any of the putative functions of CASK in synaptic function (Atasoy et al. 2007, Mori et al. 2019, Patel, PA et al. 2020) or any other functions discussed herein (Patel, PA et al. 2020) may lead to the diverse phenotypes observed either in the clinic

with single-nucleotide polymorphism cases or in murine models of cell-type and region-specific CASK deletion.

Why is the phenotypic spectrum in CASK-linked disorders so vast? Why does epileptic encephalopathy generally only present in hemizygous or homozygous mutations while heterozygous mutations seem to be entirely spared of any electroencephalographic change whatsoever? Why are these particular early post-natal ages the ones where CASK-linked disorders seem to first manifest when the gene begins expressing *in utero*? These and many such questions persist.

While the relationship between genetic function and pathology can be fraught with challenges and pitfalls (Mukherjee et al. 2022), there is a case for optimism. Despite not knowing the molecular function of CASK, great progress has been made in understanding the disorders associated with it. This progress relies on several disparate avenues: observations from the clinic (Hackett et al. 2010; Moog et al. 2015; Najm et al. 2008; LaConte et al. 2017; Patel PA et al. 2022; Mukherjee et al. 2020), molecular studies in mouse and cell culture conducted based on these observations (such as in LaConte et al. 2017), as well as basic biological investigations into the protein itself (such as in Atasoy et al. 2007; Mukherjee et al. 2008; Mori et al. 2019). Despite being rare, CASK-linked disorders now exist in a very small club of neurological disorders for which there is at least some explanation of pathology progression. This highlights most importantly the need for interdisciplinary, translational science conducted by many groups working together from different ends of the problem, and genuinely making headway into explanations and solutions for affected individuals and their families.

All References

49. Albus, J. S. (1971). “A theory of cerebellar function”. Mathematical Biosciences. **10**(1-2): 25-61.

50. Apps, R., Garwicz, M. (2005). Anatomical and physiological foundations of cerebellar information processing. Nat Rev Neurosci. 6: 297-311.

51. Atasoy, D. et al. (2007). "Deletion of CASK in mice is lethal and impairs synaptic function." Proceedings of the National Academy of Sciences of the United States of America **104**(7): 2525-2530.

52. Baumel, Y., Jacobson, G. A., Cohen, D. (2009). “Implications of functional anatomy on information processing in the deep cerebellar nuclei”. Front Cell Neurosci. **3**(14).

53. Becker, M. et al. (2020). “Presynaptic dysfunction in CASK-related neurodevelopmental disorders”. Transl Psychiatry. **10**(1): 312

54. Bohne, P. et al. (2019). “A New Projection From the Deep Cerebellar Nuclei to the Hippocampus *via* the Ventrolateral and Laterodorsal Thalamus in Mice”. Front Neural Circuits. **13**(51).

55. Boudeau, J. et al. (2006). “Emerging roles of pseudokinases”. Trends in Cell Biology. **16**(9): 443-52.

56. Bozzi, Y. et al. (2018). “Neurobiological bases of autism-epilepsy comorbidity: a focus on excitation/inhibition imbalance”. Eur J Neurosci. **47**(6): 534-48.

57. Brenner, M., Messing, A. (2021). “Regulation of GFAP Expression”. ASN Neuro. **13**:1759091420981206.

58. Buffo, A., Rossi, F. (2013). “Origin, lineage and function of cerebellar glia”. Progress in Neurobiology. **109**: 42-63.

59. Burglen, L. et al. (2012). "Spectrum of pontocerebellar hypoplasia in 13 girls and boys with CASK mutations: confirmation of a recognizable phenotype and first description of a male mosaic patient." Orphanet J Rare Dis **7**: 18.

60. Butt, A. M. et al. (2004). “Functions of optic nerve glia: axoglial signalling in physiology and pathology”. Eye (Lond). **18**(11): 1110-21.

61. Carter, S. F. et al. (2019). “Astrocyte Biomarkers in Alzheimer’s Disease”. Trends Mol Med. **25**(2): 77-95.

62. Cristofoli F. et al. (2018). “Novel *CASK* mutations in cases with syndromic microcephaly”. Hum Mutat. **39**(7): 993-1001.

63. Delion M., Dinomais, M., Mercier, P. (2017). “Arteries and Veins of the Cerebellum”. Cerebellum. **16**: 880-912.

64. Galliano, E. et al. (2013). “Silencing the majority of cerebellar granule cells uncovers their essential role in motor learning and consolidation”. Cell Rep. **3**(4): 1239-51.

65. Giovannucci A. et al. (2017). “Cerebellar granule cells acquire a widespread predictive feedback signal during motor learning”. Nat Neurosci. **20**(5): 727-34.

66. Hackett, A. et al. (2010). "CASK mutations are frequent in males and cause X-linked nystagmus and variable XLMR phenotypes." Eur J Hum Genet **18**(5): 544-552.

67. Hata, Y. et al. (1996). "CASK: a novel dlg/PSD95 homolog with an N-terminal calmodulin-dependent protein kinase domain identified by interaction with neurexins." J Neurosci **16**(8): 2488-2494.

68. Hayreh, S. S. (1969). “Blood supply of the optic nerve head and its role in optic atrophy, glaucoma, and oedema of the optic disc”. Br J Ophthalmol. **53**(11): 721-48.

69. Hess, E. J. (1996). “Identification of the *weaver* Mouse Mutation: The End of the Beginning”. Neuron. **16**(6): 1073-76.

70. Hsueh, Y. et al. (2000). “Nuclear translocation and transcription by the membrane-associated guanylate kinase CASK/LIN-2”. Nature. **404**: 298-302.

71. Jimsheleishvili, S., Dididze, M. (2021). “Neuroanatomy, Cerebellum”. In: StatPearls [Internet]. Treasure Island (FL): StatPearls Publishing; 2022 Jan-

72. Kang, K., Shapley, R.M., Sompolinsky, H. (2004). “Information Tuning of Populations of Neurons in Primary Visual Cortex”. Journal of Neuroscience. 24(15): 3726-3735.

73. Kerr, A. et al. (2019). "Non-Cell Autonomous Roles for CASK in Optic Nerve Hypoplasia." Invest Ophthalmol Vis Sci **60**(10): 3584-3594.

74. Kumoro, H., Rakic, P. (1998). “Distinct Modes of Neuronal Migration in Different Domains of Developing Cerebellar Cortex”. Journal of Neuroscience. **18**(4): 1478-90.

75. LaConte, L. E. et al. (2016). "CASK stabilizes neurexin and links it to liprin-alpha in a neuronal activity-dependent manner." Cell Mol Life Sci **73**(18): 3599-3621.

76. LaConte, L. E. W. et al. (2018). "Two microcephaly-associated novel missense mutations in CASK specifically disrupt the CASK-neurexin interaction." Hum Genet **137**(3): 231-246.

77. Liang, C. et al. (2017). "Optic Nerve Hypoplasia Is a Pervasive Subcortical Pathology of Visual System in Neonates." Investigative Ophthalmology & Visual Science **58**(12): 5485-5496.

78. Lu, C. S. et al. (2003). "Regulation of the Ca2+/CaM-Responsive Pool of CaMKII by Scaffold-Dependent Autophosphorylation". Neuron. **40**: 1185-97.

79. Lyon, M. (1961). "Gene action in the X-chromosome of the mouse (*Mus musculus* L.)". Nature **190**:372-373.

80. Marr, D. (1969). "A theory of cerebellar cortex". The Journal of Physiology. **202**(2): 437-470.

81. Martersteck, E. et al. (2017). "Diverse Central Projection Patterns of Retinal Ganglion Cells". Cell Rep. 18(8): 2058-2072.

82. McSweeney, D. et al. (2022). "Loss of Neurodevelopmental Gene *CASK* Disrupts Neural Connectivity in Human Cortical Excitatory Neurons". *BiorXiv*.

83. Miyata, T. et al. (2010). "Migration, early axonogenesis, and Reelin-dependent layer-forming behavior of early/posterior-born Purkinje cells in the developing mouse lateral cerebellum". Neural Development. **5**(23).

84. Morgan, J. L. (2017). "A connectomic approach to the lateral geniculate nucleus". Vis Neurosci. **34**: E014.

85. Moog, U. et al. (2011). "Phenotypic spectrum associated with CASK loss-of-function mutations." J Med Genet **48**(11): 741-751.

86. Moog, U. et al. (2015). "Phenotypic and molecular insights into CASK-related disorders in males." Orphanet J Rare Dis **10**: 44.

87. Mori, T. et al. (2019). "Deficiency of calcium/calmodulin-dependent serine protein kinase disrupts the excitatory-inhibitory balance of synapses by down-regulating GluN2B." Mol Psychiatry **24**(7): 1079-1092.

88. Mukherjee, K. et al. (2008). "CASK functions as a Mg2+-independent neurexin kinase." Cell **133**(2): 328-339.

89. Mukherjee, K. et al. (2020). “Survival of a male patient harboring CASK Arg27Ter mutation to adolescence”. Mol Genet Genomic Med. **8**(e1426).

90. Mukherjee, K., LaConte, L. E. W., Srivastava, S. (2022). “The Non-Linear Path from Gene Dysfunction to Genetic Disease: Lessons from the MICPCH Mouse Model”. Cells. **11**(7): 1131.

91. Najm, J. et al. (2008). "Mutations of CASK cause an X-linked brain malformation phenotype with microcephaly and hypoplasia of the brainstem and cerebellum." Nat Genet **40**(9): 1065-1067.

92. Patel, P. A. et al. (2020). "Haploinsufficiency of X-linked intellectual disability gene CASK induces post-transcriptional changes in synaptic and cellular metabolic pathways." Exp Neurol **329**: 113319.

93. Panning, B. (2008). “X-chromosome inactivation: the molecular basis of silencing”. Journal of Biology. **7**(30).

94. Plenge, R.M. et al. (2002). “Skewed X-chromosome inactivation is a common feature of X-linked mental retardation disorders”. Am J Hum Genet. **71**(1): 168-73.

95. Patel, P. A. et al. (2022). “Complete loss of the X-linked gene CASK causes severe cerebellar degeneration”. Journal of Medical Genetics. Published Online First: 11 February 2022.

96. Patil, N. et al. (1995). “A potassium channel mutation in weaver mice implicates membrane excitability in granule cell differentiation”. Nat Genet. **11**(2): 126-9.

97. Salazar, J. J. et al. (2018). “Anatomy of the Human Optic Nerve: Structure and Function”. In: Ferrari, F. M. editor, Optic Nerve [Internet].

98. Schweighofer, N., Doya, K., Lay, F. (2001). “Unsupervised learning of granule cell sparse codes enhances cerebellar adaptive control”. Neuroscience. **103**(1): 35-50.

99. Seabrook, T. A. et al. (2017). “Architecture, Function, and Assembly of the Mouse Visual System”. Annu Rev Neurosci. **40**: 499-538.

100. Srivastava, S. et al. (2016). "X-linked intellectual disability gene CASK regulates postnatal brain growth in a non-cell autonomous manner." Acta Neuropathol Commun **4**: 30.

101. Streng, M.L., Popa, L.S., Ebner, T.J. (2018). “Complex Spike Wars: a New Hope”. Cerebellum. 17(6): 735-746.

102. Rakic, P., Sidman, R. L. (1973). “Sequence of developmental abnormalities leading to granule cell deficit in cerebellar cortex of weaver mutant mice”. J Comp Neurol. **152**(2): 103-32

103. The NCBI handbook [Internet]. Bethesda (MD): National Library of Medicine (US), National Center for Biotechnology Information; 2002 Oct. Available from http://www.ncbi.nlm.nih.gov/books/NBK21101

104. van Welie I. et al. (2011). “The metamorphosis of the developing cerebellar microcircuit”. Curr Opin Neurobiol. **21**(2-14): 245-53.

105. Watson, J. D., Crick, F. H. C. (1953). “Molecular Structure of Nucleic Acids: A Structure for Deoxyribose Nucleic Acid”. Nature. **171**: 737-38.

106. Xiao L. et al. (2018). “Regulation of striatal cells and goal-directed behavior by cerebellar outputs”. Nat Commun. **9**(3133).

107. Zhang, Y. et al. (2014). “An RNA-sequencing transcriptome and splicing database of glia, neurons, and vascular cells of the cerebral cortex”. J Neurosci. **34**(36): 11929-47.